University of Puerto Rico
Rio Piedras Campus
Department of Biology
Doctoral Program

Characterizing the effects of estrogen and G15 on triple-negative Inflammatory Breast Cancer

By

Xavier S. Bittman-Soto

A dissertation submitted to the Doctoral Program in the Department of Biology of the University of Puerto Rico in partial fulfillment of the requirements for the degree of

DOCTOR IN PHILOSOPHY

February 27, 2023

Characterizing the effects of estrogen and G15 on triple-negative Inflammatory Breast Cancer

Accepted by the Faculty of the Doctoral Program in the Department of Biology of the University of Puerto Rico in partial fulfillment of the requirement for the degree of

Doctor of Philosophy

_____
Dr. Esther A. Peterson Peguero
Department of Biology
Thesis Advisor

_____
Dr. Harold I. Saavedra
Department of Basic Science
Thesis Committee Member

_____
Dr. Jose A. Rodriguez Martinez
Department of Biology
Thesis Committee Member

_____
Dr. Jose L. Agosto Rivera
Department of Biology
Thesis Committee Member

_____
Dr. Pablo L. Vivas Mejia
Department of Biology
Thesis Committee Member

February 27, 2023

Characterizing the effects of estrogen and G15 on triple-negative Inflammatory Breast Cancer

Abstract

Inflammatory breast cancer (IBC) remains the most aggressive and lethal form of breast cancer—reporting rapid progression, poor prognosis, and a unique clinical diagnosis. IBC is frequently classified as a hormone receptor-negative (HR-negative) breast cancer, where cancer cells test negative for estrogen and progesterone receptors and cannot be treated with current hormone therapies. Still, estrogen stimulation enhances cell migration and invasion phenotypes on IBC cells via activation of non-genomic (rapid) signaling cascades—which are known to be mediated by alternate ERs such as the G-protein coupled estrogen receptor (GPER). However, the estrogen-induced transcriptome on IBC cells remains unknown, and the involvement of GPER on estrogen-response signals remains unclear. An extensive understanding of the effects induced by estrogen and G15 (GPER-specific antagonist) on IBC cells provides a new opportunity to address the current need for alternative approaches against IBC patients. Here, RNA sequencing was performed on IBC cells SUM149 to characterize the transcriptome induced by 17β-estradiol (E2) at different time points. In addition, IBC cells SUM149 and SUM190 were treated with G15 alone and combined with E2 to identify the drug's effects on estrogen-response signals and IBC's aggressiveness—possibly elucidating GPER's role. RNA-seq analysis on IBC SUM149 revealed an E2-induced enhancement in the expression of genes associated with transcription factors, signaling cascade mediators, and growth factor ligands—some of which G15 treatment was able to disrupt. Furthermore, G15 reduced the cell viability, growth rate, and colony size of IBC cell SUM149 and inhibited the cell viability and growth rate of IBC SUM190. G15 also inhibited the E2-induced expression of Cyclin-E1 (a cell cycle progression marker), inhibited the anti-apoptotic regulator B-cell lymphoma 2 (BCL-2), and increased the pro-apoptotic marker cleave caspase-3 on IBC SUM149. Regarding non-genomic signals, G15 disrupted the regulatory mechanism of the E2-induced ERK and AKT signaling on IBC cells SUM149, reporting a sustained activation of the ERK and AKT signals. These findings suggest a protective role of GPER on two IBC cell models and provide novel insight into the estrogen sensitivity of TN-IBC SUM149, which can guide future therapeutic efforts against GPER-positive IBC patients.

Dedication

To my mother **Carmen M. Soto González**, my father **Carl X. Bittman Diez**, and my brother **Carl F. Bittman Soto**, who are my greatest motivation.

To **Laura Mendez** and **Jesus Acevedo**, who shared their advice and encouragement throughout the process.

Acknowledgments

"Last but not least, I want to thank me."

"I want to thank me for believing in me, I want to thank me for doing all this hard work. I want to thank me for having no days off. I want to thank me for never quitting. I want to thank me for always being a giver and trying to give more than I receive. I want to thank myself for trying to do more right than wrong. I want to thank me for always being myself."   Snoop Dog

Table of Contents

Chapter 3: Results

List of Table

Table 1. Breast cancer subtypes and molecular characteristics

Table 2. List of GPER agonist and antagonist molecules

Supplementary data

Table S1. List of RT-qPCR primers

Table S2. Top 100 most statistically significant E2-regulated genes at 45 min

Table S3. Top 100 most statistically significant E2-regulated genes at 90 min

Table S4. Top 100 most statistically significant E2-regulated genes at 180 min

List of Figures

Supplementary data

List of Symbols and Abbreviations

AC	adenylyl cyclase
AKT	ak strain transforming
p-AKT	phosphorylated ak strain transforming
AP-1	activator protein 1
BC	breast cancer
BCL-2	b-cell lymphoma 2
CAF	cancer-associated fibroblast
cAMP	cyclic AMP
CDK	cyclin-dependent kinases
CK	cytokeratins
CREB	cAMP response element binding
DCIS	ductal carcinoma in situ
DUSP6	dual-specificity phosphatase 6
E2	17β-estradiol
EGFR	epidermal growth factor receptor
EGR1	early growth response protein 1
ER	estrogen receptor
ERα	estrogen receptor α
ERβ	estrogen receptor β
ERE	estrogen regulatory element
ERK1/2	extracellular regulated protein kinase
ETS	erythroblast transformation specific
EZR	ezrin
GAPDH	glyceraldehyde 3-phosphate dehydrogenase
GO	gene ontology
GPCR	G-protein coupled receptor

GPER	G-protein coupled estrogen receptor
GRV	growth rate value
HB-EGF	heparin-binding EGF-like growth factor
HER2/neu	human epidermal growth factor receptor 2
HIF1α	hypoxia-inducible transcription factor-1α
IBC	inflammatory breast cancer
IL-17	interleukin 17
MAPK	mitogen-activated protein kinase
MMP	matrix metalloproteinase
NF-κB	nuclear factor-kappa B
PCR	polymerase chain reaction
PI3K	phosphoinositide 3-kinase
p-ERK1/2	phosphorylated extracellular regulated protein kinase
PKA	protein kinase A
PR	progesterone receptor
qPCR	quantitative polymerase chain reaction
RAF	rapidly accelerated fibrosarcoma
RAS	rat sarcoma virus
RCV	relative cell viability
SDS-PAGE	sodium dodecyl-sulfate polyacrylamide gel electrophoresis
SERD	selective estrogen receptor dysregulator
SERM	selective estrogen receptor modulator
siRNA	small interfering RNA
SRC	steroid receptor coactivator
TF	transcription factor
TNBC	triple-negative breast cancer
TN-IBC	triple-negative inflammatory breast cancer
VEGF	vascular endothelial growth factor

Chapter 1: Introduction

1. Breast cancer

Breast cancer is the most common non-cutaneous cancer in women worldwide—and over 12% of all women in the United States are estimated to be diagnosed over their lifetime [1-2]. Breast cancer occurs almost entirely in women, but men can also be diagnosed with breast cancer. Breast cancer can start from different parts of the breast (e.g., lobules and ducts) and can further spread (metastasize) into the blood or lymph system, where the cancer cells can migrate to other body parts. It is estimated that 62% of breast cancer cases are confined to the breast at the time of diagnosis, while an additional 31% will have spread to regional lymph nodes. Still, not all women with cancer cells in their lymph nodes develop metastases, and some women with no cancer cells in their lymph nodes might develop metastases later. Only 6% of breast cancers are metastatic at diagnosis—defined as the involvement of sites distant from the breast and its regional lymph nodes [3].

Breast cancers are classified into subtypes based on the specific kind of cells affected in the breast. Most breast cancers are carcinomas, which are cancers that form in epithelial tissue. However, cancers such as ductal carcinoma in situ (DCIS) and invasive carcinoma are adenocarcinomas since cancer starts on the gland cells in the milk ducts or the lobules (milk-producing glands). Other cancers, like angiosarcoma or sarcoma, can grow in the breast but are not considered breast cancer since they start in different cells (e.g., connective tissues). The most common breast cancer histology is invasive ductal carcinoma (50-75% of patients), followed by invasive lobular carcinoma (5-15% of patients), mixed ductal/ lobular carcinomas, and other rare histology [4]. Screening mammograms detect half of the breast cancer cases in the United States,

and approximately one-third are diagnosed as palpable breast masses [5]. Palpable axillary mass, nipple discharge, nipple inversion, breast asymmetry, breast skin erythema, and breast skin thickening (peau d'orange) are fewer presentations of breast cancer [6].

Currently, metastatic breast cancer prevails as a near-fatal disease among nearly all affected patients—relying mostly on systemic therapy approaches. This can be administered preoperative (neoadjuvant), postoperative (adjuvant), or both. Local therapy modalities, such as surgery and radiation, are typically used for palliation only in metastatic disease. However, for nonmetastatic breast cancer, the main goals of therapy are eradicating tumors from the breast and regional lymph nodes and preventing metastatic recurrence. Local treatment for nonmetastatic breast cancer consists of surgical resection and sampling or removal of axillary lymph nodes, with consideration of postoperative radiation [7].

1.1 Stage and molecular subtyping of breast cancer

Cancer can be staged by its characteristics—such as the extent (size) of the tumor and the spread (metastasis) to distant sites. The stage is usually represented on a scale of 0 through IV. Stage 0 describes non-invasive cancers that remain within their original location, while stage IV describes invasive cancers that have spread outside the breast to other body parts [8]. However, in 2018, the cancer staging guidelines were updated to add other cancer characteristics, including the cancer cells' molecular composition. The breast cancer subtypes are commonly grouped into four categories based on the immunohistochemical expression (IHC) of hormone receptors: estrogen receptor-positive (ER+), progesterone receptor positive (PR+), human epidermal growth factor receptor positive (HER2+), and triple-negative (TNBC), which is characterized by

the lack of expression of any of the above receptor or by molecular subtyping by gene expression profiling (**table 1**). Ki-67 expression also characterizes the proliferation index (PI) of the cells—defined as the percentage of Ki-67-positive cells among the overall cell population.

Table 1. Molecular subtypes of breast cancer based on immunohistochemical characterization

	Luminales		HER2		Triple-negative	
Frequency	50%	15%	20%		15%	
Molecular type	**Luminal A**	**Luminal B**	**Luminal**	**Enriched**	**Non Basal-like**	**Basal-like**
Estrogen receptor	+++	++	++	-	-	-
Progesterone receptor	+++ (>20%)	+/-	+/-	-	-	-
HER2	-	-	+++	+++	-	-
CK 5/6	-	-	-	-	-	+++
EGFR	-	-	-	-	-	+++
Histological grade	I & II	II & III	III	III	III	III
Ki67	<14%	14-30%	>14%	High	High	High
Mutations		BRCA2		p53 (40-80%)		p53(100%) 85% of BRCA1
Histological forms	Tubular CA ICD low-grade UC					Poorly differentiated ICD, metaplastic and some with a better prognosis: medullary CA, adenoid-cystic, apocrine, fibromatosis-like, ect
Prognosis	Good	Intermediate	Intermediate	Bad	Bad	
Treatment	Hormone therapy	CT Hormone therapy	CT Herceptin Hormone therapy	Ct Herceptin	CT and others currently under investigation	
Chemotherapy (CT) response	Low	Intermediate	High	High	High	

The content of this table was obtained from table 1. at Horvath, E. et al., 2021 [188].

Breast cancer stage and molecular classification guides prognosis (outcome) predictions and potential responses to targeted treatments [10, 11]. The staging system classifies triple-negative breast cancer at a higher stage and most hormone receptor-positive breast cancer at a lower stage. Stage I breast cancers—defined anatomically as a breast tumor smaller than 2 cm and no lymph node involvement—have a 5-year overall survival rate of at least 99%, at least 94%, and at least 85% for HR+, HER2-amplified, and triple-negative subtypes, respectively [36]. Stage IV breast cancers have a median overall survival rate of approximately five years for HR+ or HER2-amplified subtypes and 1 year for triple-negative [12-15]. Some targeted therapies for all HR+ tumors include endocrine therapy (with some patients requiring chemotherapy), trastuzumab-based HER2-directed antibody therapy, and chemotherapy for all HER2-amplified or HER2-positive tumors chemotherapy alone for triple-negative breast cancers [2].

1.2 Triple-Negative Breast Cancer

About 10-15% of all breast cancer cases are classified as triple-negative breast cancers (TNBCs)—where cells lack the expression of ERα, PR, and HER2-amplification [16, 17]. TNBC accounts for more than 50% of all breast cancer mortality, and less than one-third of women with metastatic TNBC will survive a 5-year rate [18-21]. TNBCs are likely to occur in younger (~40 years old) women, and with black or Hispanic ethnicity [22]. TNBCs tend to have a more aggressive clinical course—growing (larger tumor size) and spreading (higher grade of lymph node involvement) at a much higher rate compared to other types of invasive breast cancers [20].

To date, TNBC patients report significantly higher death rates and fewer treatment options than ER-positive breast cancer [23]. Unfortunately, TNBC patients do not benefit from targeted

therapies such as tamoxifen or trastuzumab, which are directed against ERα and HER2, respectively. Instead, chemotherapy is generally administered to all patients with triple-negative breast tumors larger than 5 mm, even with negative axillary node involvement. Some specific targeted therapies for TNBC patients are bevacizumab—an agent that targets angiogenesis in TNBC patients with high levels of vascular endothelial growth factor (VEGF) [24], poly (ADP-ribose) polymerase (PARP) inhibitors—used in TNBC patients with BRCA gene mutations [25, 26], and cetuximab—an epidermal growth factor receptor (EGFR) inhibitor [27]. However, there is still an urgent need to develop novel targeted therapeutics for TNBC patients.

1.3 Inflammatory breast cancer (IBC)

Inflammatory Breast Cancer (IBC) is the most aggressive and highly metastatic form of breast cancer—with an overall 5-year survival rate of around 19% when metastasized [28, 29]. Unlike other breast cancer types, a palpable tumor mass is not typically present in IBC patients as the formation of tumor emboli instead marks the disease —cancerous cells forming a blockage in the lymph vessels of the skin of the breast [37]. As a result, the phenotype of IBC—including symptoms of breast enlargement, redness, itchiness, and "peau-d'orange" caused by erythema and edema [15, 31]—is often confused with the benign condition mastitis or other inflammatory conditions of the breasts (breast infection), leading to misdiagnosis. In addition, because of the high rate of metastases at presentation in IBC patients (approximately 30%), accurate initial staging is crucial to plan adequate systemic and locoregional treatment [32].

The current management of non-metastatic IBC includes neoadjuvant chemotherapy, ablative surgery—if a tumor-free resection margin is expected (in case of axillary lymph node

involvement combined with lymph node dissection), and locoregional radiotherapy in combination with peri-adjuvant trastuzumab and adjuvant hormone therapy in case of HER2 or ER/PR positive tumors, respectively. This multimodal therapeutic approach has significantly improved patient survival in recent years, which might, in part, be explained by more targeted therapy becoming available [33-36]. Nevertheless, IBC still has a poor outcome, with a median disease-free survival of fewer than 2.5 years and overall survival of 30–40% at five years [37]. The poor prognosis for IBC patients and the lack of targeted therapies emphasizes the need for a better understanding of the pathogenesis of the disease with the long-term goal of developing effective targeted therapeutics.

Regarding molecular composition, IBC cases are more frequently characterized as negative for hormone and growth receptors expression than non-inflammatory breast cancer (NIBC), associated with a more aggressive clinical course and decreased survival [38, 39]. Up to 83% of IBC tumors lack estrogen receptor (ER) expression compared with other locally advanced breast cancers—mainly classified as ER-positive [40]. However, research studies on IBC patients have identified the expression of novel estrogen receptors in IBC patients—including the G-protein coupled estrogen receptor (GPER). GPER is a seven-transmembrane receptor belonging to the G-protein coupled receptor (GPCRs) family reported to be expressed in 69% of IBC cancers [185]. GPER is known to regulate cellular and physiological responsiveness to estrogen in many breast cancers—including IBC. Therefore, despite the absence of canonical or classical ERα expression on IBC, hormone production still plays a role in IBC tumorigenesis. In addition, it may be possible to identify novel potential therapeutic targets through non-classical estrogen-dependent pathways—explained in more detail in **Fig. 3**.

Additionally, over 50% of IBC cases overexpress the epidermal growth factor receptor (EGFR), which plays an essential role in cell proliferation, survival, migration, and differentiation [42]. EGFR overexpression has been associated with a significantly worse 5-year overall survival rate compared to EGFR-negative IBC and an increased risk of IBC recurrence [43]. Furthermore, HER2—a transmembrane tyrosine kinase receptor involved in signal transduction pathways leading to cell growth and differentiation—has also been overexpressed in some IBC cases [44. Some studies using dual inhibitors of the EGFR and HER2 receptors (e.g., Lapatinib) in combination with neoadjuvant and adjuvant chemotherapy have shown significant improvement in pathological response in both breast tissue and axillary lymph nodes [45]. However, IBC patients continue to have a high risk of locoregional recurrence and, relatively early recurrence in the brain even when a complete pathological response is reached [46]. In addition, there is still no effective targeted therapy for patients with the triple-negative subset of inflammatory breast cancer—which accounts for 20-40% of IBC cases [47-49]. Thus, there is an urgent need to further characterize the molecular mechanisms associated with IBC aggressiveness and progression with the goal of identifying possible candidates for developing effective targeted therapeutics.

2. Estrogen Signaling in breast cancer

2.1 Estrogens

Estrogens are steroidal hormones that function as the primary female sex hormone. Estrogens are produced in the ovaries, but smaller amounts can also be made by other tissues such as the liver, adrenal glands, and mammary glands [50]. There are three primary forms of estrogen, namely estrone (E1), estradiol (E2), and estriol (E3). 17-β-estradiol (E2) is the

predominant estrogen in nonpregnant females, while estrone and estriol are primarily produced during pregnancy and following the onset of menopause [51], respectively. Previous studies have suggested that estrogens are associated with the development and growth of mammary, ovarian, and endometrial cancers [52, 53]. In addition, reproductive factors such as early menarche, late menopause, and late pregnancies are known to affect the risk of breast cancer through changing exposures of ovarian hormones—including 17-β-estradiol and progesterone (P4) [54].

17-β-estradiol has been linked to the initiation, development, and progression of breast cancer—via the activation of diverse estrogen receptors like ERα and ERβ. Upon activation, these nuclear ERs form dimers that bind to specific estrogen response elements (EREs) in the regulatory sequences and/or promoters of target genes to regulate their transcription—a process known as estrogen genomic signaling [2, 5-6]. An extensive profile of genes is known to be regulated by estrogen, some of which are protein-coding for transcription factors (e.g., JUN, FOS, MYC, and NR1B1), intracellular signaling molecules (e.g., BCL2, and HRAS), growth factors and hormones (e.g., IGF1, and TGF-α), membrane proteins, and proteases (e.g., CTSD) [55]. In addition, estrogen-responsive genes, including IGF1, cyclin D1, MYC, and Efp, are essential for cell proliferation and survival [56-57]. Some of these genes are assumed to directly mediate estrogen actions in normal tissues, cancer, and other diseases.

However, regulation of some of these genes in breast cancer cells appears insufficient to explain the estrogen actions behind tumorigenesis. Therefore, a genomic-wide comprehensive analysis for each breast cancer subtype is required to fully elucidate estrogen-regulated genes and signaling networks.

Furthermore, cellular responses to estrogen can also start at the plasma membrane, where ERs form protein complexes with many signaling molecules leading to rapid activation of cytoplasmic signal transduction cascades—known as estrogen non-genomic signaling [3, 17]. Estrogen non-genomic effects have been attributed to the increase of intracellular calcium concentration [58], activation of Gα and Gβ proteins [59], regulation of potassium channels, activation of MAPK cascades (e.g., SRC, ERK, and AKT), activation of lipid kinases (e.g., PI3K) and adenylate cyclase [60]. However, only a small fraction of ERs is associated with the rapid effects of E2 at the plasma membrane level, including some ERα-splices variants (e.g., ERα36 and ERα46) and the alternate estrogen receptor GPER. Therefore, a complete understanding of the mechanisms underlying the nongenomic estrogen signaling, with the aim of abrogating a specific step in the signaling pathway (signaling cascades), is a strategy that might lead to more targeted-treatment options for hormone dependent-breast cancer.

2.2 Estrogen receptors

2.2.1 ER-alpha (ERα) and splice variants

ERα, coded by the ESR1 gene, is a classical transcription factor that mediates the effect of estrogens in both standard and malignant mammary tissues. E2 binding to ERα leads to dimer formation and a series of conformational changes in the protein structure of ERα—which uncovers areas on the external surface of ERα responsible for the binding of coactivator molecules—facilitating gene transactivation in the nucleus. ERα and its regulated genes are significant drivers of about 70% of breast cancers and inhibition of ER signaling is the mainstay of ER-positive BC therapy and has substantially improved patient survival [3, 61].

Structurally, the classical ERα molecule contains 6 domains, named A to F, which can be functionally divided into a hormone-independent activation function (AF-1) region, the DNA binding domain (DBD), a hinge region containing three nuclear localization sequences (NLS) that mediate the translocation of the receptor from the cytosol to the nucleus, and a hormone-binding domain (HBD) on the C-terminus of the receptor possessing dimerization and hormone-dependent activation function (AF-2). However, two physiologically relevant splice variants of ERα have been identified and named ERα46 and ERα36—reflecting their molecular weight [62].

As seen in **Figure 1,** ERα46 and ERα36 are truncated in the amino-terminus (173 amino acids) and lack the first transcriptional activation domain (AF1). ERα46 is identical to ERα66 in the remaining protein sequence. ERα36 lacks the second transcriptional activation domain (AF2) and has a unique C-terminus. The ERα36 protein is identical to the full-length receptor in its DNA binding domain and part of its dimerization and ligand binding domains. Because ERα66 and ERα36 have different ligand binding domains, ERα36 may be capable of interacting with molecules different than ERα66—like G-1 for instance [64].

Notably, these ERα spliced variants are localized mainly in the plasma membrane and cytoplasm [65], where they bind to a diverse membrane or cytoplasmic signaling molecules such as the mitogen-activated protein kinase (MAPK) [66-67]—which initiate cell survival and proliferation signals. Additionally, these signaling molecules can phosphorylate the ERα and its co-regulators to augment nuclear ERα signaling [68]. Therefore, the genomic and non-genomic actions of ERs play a crucial role in breast epithelial cell proliferation and survival, as well as mammary tumorigenesis [68]. However, their contribution to estrogen signaling in many breast cancers remains elusive. Thus, an understanding of the tissue-specific expression of the various

estrogen receptors is necessary for identifying the individual functional roles that each may play under physiologic conditions.
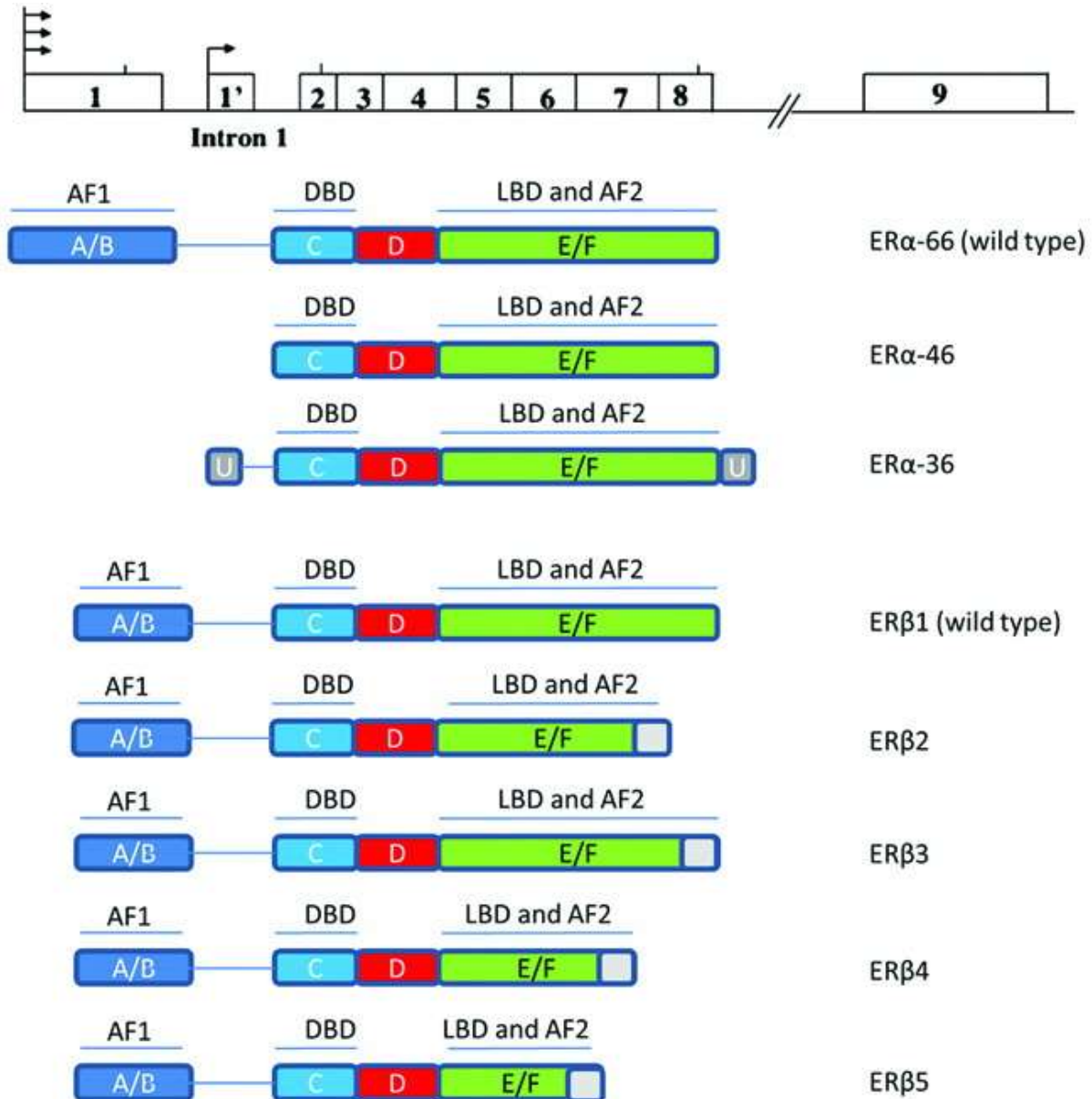
Figure 1. **Schematic representation of the different domains of the estrogen receptors**.
Only exons are shown in the Figure, except for (1) the intron between A/B and C domains, in which an alternative transcription initiation site has been reported; (2) intron 8, as exon 9 is included only in the sequence of ERα36. Grey boxes represent the alternative specific amino acid sequences for each isoform; in the sequence of the ERα36, this refers to the transcription of a novel exon 9 (shown in A), while in the ERβ isoform, it represents sequence differences in exon 8. Figure obtained from a review published by Kampa M, et, al. 2013 [63].

2.2.2 ER-beta (ERβ)

ER-beta (ERβ), coded by the ESR2 gene, has functions and expression patterns distinct from ERα. ERβ-specific effects on gene regulation can result from the modulation of ERα actions or differential gene regulation in the absence of ERα. ERβ, like ERα, can also modulate gene expression in a ligand-independent manner [4]. However, since ERα can also regulate most ERβ-targeted genes, the overall actions of ERβ on the genome of hormone-responsive cells depend mainly on the relative concentration of both ERs in the cell. In the normal mammary gland, ERβ is the most widely expressed ER, but its expression is known to decrease during malignant progression up to total absence in some invasive breast tumors [22]. Although the role of ERβ in breast cancer is still controversial, there is profound evidence from *in vitro* and *in vivo* studies that this receptor has tumor-suppressive properties. Various *in vitro* studies reported ERβ to suppress the growth and invasion of breast cancer cell lines [13-15].

2.2.3 G protein-coupled estrogen receptor 1 (GPER/GPR30)

GPER, also known as GPR30 or GPER, was discovered in human breast cancer tissue in 1996 [69] and cloned in 1997 via differential cDNA library analysis of the human breast adenocarcinoma cell lines MCF-7 (ER+) and MDA-MB-231 (TNBC) [70-71]. As a member of the G protein-coupled receptor (GPCR) family, and with a sequence of high homology to the interleukin 8 receptor and the angiotensin II receptor type 1 [70, 72], it was initially termed as a GPCR Class B receptor (GPCR-Br). However, chemokines and peptides treatment failed to evoke a response in GPR30 transfected cells [70, 73], which was later suggested as an orphan GPCR without cognate endogenous ligands and renamed GPR30. In 2005, different research groups provided

evidence demonstrating that E2 could directly bind to GPR30, suggesting it as a membrane-bound ER [72, 74-75]. Follow-up studies later confirmed that the GPER receptor is highly specific to E2 and related analogs [76] and could mediate a rapid non-genomic estrogen response in clonal cell-based experiments and was officially named GPER by the International Union of Basic and Clinical Pharmacology in 2007 [77].

2.2.3.1 GPER gene and protein

GPER gene is located on chromosome 7p22.3 and contains an open reading frame with a single exon of 1,125 bp that encodes a 375 amino acid receptor [69, 71]. GPER receptor is a multi-pass (7 transmembrane α-helical regions, 4 extracellular and 4 cytosolic segments) membrane protein from the G-protein coupled receptor 1 family—which expression and localization within the cell remain unclear to date. Several studies have reported that GPER is expressed both along the cell membrane surface and intracellularly within the endoplasmic reticulum and Golgi apparatus (78, 79). After several decades, it is recognized that although GPER expression exists within the cell membrane, the expression level is substantially less than the subcellular expression [79]. This has important implications for drug discovery in that GPER ligands may need to be lipophilic and able to cross the cell membrane to access the receptor.

2.2.3.2 GPER ligands and signaling

Recently developed genetic tools and chemical ligands have greatly facilitated researchers in determining the physiological roles of GPER in different tissues. However, there is a limited number of available GPER-specific ligands (**Table. 2**)—primarily attributed to a lack of

clarity in the localization and the complex pharmacology associated with GPER. For 17β-estradiol (E2), the estimated binding affinity to GPER is 3–6 nM [80-81], which is considerably higher as compared with its binding affinities for classical ERs (0.1–1 nM) [82]. Other 17β-estradiol-based steroids, such as estriol (E3), E3-sulfate (estriol-3-sulfate and estriol-17-sulfate), and estrone also interact with GPER [83-84]—and are known to function as GPER antagonists [85]. In addition, other estrogenic compounds—like genistein, quercetin, and bisphenol A—can directly bind to GPER and initiate non-genomic cellular responses in normal and cancer tissue [86-89]. In addition, classical Ers modulators and antagonists like tamoxifen, raloxifene, and fulvestrant act as GPER agonists [90-91]. The binding affinity and GPER-agonist properties of tamoxifen are believed to contribute to tamoxifen resistance in breast malignancy. Indeed, studies have indicated an increased expression of GPER in breast tumors with an acquired tamoxifen resistance [2].

In addition, the identification and synthesis of the highly selective GPER agonist, G-1 [92] has allowed the analysis of GPER-specific signaling pathways and actions in diverse cell contexts. Indeed, binding experiments reported that G-1 has a high affinity for GPER (Kd = 10 nM), but it also binds to Ers at concentrations of 10μM [93]. Two other novel GPER-specific agonists—GPER-L1 and GPER-L2—with binding affinities of about 100 nM have also been synthesized [94]. Moreover, it was reported that propyl pyrazole triol (PPT), usually used as Erα specific agonist, may also act as a GPER agonist at concentrations as low as 10–100 nM, while the Erβ specific agonist diarylpropionitrile (DPN) has no effects on GPER activity [95].

Table 2. **List of GPER agonist and antagonist**

Compound	Function	Binding affinity (Kd)	Comment	References
G1	Agonist	10nM	No binding to ERα/β at concentrations as high as 10 µM	96
G15	Antagonist	1uM	Minimal binding to ERα/β (Kd >10 µM)	97-98
E2	Agonist	3-6nM	Considerably higher for GPR30 as compared with classical ERs binding affinities (0.1–1 nM)	99-101, 103, 105-106
ICI182,780 (ICI); fulvestrant	Agonist	30-50nM	Selective ERα/β antagonist	102
Genistein	Agonist		Phytoestrogen belonging to the class of soy isoflavones	103-105
G36	Antagonist		Generated to restore the steric bulk of G-1 and the ER counter selectivity	107
GPER-L1 & L2	Agonist	100nM	Synthesized in 2012	108
MIBE	Antagonist		Reported to bind and block both ERα and GPER activity in breast cancer cells	109
Propyl pyrazole triol (PPT)	Agonist	10-100nM	Widely used ERα specific agonist	110
Diarylpropionitrile (DPN)	No effect	10uM	ERβ specific agonist	111
Dichlorodiphenyltrichloroethane (DDT)		2.8-10nM	Affinity depends on the isomer structure	112

Additionally, G-15 was found as a selective GPER antagonist by screening in a library of small molecules (NIH-MLSMR) [113]. G-15 is a synthetic substituted dihydroquinoline with a similar structure as G-1 but lacking the ethanone moiety of the molecule [93, 113]—as shown in **Figure 2**. G-15 shows a GPER binding affinity of 20 nM and only a minimal binding to ERs (Kd > 10 µM) [77]. G15 was tested in the GPER expressing breast cancer cells SKBr3 and could block calcium mobilization by E2 [114]. Restoring the steric bulk of G-1, another GPER-specific

antagonist, G-36, with an improved affinity to GPER, has also been developed [93]. G-1, G-15, and G-36 have now been used in over 150 publications to study the effects of GPER in systems from cells to tissues and organs to live animals [115].
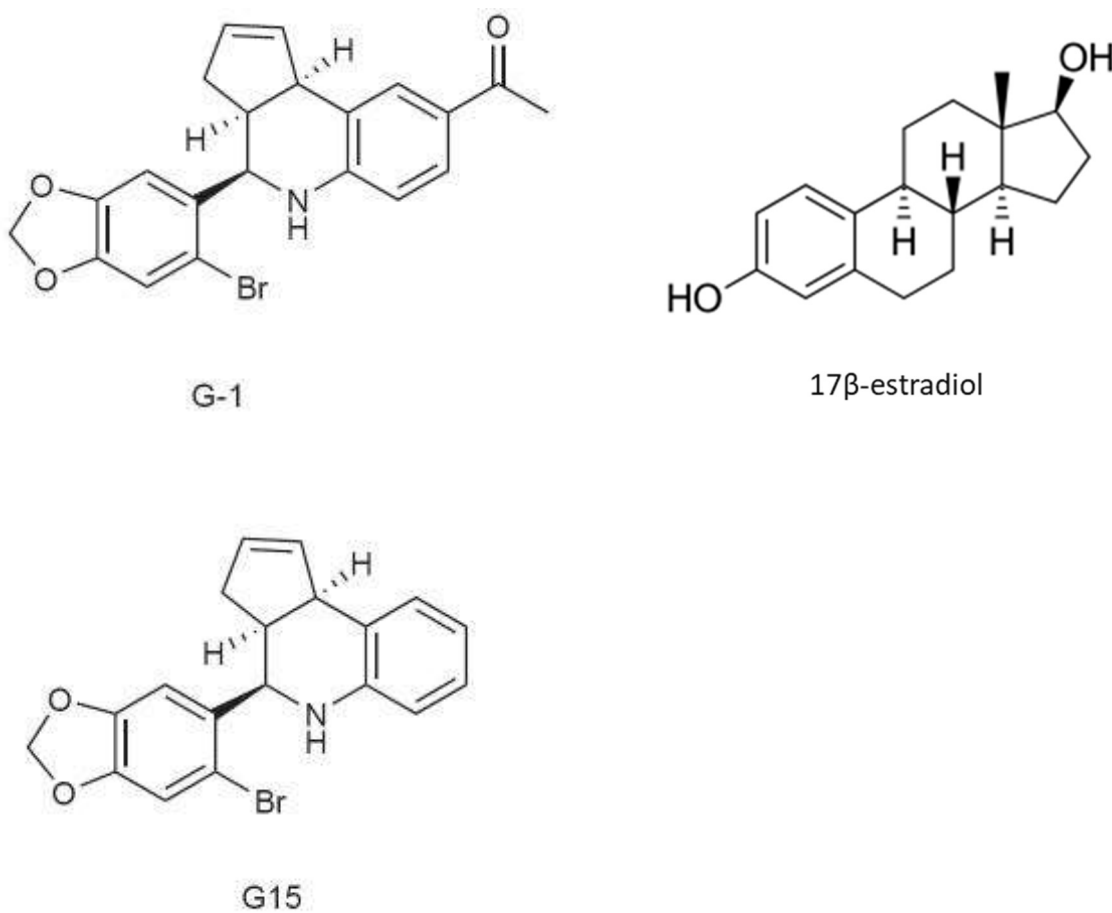
Figure 2. Molecular structure of G-1, 17β-estradiol, and G15. G15 molecular structure closely resembled the G-1 molecule but lacks the ethanone moiety present in G-1. Based on the structural overlap of G-1 with estrogen and the similar but not identical spacing of oxygen atoms at the extremes of the molecules, it is speculated that the ketone functionality of G-1 might play an important role as a hydrogen bond acceptor by inducing conformational changes that activate GPER [114].

Further experimental data have shown that in breast cancer cells the synthetic molecule MIBE (ethyl 3-[5-(2-ethoxycarbonyl-1-methylvinyloxy)-1-methyl-1Hindol-3-yl] but-2-enoate) might bind to and block both ERα and GPER activity—with an affinity for both receptors greater than 10 µM [94]. More recently, ERalpha17p–a peptide corresponding to part of the hinge region/AF2 domain of the human estrogen receptor α has been identified as a GPER inverse agonist (binds to the same receptor-binding site as the agonist) [82, 116]. ERalpha17p has shown anti-tumoral activity in breast cancer cells—including triple-negative breast cancers—and it is claimed as the first peptidic GPER disruptor [117-119].

Growing evidence has shown that activation of GPER in several cancer cells may induce the expression of diverse genes, like c-fos, cyclin D1, and CTGF—involved in critical biological effects, including cell proliferation and migration [87]. Moreover, GPER signaling triggers HIF-1α-dependent VEGF expression supporting its involvement in angiogenesis and progression of breast cancer [88]. Interestingly, estrogenic GPER activation can regulate the expression of the pro-inflammatory cytokine IL1β and its receptor IL1R1 in breast cancer cells, suggesting a positive feedback loop, which links the tumor microenvironment with tumor cells toward the progression of breast cancer [89]. In addition, GPER stimulation by G-1 is associated with cytoskeleton reorganization in human fibroblasts, such as re-organization of focal adhesion and changes in cell shape through activation of ERK1/2 signaling [120]. GPER—upon stimulation with E2, estrogenic compounds (e.g., genistein, hydroxytamoxifen), or G1—is associated with enhanced cancer cell proliferation in ER-negative breast cancer cells, and in the thyroid [121], endometrial [122], and ovarian cancer cells [123].

2.3 Estrogen signaling in ERα-negative breast cancer

Although TNBC cells do not express canonical Erα-66, they are estrogen-responsive via ERα-independent pathways. A recent study using a TNBC experimental metastasis model reported that estrogens promote the metastatic brain colonization of TNBC cells, while ovariectomy decreased the frequency of brain metastases of TNBC cells by 56% compared to estrogen supplementation—and the combination of ovariectomy and aromatase inhibitor letrozole further reduced the frequency of large lesions to 14.4% of the estrogen control [30]. Furthermore, it was demonstrated that increasing levels of circulating estrogens was sufficient to promote the formation and progression of TNBC [54]. Furthermore, the effects of estrogen were shown to act via a systemic increase in host angiogenesis, increasing mobilization and recruitment of bone marrow stromal-derived cells into sites of angiogenesis and to a growing tumor mass—suggesting that estrogen may promote the growth of ERα-negative breast cancers like TNBC by acting on cells distinct from the cancer cells to stimulate angiogenesis [54].

However, E2-induced effects in TNBC have been shown to also be antitumoral—by activating ERβ for example. ERβ is found in 30% to 60% of TNBCs and has been proposed as a tumor suppressor [144]. However, a recent study presented evidence that the tumor-suppressive functions of ERβ are severely compromised due to the downregulation of tethering partners of ERβ (Fos, Jun, Fra1) in TNBC [82, 124]. Thus, ERβ agonists are unlikely to be helpful for treating TNBC. Instead, there is the danger that at estrogen response elements, ERβ may be acting as ERα and increase proliferation [125].

GPER and other estrogen-related receptors (ERRs) are known to activate or modulate estrogen signaling in TNBC and thus are additional potential targets for the therapy of this cancer entity. Before the discovery of GPER, ERα36 had been suspected of mediating most of the extranuclear effects induced by estrogen. ERα36 is primarily located in the plasma membrane and is suspected of mediating the E2-mediated anti-apoptotic effects in TNBC, HCC38—and suggested as a potential target for therapy in TNBCs. ERα36 regulates estrogen non-genomic signaling by activating ERK and AKT in breast and endometrial cancer and is believed to be involved in EGFR-mediated carcinogenesis [126]. In addition, ERα36 has been proposed as an effector of GPER-dependent signals—suggesting a crosstalk between GPER and ERα36, which should be considered when assessing possible pathogenic and therapeutic questions related to the activation or inhibition of estrogen receptors [127-128].

Furthermore, the expression of GPER in estrogen-sensitive tumors has been associated with activating several cascade responses leading to critical biological events—like cell growth, migration, and angiogenesis [129-132]. The network of signal transduction pathways mediated by GPER also includes EGFR, PI3K/Akt cascades, calcium mobilization, and intracellular cyclic AMP production. In human breast cancer cells, the activation of MAPK/ERK signaling by E2-GPER involves the heterotrimeric G-proteins βγ-subunits and the cytosolic kinase src activation, suggesting the contribution of the heparin-bound EGF cleavage [133]—as shown in **Fig. 3**. Regarding this pathway, estrogenic GPER stimulation leads to the release of intracellular calcium from the endoplasmic reticulum and the consequent activation of integrin α5β1, which induces matrix metalloproteinase-dependent activation of the EGFR by the release of membrane heparin-bound EGF [14].

In this manner, estrogenic action via GPER coordinates the release of local EGF-related polypeptides and EGFR phosphorylation, which, activating STAT5 and MAPK/ERK pathways, induces cellular activities associated with cell survival [14]. Besides ERK activation, the transactivation of the EGFR by E2 also activates PI3K/Akt pathway [86]. It has also been reported that, in breast cancer cells, the estrogenic stimulation of GPER causes activation of the Gαs protein which, in turn, leads to adenylyl cyclase activation and cAMP accumulation [4,12].
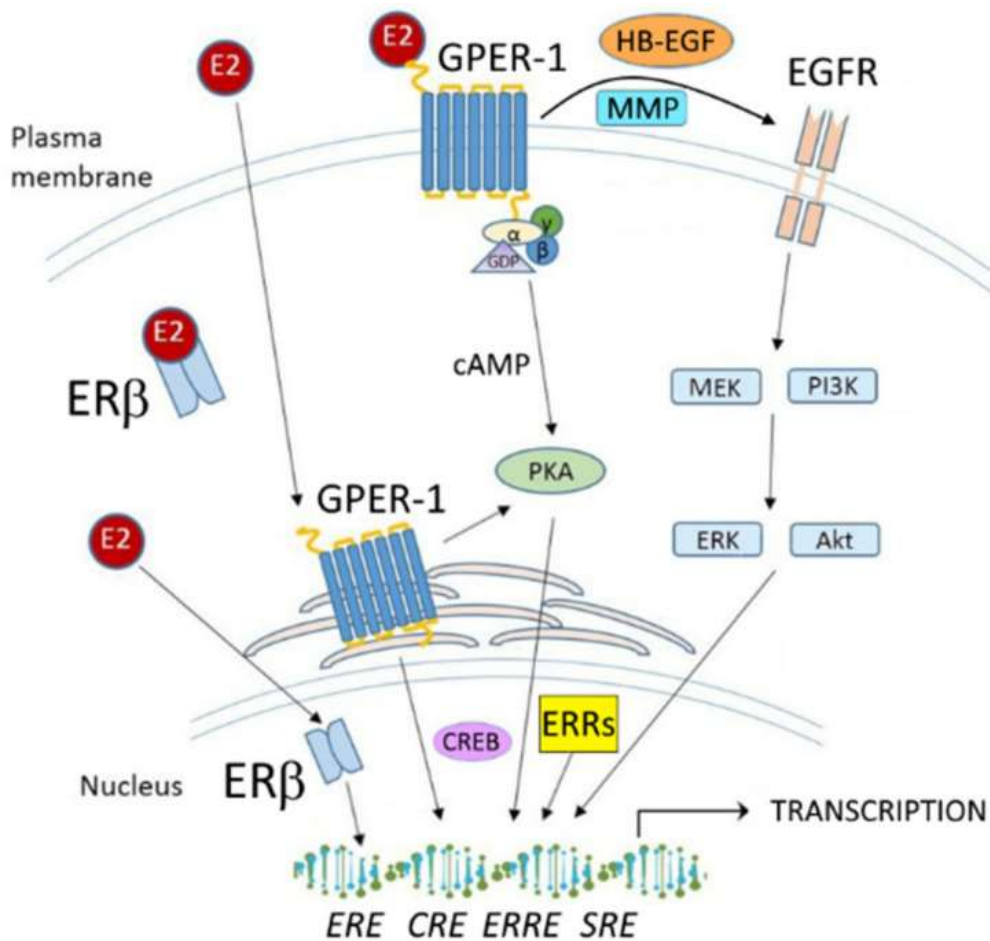
Figure 3. **Schematic overview of estrogen signaling in TNBC cells**. cAMP: cyclic adenosine monophosphate; PKA: protein kinase A; CREB: cAMP-response element binding protein; CRE: cAMP-response element; SRE: serum response element; MMP: matrix metalloproteinase; HB-EGF: heparin-binding EGF-like growth factor; EGFR: epidermal growth factor receptor; MEK: Mitogen-activated protein kinase kinase; ERK: extracellular signal-regulated kinase; PI3K: Phosphoinositide 3-kinase; AKT: Protein kinase B (PKB). Figure from Treeck te. At., 2020 [137].

2.3.1 GPER in Triple-negative IBC and non-IBC breast cancer

GPER is strongly expressed in TNBC cell lines—as reported in MDA-MB-468, MDA-MB-436, and other TNBC cell lines [135]. Treatment with E2, tamoxifen, and the GPER-specific agonist G1 is believed to lead to the rapid activation of ERK1/2 in TNBC and TN-IBC cells through the GPER signaling. The estrogen/GPER/ERK signaling pathway is known to be involved with increased cell growth, survival, migration, and invasion through upregulating the expression of cyclin A, cyclin D1, cyclin E, Bcl-2, and c-fos [136]—genes associated with the cell cycle, anti-apoptosis, and proliferation, respectively. Clinical studies have related GPER/ERK1/2 positivity with large tumor size and advanced stage, indicating that the GPER/ERK signaling might also contribute to the tumor progression in TNBC patients. Indeed, pretreatment with GPER antagonist G15, the ERK1/2 inhibitor U0126, or the transfection with the siRNA against the GPER has been shown to abolish these effects [137]. In addition, the enhancement of cell proliferation in TNBC cells MDA-MB-435 and HCC1806 was entirely inhibited by siRNA transfection against the GPER [136]—as well as the increased activity of the SRC kinase, EGFR transactivation, and c-fos expression.

Furthermore, a study on TNBC cells MDA-MB-231 showed evidence that estrogen binding to GPER can activate the MAP kinase pathways by triggering the release of heparin-binding EGF-like growth factor (HB-EGF), which in turn activates the EGFR signaling [138]. In addition, estrogen binding to GPER has been reported to stimulate adenylyl cyclase and cAMP production on TNBC—regulating the EGFR-induced MAPK phosphorylation [139]. Since the discovery of this GPER and growth factor receptor signaling crosstalk, it has been implied that ER-negative breast cancers might use this relationship to drive EGFR cellular responses—since the administration of EGFR-antagonist gefitinib inhibited estrogen non-genomic action mediated by GPER in TNBC cells

[128]. This experimental intervention is now suggested to be a potential therapeutic approach for GPER-expressing TNBC [42-43].

Furthermore, suppression of GPER protein was recently shown to reduce the metastatic behavior of TNBC cells by improving the anti-invasive efficacy of selective ERβ agonists and 4OH-tamoxifen sensitivity—suggesting a crosstalk between ERβ and GPER that could be a novel therapeutic approach for reducing cancer cell malignancy [140].

However, the exact role of GPER in TNBC is still controversial as some studies characterized this receptor as tumor-promoting, whereas others reported GPER as a putative tumor suppressor. The first studies suggesting GPER has tumor-suppressor in TNBC claimed that GPER agonist G-1 inhibits TNBC cell growth via induction of cell cycle arrest in the G2/M phase, enhanced phosphorylation of histone H3, and caspase-3-mediated apoptosis [62]. In another study using G-1 as a GPER agonist, GPER activation inhibited EMT and metastasis of TNBC cells via NF-κB signaling [86]. A further report on G-1 triggering GPER activation observed that after the trigger, there is significant inhibition of interleukin 6 (IL-6) and vascular endothelial growth factor A (VEGF-A)—resulting in the suppression of migration and angiogenesis of TNBC [87]. Moreover, E2 binding to GPER inhibited *in vivo* tumor growth and angiogenesis and reduced the expression levels of VEGF, NF-κB/p65, STAT3, and the endothelial marker CD34 in TNBC cell xenograft tumors [88]. Finally, a very recent report demonstrated the activation of GPER by E2 or G-1 to inhibit TNBC cell viability, proliferation, migration, invasion, angiogenesis, and EMT process [89].

The discrepancy in the role of GPER in some cancer cells is believed to be mainly associated with the contradictory effects seen after the use of G-1 [39]. For example, the G-1 has been shown to induce the phosphorylation of ERK1/2 in GPER-negative HEK293 cells stably transfected with ERα36 [141]—a variant of human ERα66. Additionally, the knockdown of ERα-36 in MDA-MB-231 and SKBr3 cells suppressed the phosphorylation of ERK1/2 and intracellular calcium mobilization stimulated by G-1, suggesting that G-1 also modulates ERα-36, and therefore it may not be specific for GPER [142]. Therefore, the role of GPER in breast cancer is believed to be tissue-specific, and a deep understanding of the estrogen nongenomic signaling effects of GPER in TN-IBC is imperative to elucidate these controversies. Studies on the protein level, including the use of specific GPER-antagonist molecules, are further needed to unravel the present discrepancy in the role of GPER in triple-negative and non-TN IBC breast cancer.

Characterizing the effects of estrogen and G15 on triple-negative Inflammatory Breast Cancer

Specific Aims

Up to 40% of IBCs are classified as TNBC—and the absence of ERα makes it challenging to treat with current endocrine therapy. There is evidence that estrogen promotes oncogenic phenotypes in TN-IBC cells, however, the transcriptome induced by estrogen and how these gene regulations affect TN-IBC migration and invasion phenotypes is far from clear. Alternate estrogen receptors such as GPER are believed to mediate estrogen-induced signals promoting cell migration and invasion enhancement— which brings the possibility to develop new targeted therapeutics for TN-IBC patients. Nonetheless, there is still a lack of evidence on whether GPER plays a significant role in mediating estrogen signaling in TN-IBC. Additionally, there is still a debate about whether GPER has a tumor-promoting or suppressor role in TNBC since the administration of the GPER-specific agonist G-1 has been shown to inhibit cell proliferation, induce G2 cell-cycle arrest in vitro, and suppress ER-negative breast cancer growth in vivo. Here, we hypothesize that GPER has a direct role in regulating estrogen-mediated signals leading to TN-IBC tumorigenesis progression. Therefore, the overall objective of this proposal is to define the biological processes and molecular functions associated with the actions of E2 on TN-IBC cell's aggressive phenotypes and to provide novel knowledge on the role of GPER in estrogen signals—which can be significant for the design of potential targeted therapeutics for TN-IBC cancers. This understanding will also be a significant step forward in the search for causes, prevention, and diagnosis for TN-IBC patients.

We accomplish these goals through the following aims:

AIM # 1: Characterize the transcriptional profile induced by estrogen on TN-IBC

Estrogen stimulus has been associated with gene expression changes associated with stemness and metastasis enhancement in TNBC (Wang, 2018). We hypothesize that estrogen signaling has an active role in the pathogenesis of TN-IBC and contributes to the formation or maintenance of IBC carcinogenesis. Therefore, after estrogen stimulation, RNA-seq analysis was performed on TN-IBC SUM149 cells to elucidate the estrogen-regulated genes and signaling networks.

AIM #2: Characterize the effects of GPER-specific antagonist G15 on the estrogen signals on TN-IBC

Several studies have shown that estrogen can exert nongenomic effects in IBC and non-IBC TNBCs leading to oncogenic behaviors enhancement—believed to be mediated by the expression of alternate estrogen receptors like GPER. We hypothesize that GPER has a direct role in estrogen-mediated signals in IBC cells—acting as a tumor promoter. The GPER-specific inhibitor G15 was used to identify the drug's effects on estrogen-mediated signaling cascade activation (ERK1/2 and AKT) and gene transcription regulations.

AIM #3: Identify the effects of G15 on IBC's oncogenic phenotypes

GPER expression positively correlates with tumor size progression, metastasis, and biological aggressiveness in TNBC. We hypothesized that G15 administration reduces TN-IBC's viability, growth rate, and migration phenotypes. We measured IBC cell viability, growth rate, migration, and three-dimensional (3D) colony formation after the administration of the specific GPER-antagonist G15 in the presence or absence of E2.

Chapter 2: Materials and Methods

General methods

    A. Cell culture

Breast cancer cell lines MCF7, MDA-MB-231, SUM149, and SUM190 were purchased from the American Type Culture Collection (ATCC). To guarantee the identity of the cell lines over the years, cells were expanded after purchase, and aliquots were stored in 10% DMSO/Fetal bovine serum (FBS) at 80^OC. Cells were cultivated in tissue culture treated plates (100 mm) at 37^OC in a humidified atmosphere with 5% CO2 in their corresponding media; MCF7 (DMEM, 10% FBS, and 1% Pen/strep), MDA-MB-231 (RPMI, 10% FBS, and 1% Pen/Strep), and SUM149 and SUM190 (F-12; Sigma N6658, 10% FBS, 1% Pen/strep, 0.1% hydrocortisone, and 0.05% Insulin). Cells were used for experiments until passage 7.

    B. Starving media and treatments

After the cells have reached the desired confluency, the growth media is removed, the cells are washed with HBSS 1X (Hank's Balanced Salt Solution), and the growth medium is replaced with phenol red-free DMEM/F12 medium (Sigma; D6434) supplemented with 1% charcoal-stripped FBS and 1% pen/strep to starve the cells. After 48 h, serum-starved cells are stimulated with DMSO (solvent; 0.2%), E2 (10 nM), and G15 (10 µM) alone and in combination with E2 in time points; final concentrations. G15 was used at a concentration of 10 µM since it is the IC:50 value reported in a dose-response curve performed on TN-IBC in our lab and because G15 has no binding abilities to other ERs (ERα and ERβ) at concentrations up to 10 µM.

C. RNA isolation, cDNA synthesis, and Reverse Transcription PCR (RT-qPCR)

Total RNA was purified using the RNeasy-kit (Qiagen, Cat. No 74104) following the manufacturer's protocol—followed by quantification using a Nanodrop spectrophotometer. For reverse transcription, 1 µg total RNA was transcribed using iScript Reverse Transcription Supermix (BioRad, Cat. No. 1708841) following the manufacturer's protocol. Real-time PCR reaction was performed using SYBR Green Mix (Bio-rad, Cat. #1725121). Cycling conditions were denaturation at 95°C for 2 min, followed by 35 cycles of 95°C for 15 s, 58°C for 30 s, and 72°C for 30 s. Optimal PCR conditions for each gene were ascertained. In brief, a 1:8 dilution of a 1 µg complementary DNA (cDNA) synthesis reaction was mixed with 400 nM of primers per group. Relative expression of the targeted genes was normalized to GAPDH, and results were expressed as fold changes ($2^{-\Delta\Delta Ct}$ method) or relative expression ($2^{-\Delta Ct}$) to control (vehicle). All the primers involved in this study were designed and synthesized by IDT (Integrated DNA Technologies, USA), and sequence information is listed in **Supplementary Table 1**. PCR products were separated on a 3% agarose gel in 0.5× TBE buffer at 100 V for 60 min. Gels were stained in ethidium bromide (3 µg/ml) for 30 min and photographed using Azure Imaging technology.

D. Cell extracts and immunoblotting

Cells were lysed for 10 min on 4°C using 1X Cell lysis buffer (Cell Signaling Technology, 9803S) supplemented with a phosphatase/protease inhibitors cocktail (Cell Signaling Technology, 5872S), and further harvested with a scraper. Cell lysates were cleared at 12,000g for 20 min at 4°C, and protein concentration was measured by BCA (Bicinchoninic acid assay) protein kit (Thermo Scientific, Cat. No. 23227). 30-40 µg of each sample were electrophoresed with 4-15% sodium sulfate-polyacrylamide gel electrophoresis (Mini-PROTEAN® TGX™ Precast Gel; Bio-Rad)

and transferred on PVDF-membrane sequentially. Then, the membrane was blocked for 1hr at room temperature with blocking/dilution buffer, constituted of 2.5% bovine serum albumin (BSA) dissolved in 1X TBST (0.1% Tween-20). The membrane was incubated with the primary antibody on a shaker overnight at 4℃. Primary antibodies were applied as follows: anti-phospho-ERK1/21/2 (Cell Signaling Technology, #4370; 1:1000), anti-ERK1/21/2 (Cell Signaling Technology, #4695; 1:2000), anti-phospho-AKT (Cell Signaling Technology, #4060), anti-AKT (Cell Signaling Technology, #9272; 1:1000), and anti-β-Tubulin (Cell Signaling Technology, #86298; 1:1000) anti-CDK2 (Cell Signaling Technology, #2546T;1:1000), anti-BCL-2 (Cell Signaling Technology, #15071T; 1:1000), anti-Cyclin E1 (Cell Signaling Technology, #4129; 1:1000), anti-GAPDH (Cell Signaling Technology, #2118; 1:1000), and anti-GPER (Abcam, #260033; 1:1000). All antibodies were diluted following the manufacturer's instructions. After three washes in 1X TBST, horseradish peroxidase-conjugated secondary antibodies for mouse IgG (Cell Signaling Technology, #7076; 1:10000) and rabbit IgG (Cell Signaling Technology, #7074; 1:10000) incubation was carried out at room temperature for one h. After 1X TBST wash (X3), protein bands were detected using a chemiluminescence reagent (ECL) on the Azure imaging system. The intensity levels of the bands were quantified using Image lab software (Bio-Rad, USA), and results were expressed as a relative expression if normalized with loading control (GAPDH or β-Tubulin) or as fold-change if normalized with the control group.

E. Immunocytochemistry

$1X10^4$ cells were cultured in a tissue-culture chamber slide and incubated at 37℃ in a humidified atmosphere with 5% CO2. After treatment (24 h), the cells are washed with PBS, fixed with 4% paraformaldehyde (10 min), permeabilized with 0.1% PBS-Tween (10 min), and then

blocked with 1% BSA/10% normal goat serum in 0.1%PBS-Tween for 1 h. Cells are then incubated overnight at 4°C with a rabbit anti-cleaved caspase-3 antibody (Cell signaling; #9661; 1:400), and anti-GPER (Abcam, #260033; 1:50). Cells are further incubated with Goat polyclonal Secondary Antibody to Rabbit IgG - H&L (Alexa Fluor® 594; ab150081) at 2 µg/ml for 1 h at room temperature in the dark. Nuclear DNA was labeled with DAPI (shown in blue). Images were taken in an inverted fluorescent microscope using a 40X objective and further analyzed by ImageJ.

F.   RNA sequencing analysis

RNA was sequenced using the Illumina NextSeq (2x75bp). The quality of the data was assessed using FastQC [71]. High-quality reads were aligned, annotated, and quantified to the human genome (HG38) using STAR and RSEM algorithms [72-73]. Gene expression analysis was performed in R statistical software (packages tximport and DESeq2). Gene ontology analysis, volcano plots, and bar graphs were performed in R statistical software (packages enrichR, ggplot2, dplyr, stringr, viridis, ggrepel, and tidyverse)

G.   Cell Viability and growth assay

Cell viability and proliferation assays for 17β-estradiol (E2) and G15 were performed on IBC cells pre-cultured for 48 h in a starving medium (phenol red-free medium supplemented with 1% charcoal-depleted serum). In brief, 10,000 cells/well were seeded into 96-well plates in a 200 µl starve medium containing DMSO (solvent; 0.2%), E2 (10 nM), G15 (10 µM), and a combination of E2 + G15; final concentrations. Cells were seeded in triplicates per treatment and grown for 1-3 days at 37°C, 5% CO_2, and saturated humidity. Cell number was determined by a colorimetric method using alamarBlue (Invitrogen, Cat. No A50101). Fluorescence was measured on a plate reader (Tecan Infinite 200 PRO) at a wavelength of 550 nm. Assays were performed at least three

times in triplicates. Results are presented as means ± standard deviations of three independent experiments. For growth rate measurements, we used the same data generated in the dose-response curve. We calculated GR values using the GR calculator program from Dr. Sorger's Lab at Harvard Medical School reference needed. GR values are presented as cell growth (GR > 1), partial cell growth inhibition (1 > GR >0), Cytostatic or cell cycle arrest (GR = 0), and Cytotoxic or cell death (GR < 0).

H. Wound-healing assay

In brief, TN-IBC SUM149 cells were cultured in their corresponding medium to 50-60% confluency, then transferred to starving media (phenol red-free medium supplemented with 1% charcoal-stripped FBS) for 48 h until cells reached a 100% confluency. The wound area was performed by scraping the monolayer culture in a straight line using 10 μl micropipette tip. Cells were further treated with E2 (10 nM) alone and in combination with G15 (6 μM), and DMSO (vehicle) for 19 h. An inverted microscope captured the closure of the wound area (200 x magnification). Wound-closure area measurements were analyzed using ImageJ software and GraphPad, with three pictures per group.

I. 3D Colony formation assay

A colony formation assay was performed through a 3D-culture technique using Matrigel. In brief, TN-IBC SUM149 cells (10,000 cells) were incubated for 2 h at 37°C in a 24-well culture plate previously exposed with Matrigel (30 min at 37°C). Then, a solution of 5% Matrigel with corresponding growth medium and G15 (10 μM) or DMSO (control) was applied to the different wells. The medium with the drug was changed every 2 days for 10 days. A full description of the protocol is presented in the protocol section. Finally, the area per pixel of approximately 150-200

colonies per well was counted for each treatment. The colony size was measured through ImageJ software. Extreme values were checked using quartiles to identify outliers and remove them from the data. Statistical analysis of 3 independent biological replicates per treatment was performed by GraphPad prism9 software by two-tailed Unpaired test-test.

I. Statistical analysis

Statistical computing and graphics were generated using R software environment and GraphPad prism 9. Results are mean + SD of three independent experiments, each performed in triplicates. Relative expression values were obtained after normalization with a reference gene, and fold changes were obtained after normalization to the control group. Student T-test and ANOVA analysis followed by Tukey or Dunnett were performed for multiple comparisons. Adj. P-values are presented as $*P < 0.05$; $**P < 0.01$; $***P < 0.001$; $****P < 0.0001$.

Chapter 3: Results

I. **Aim 1: Characterize the transcriptional signature induced by estrogen on TN-IBC**

A. *Transcriptional signature induced by E2 stimulus on TN-IBC*

Gene expression profiling helps scientists measure the activity of thousands of genes affected by a ligand's stimulus (e.g., estrogen), creating a global picture of cellular function. Here, differential RNA-Seq analysis was performed on TN-IBC SUM149 cells to identify the transcriptional signature induced by estrogen stimulus at time points (45, 90, and 180 min). Each time point consisted of three independent biological replicates. Principal Component Analysis (PCA) was performed for quality control of the experiment. PCA centers and scales the means of the data to unit variance, summarizing into two principal components: PC1 and PC2. PC1 is the line that represents the maximum variance direction in the data (also known as a score), while PC2 is oriented such that it reflects the second largest source of variation in the data (being orthogonal to PC1). Here, the values of variation for PC1 were 44% and 17% for PC2.

After differential expression analysis, statistically significant gene expression regulations were observed exclusively and commonly among the E2 time points (**Fig. 4B).** After 45 min, 211 genes were regulated by E2, where 19 were exclusive for that time point, 68 were shared with the 90 min group, and 19 shared with the 180 min group. At 90 min, 1,389 genes were regulated by E2, with 542 being exclusive to that time point, 68 shared with the 45 min group, and 573 shared with the 180 min group. The 180 min E2-treated group reported 4,527 genes regulated, where 3,587 were exclusive for that time point, and 19 and 573 were shared with the 45 min and the 90 min group, respectively. 86 genes were shared among all groups. In addition, 73% of all the genes with differential expression statistically significant were observed at 3 h of E2 stimulus.
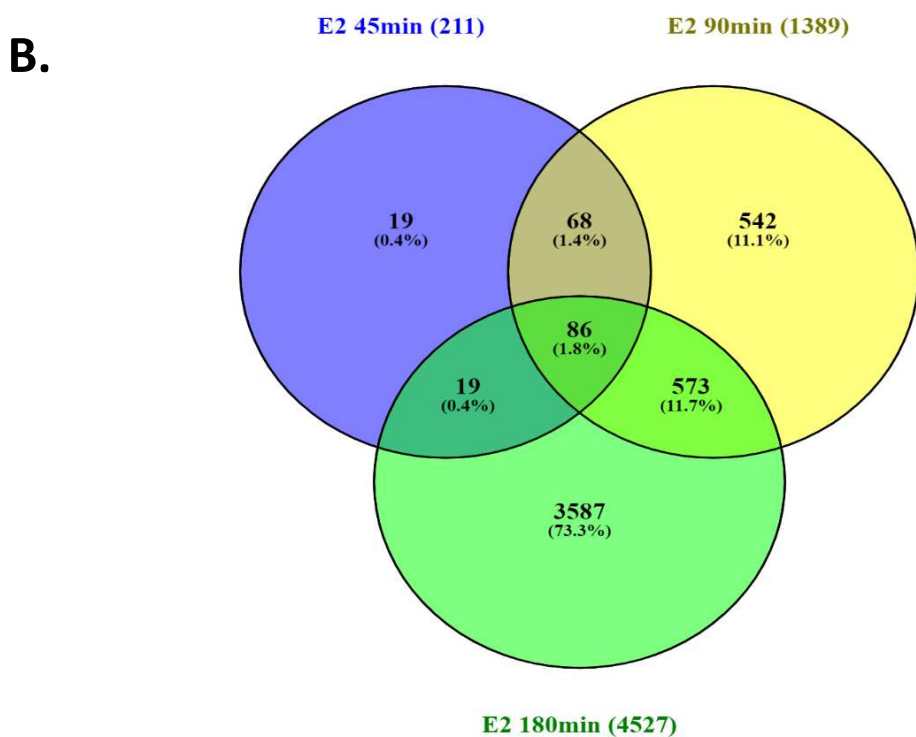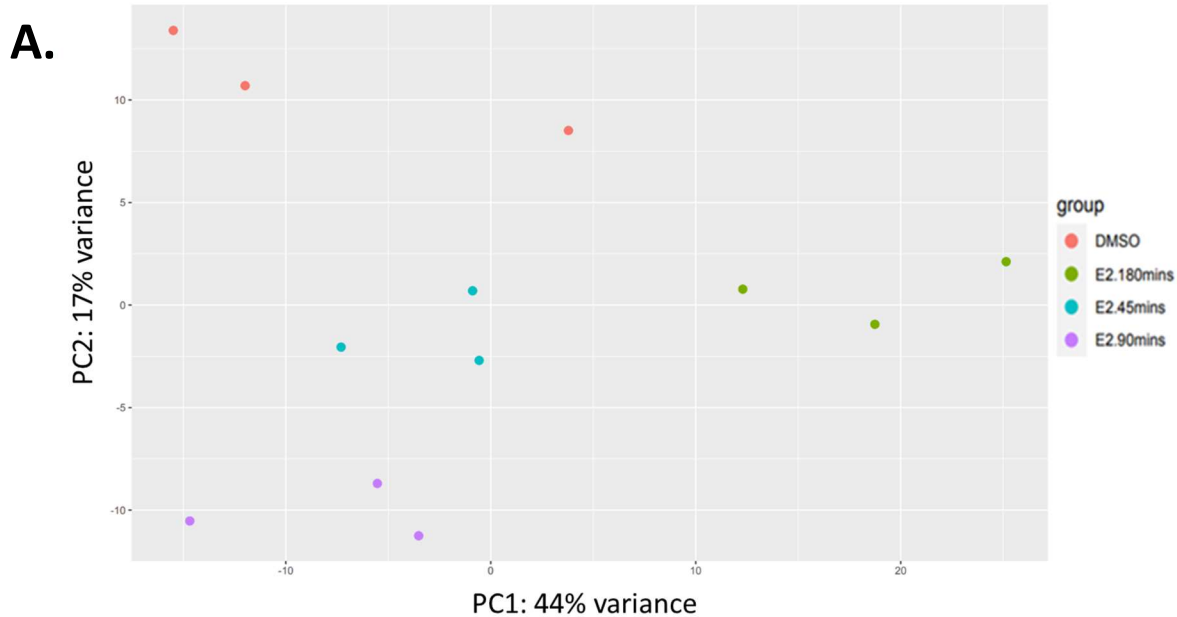
Figure 4. Quantification and differential expression of genes across E2 time points on TN-IBC.
(A) PCA plot with principal components (PCs) of transcription quantification for each time point. The first component (PC1) reported a 44% variation, and the second component (PC2) reported a 17% variation. (B) The Venn diagram shows the intersections of the E2-regulated genes across time points. Each circle contains the genes that had statistically significant (Adj. P-value < 0.05) expression differences relative to the control group (DMSO). E2 treatment significantly regulated the expression of 211 at 45 min, 1,389 at 90 min, and 4,527 at 180 min, relative to DMSO. Percentage value (%) represents the abundance of all the E2-regulated genes per group. Venny 2.01 interactive tool created the diagram (Olivero, J.C. 2015).

Furthermore, the genes with statistically significant (Adj. p-values < 0.05) differential expression for each time point of E2 treatment on our RNA-seq analysis were plotted in a volcano plot to identify the genes that were up and downregulated (**Fig. 5**). The volcano plot shows the statistical significance (-log10Adj. p-value) versus the magnitude of change (log2 fold change) for each gene. A log2 Fold Change (FC) > 0.58 was considered up-regulated, while log2FC < -0.58 down-regulated. Of the 211 genes reported on the E2-treated 45 min group, 106 were reported up-regulated, while 24 were down-regulated. The top five up-regulated genes were *CCN2* (log2FC 4.63), *KLF6* (log2FC 2.23), *CCN1* (log2FC 2.54), *JUN* (log2FC 3.52), and EGR1 (log2FC 3.73), while the top 5 down-regulated were CLK1 (log2FC -1.09), *STK36* (log2FC -0.62), *CLK4* (log2FC -0.76), *PTBP2* (log2FC -0.66), and *RPL32P3* (log2FC -0.86) **(Fig. 5A)**.

Of the 1,372 genes in the E2-treated 90 min group, 308 were up-regulated, while 270 were downregulated. The top five up-regulated genes were *CCN2* (log2FC 4.67), *CCN1* (log2FC 2,77), *KLF6* (log2FC 2.07), *CDKN1A* (log2FC 1.98), and *FOSL1* (log2FC 3.16), while the top 5 down-regulated were *CLK1* (log2FC -1.07), *RSRP1* (log2FC -1.04), *ARRDC3* (log2FC -1.38), *HERC2P3* (log2FC -1.01), and *RBM5* (log2FC -0.69) **(Fig. 5B)**. Furthermore, 1,125 of a total of 4,526 genes from the E2-treated 180 min group were reported to be up-regulated, while 608 were down-regulated. The top five up-regulated genes were *EZR* (log2FC 0.87), *PDLIM5* (log2FC 1.24), *S1PR3* (log2FC 1.12), *PGBD5* (log2FC 1.77), and *PALM2AKAP2* (log2FC 1.08), while the top 5 down-regulated were *EGR1* (log2FC -2.43), *GRHL2* (log2FC -0.71), *CUTALP* (log2FC -0.71), *PDE7A* (log2FC -1.11), and *CHROMR* (log2FC -0.76) **(Fig. 5C)**.
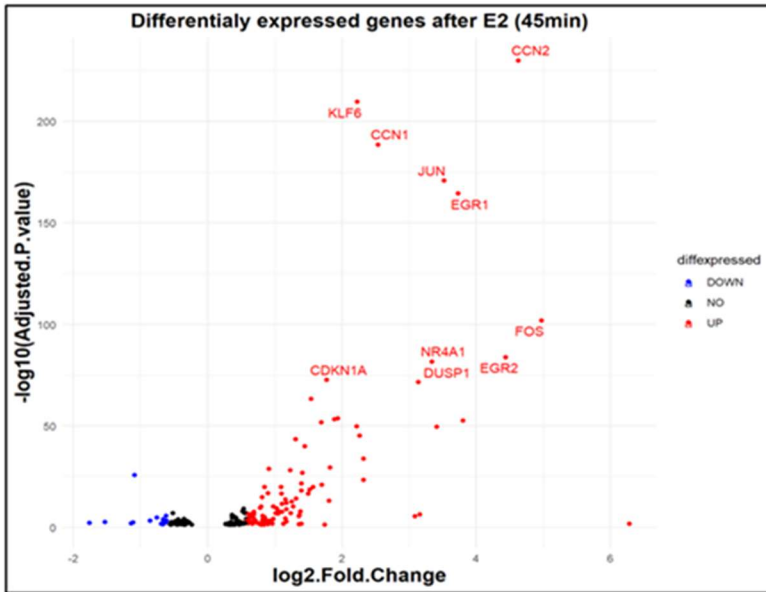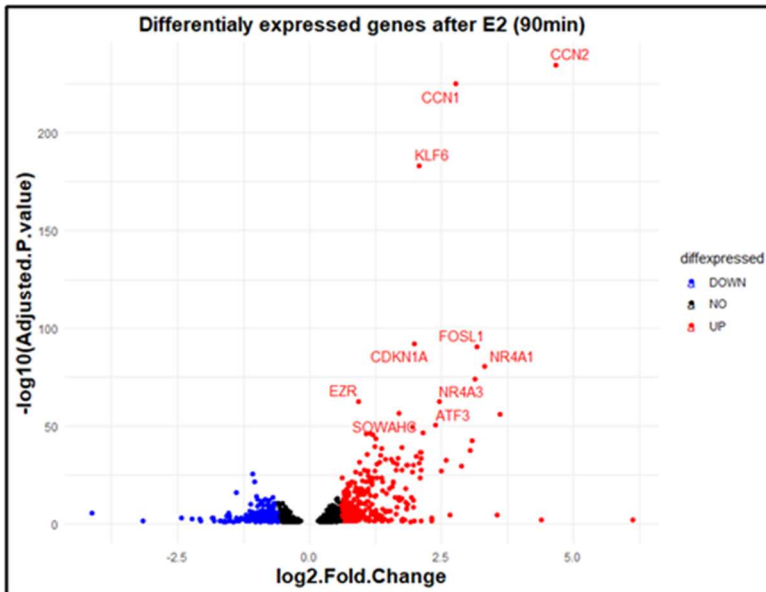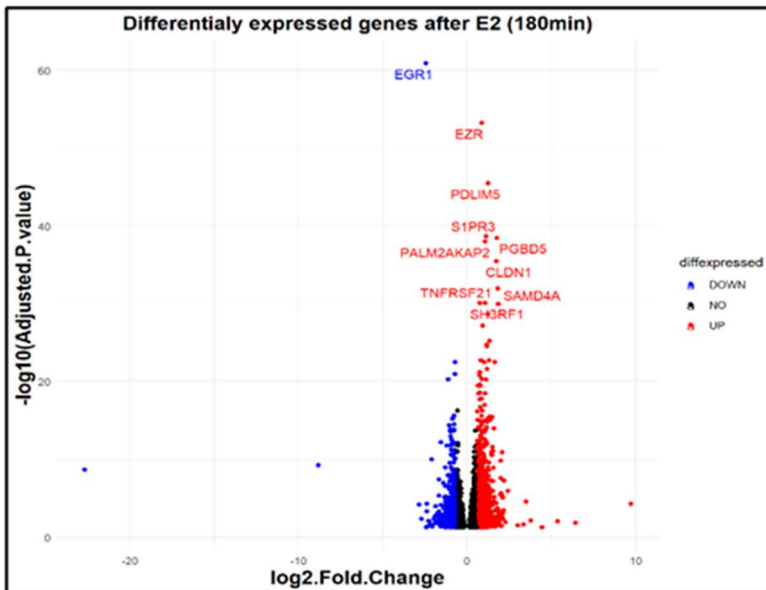
Figure 5. **Volcano plot of differentially expressed genes across E2 time points on TN-IBC**

Volcano plots presents the list of genes with statistically significant log2-fold changes after E2 treatment at the time point of 45 min (A), 90 min (B), and 180 min (C). Log2 Fold Change (FC) values > 0.58 were considered up-regulated (red), while log2FC < -0.58 down-regulated (blue). The plots were generated using R studio from the list of genes per group that reported statistical significance in differential expression (Adj. p-value < 0.05).

By RT-qPCR, we validated the upregulation in mRNA expression of *EGR1*, *HB-EGF*, and *DUSP6* induced by E2 (**Fig. 6)**. The Ct values for each set of primers were: GAPDH: 18, EGR1: 27, HB-EGF: 25, and DUSP6: 26. mRNA expression of the early-growth response 1 (*EGR1)* gene reported an E2-induced upregulation in a time-dependent manner when compared to the control group (DMSO), with a fold change of 1.7 + 0.1 (Adj. p-Value 0.003) at 45 min, 1.4 + 0.0 (Adj. p-Value 0.02) at 90 min, and 1.2 + 0.1 at 180 min (**Fig. 6A**). Furthermore, E2 stimulus on TN-IBC cells also induced the expression of the Heparin-binding epidermal growth factor-like growth factor (*HB-EGF*), with a fold change of 2.1 + 0.3 (Adj. p-Value 0.003) at 45 min, 3.2 + 0.2 (Adj. p-Value 0.0001) at 90 min, and 1.3 + 0.2 at 180 min (**Fig. 6B**). In addition, the mRNA expression of the dual-specificity phosphatase 6 (*DUSP6*) was regulated by E2 stimulus in a time-dependent manner, with fold changes of 1.5 + 0.02 at 45 min, 1.9 + 0.06 at 90 min, and 0.6 + 0.01 at 180 min when measured by RT-qPCR (**C**). Fold change values were obtained after normalization to the control group (DMSO).

A. Expression values reported on our RNA-seq analysis

Gene Symbol	E2 time-point	Fold Change	p-Value	Adj. p-Value
EGR1	45min	13.3	10.0E-169	3.3E-165
	90min	1.02	0.8	1.0
	180min	0.2	7.4E-66	1.2E-61
HBEGF	45min	2.6	1.7E-08	4.0E-06
	90min	3.8	1.7E-16	2.4E-14
	180min	1.4	4.9E-02	1.3E-01
DUSP6	45min	1.8	1.3E-06	2.3E-04
	90min	1.3	0.03	0.2
	180min	0.7	2.0E-02	6.8E-02

B. Expression values reported after RT-qPCR analysis:
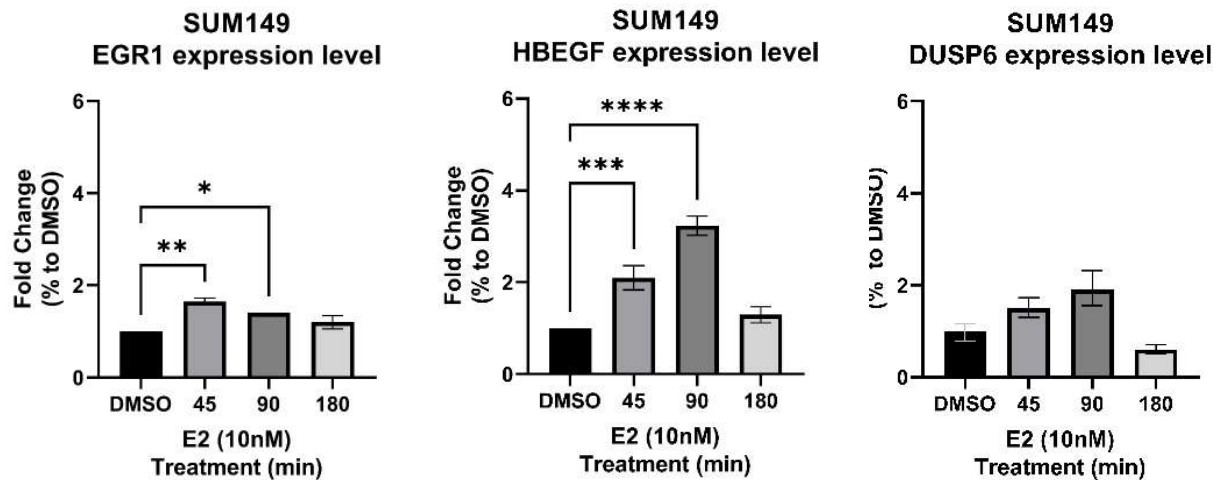
Figure 6. Real-time RT-PCR analysis of gene induction after E2 stimulus on TN-IBC
TN-IBC SUM149 cells were treated with E2 (10 nM) at 45, 90, and 180 min. (A) Fold changes and p-values of the RNA-seq analysis. Real-time RT-PCR relative quantified the mRNA expression of EGR1, HB-EGF, and DUSP6 to control (DMSO) (B). Results are mean $\pm$ SD of three independent cDNA samples. Fold change values were obtained after normalization to the control group (DMSO). Adj. P-values were calculated after an ordinary one-way ANOVA analysis with a Dunnett's multiple comparison test, represented as *P < 0.05; **P < 0.01; ***P < 0.001; ****P < 0.0001.

B. *Gene Ontology and enrichment analysis*

To date, gene ontology (GO) is an excellent tool for studying the potential function of thousands of genes. Using several gene ontology resources, we explored what kind of genes were regulated by E2 stimulus on TN-IBC SUM149. In addition, EnrichR is a web-based tool that allows the analysis of gene sets to identify statistically enriched terms and group them as clusters. The most statistically significant term within a cluster will represent the cluster. Here, we used a list of genes for each E2-treated group that had statistical significance (adj. p-value < 0.05) in differential expression after normalization with the control group (DMSO) and targeted them for enrichment analysis. We screened by GO and enrichment analysis in three aspects including the cellular component organization (CC), biological process (BP), and molecular function (MF).

Below are the top ten enriched terms for GO biological processes per gene list (E2-treated group per time points) with statistical significance (adj. p-value < 0.05) are listed below. The number of genes per enriched term is provided as an overlap. Visualization via graph plot is provided in **Fig. 7**.

GO term: Biological process, E2 45 min	Overlap	log10pValue
regulation of transcription by RNA polymerase II (GO:0006357)	66/2206	17.25
positive regulation of transcription, DNA-templated (GO:0045893)	43/1183	13.65
regulation of transcription, DNA-templated (GO:0006355)	60/2244	13.27
positive regulation of transcription by RNA polymerase II (GO:0045944)	35/908	11.78
cellular response to cytokine stimulus (GO:0071345)	24/482	10.35
negative regulation of transcription by RNA polymerase II (GO:0000122)	27/684	9.33
positive regulation of nucleic acid-templated transcription (GO:1903508)	23/511	9.07

negative regulation of transcription, DNA-templated (GO:0045892)	30/948	8.08
regulation of apoptotic process (GO:0042981)	26/742	7.92
positive regulation of fat cell differentiation (GO:0045600)	8/51	7.55

GO term: Biological Process, E2 90 min	Overlap	log10pValue
regulation of transcription by RNA polymerase II (GO:0006357)	305/2206	41.67
regulation of transcription, DNA-templated (GO:0006355)	291/2244	34.21
positive regulation of transcription, DNA-templated (GO:0045893)	146/1183	14.55
negative regulation of transcription by RNA polymerase II (GO:0000122)	99/684	14.13
positive regulation of transcription by RNA polymerase II (GO:0045944)	116/908	12.59
negative regulation of transcription, DNA-templated (GO:0045892)	119/948	12.38
regulation of epithelial to mesenchymal transition (GO:0010717)	23/76	9.81
regulation of gene expression (GO:0010468)	114/1079	7.37
negative regulation of MAPK cascade (GO:0043409)	22/94	7.14
regulation of cell differentiation (GO:0045595)	29/156	6.82

GO term: Biological process, E2 180 min	Overlap	log10pValue
positive regulation of transcription, DNA-templated (GO:0045893)	342/1183	9.86
ncRNA processing (GO:0034470)	82/201	9.54
ribosome biogenesis (GO:0042254)	79/192	9.43
rRNA metabolic process (GO:0016072)	69/162	9.09
rRNA processing (GO:0006364)	72/173	8.91
regulation of transcription by RNA polymerase II (GO:0006357)	573/2206	7.75
positive regulation of transcription by RNA polymerase II (GO:0045944)	262/908	7.57
negative regulation of transcription, DNA-templated (GO:0045892)	271/948	7.41
translation (GO:0006412)	79/214	6.94
regulation of transcription, DNA-templated (GO:0006355)	571/2244	6.41
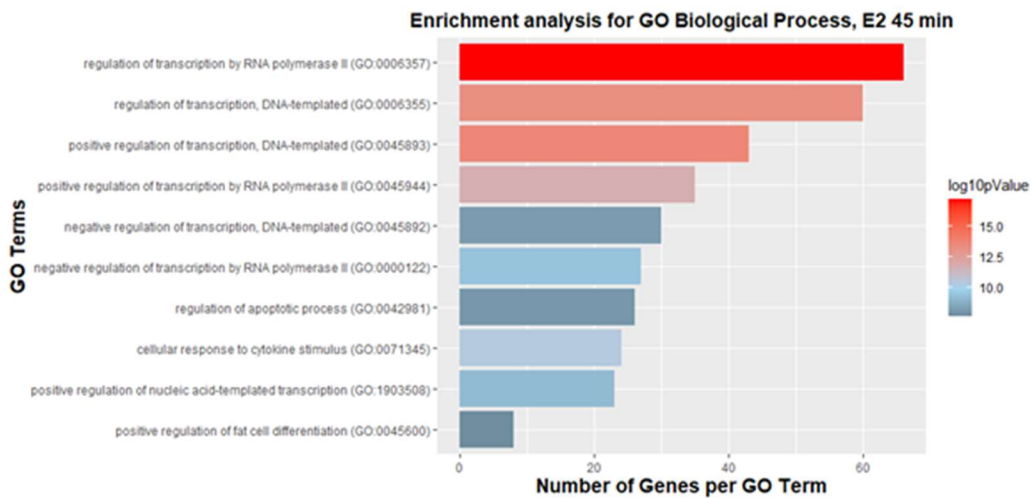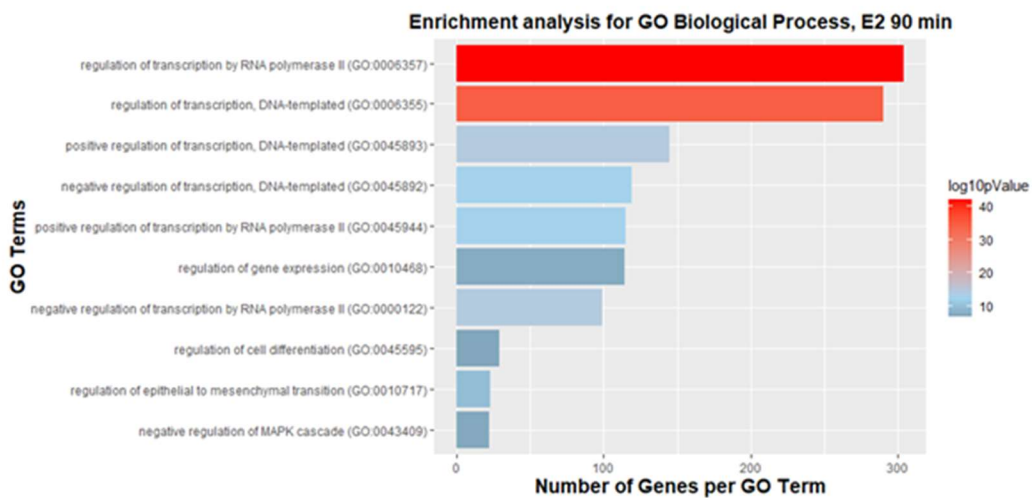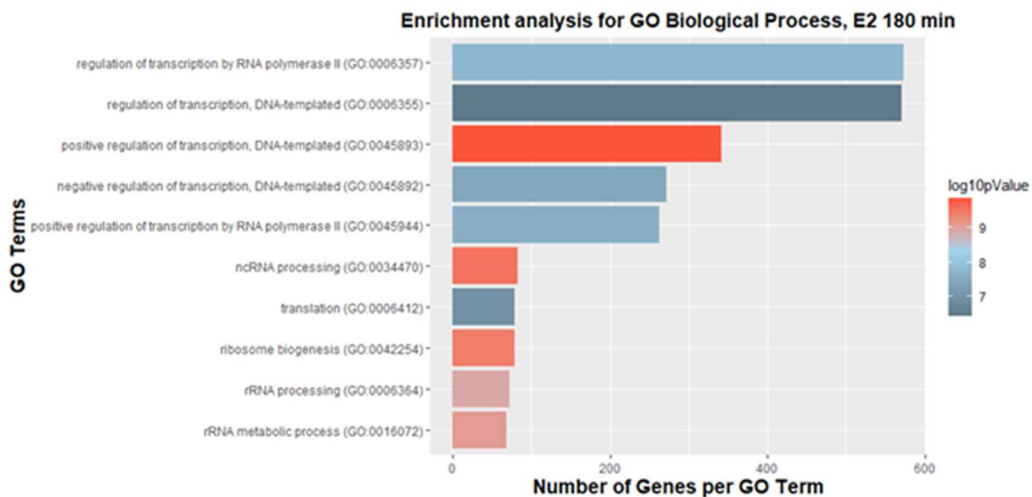
Figure 7. Top 10 GO biological processes terms associated with E2-regulated genes on TN-IBC. The EnrichR tool was used to identify the enriched Gene Ontology (GO) related to the list of genes that were significantly (Adj. p-value < 0.05) regulated by E2 treatment compared to the control (DMSO). The bar graph represents the top 10 detected terms of biological processes associated with E2-regulated genes in time points of 45 min (A), 90 min (B), and 180 min (C). The values at the X-axis represent the number of genes associated with a term, and the bars are colored based on the p-values.

Below are the top ten enriched terms for GO Molecular Functions per gene list (E2-treated group per time points) with statistical significance (adj. p-value < 0.05) are listed below. Visualization via graph plot is provided in **Fig. 8**. The number of genes per enriched term is provided as an overlap.

GO term: Molecular functions, E2 45 min	Overlap	log10pValue
sequence-specific DNA binding (GO:0043565)	36/707	15.79
sequence-specific double-stranded DNA binding (GO:1990837)	33/712	13.30
RNA polymerase II cis-regulatory region sequence-specific DNA binding (GO:0000978)	41/1149	12.73
cis-regulatory region sequence-specific DNA binding (GO:0000987)	41/1149	12.73
double-stranded DNA binding (GO:0003690)	29/651	11.27
RNA polymerase II transcription regulatory region sequence-specific DNA binding (GO:0000977)	42/1359	11.00
transcription regulatory region nucleic acid binding (GO:0001067)	14/212	7.74
DNA binding (GO:0003677)	26/811	7.15
RNA polymerase II-specific DNA-binding transcription factor binding (GO:0061629)	12/190	6.50
transcription cis-regulatory region binding (GO:0000976)	19/549	5.82

GO term: Molecular Function, E2 90 min	Overlap	log10pValue
RNA polymerase II transcription regulatory region sequence-specific DNA binding (GO:0000977)	208/1359	33.59
cis-regulatory region sequence-specific DNA binding (GO:0000987)	185/1149	32.57
RNA polymerase II cis-regulatory region sequence-specific DNA binding (GO:0000978)	183/1149	31.58
DNA-binding transcription activator activity, RNA polymerase II-specific (GO:0001228)	61/333	13.32
DNA-binding transcription repressor activity, RNA polymerase II-specific (GO:0001227)	49/256	11.54
transcription cis-regulatory region binding (GO:0000976)	77/549	10.40
sequence-specific double-stranded DNA binding (GO:1990837)	92/712	10.33
sequence-specific DNA binding (GO:0043565)	91/707	10.13
double-stranded DNA binding (GO:0003690)	80/651	8.04
transcription regulatory region nucleic acid binding (GO:0001067)	34/212	6.27

GO term: Molecular functions, E2 180 min	Overlap	log10pValue
RNA binding (GO:0003723)	428/1406	16.23
cadherin binding (GO:0045296)	129/322	13.89
protein kinase binding (GO:0019901)	165/506	8.80
kinase binding (GO:0019900)	152/461	8.52
purine ribonucleoside triphosphate binding (GO:0035639)	138/460	5.20
DNA-binding transcription factor binding (GO:0140297)	70/208	4.62
RNA polymerase II-specific DNA-binding transcription factor binding (GO:0061629)	65/190	4.58
ATP binding (GO:0005524)	86/278	3.98
ribosomal large subunit binding (GO:0043023)	912/2022	3.98
ubiquitin-like protein ligase binding (GO:0044389)	87/282	3.98
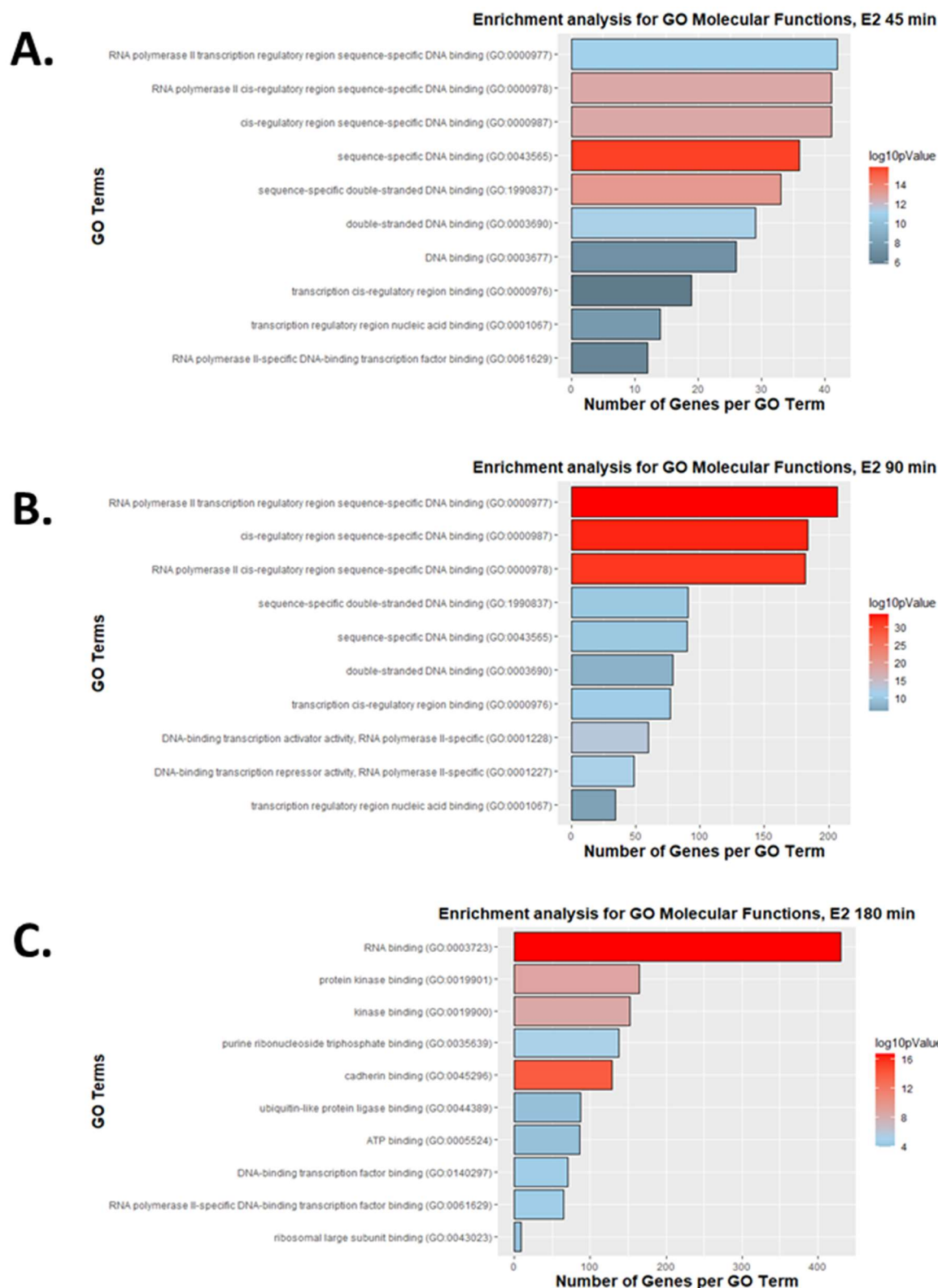
Figure 8. Top 10 GO molecular function terms associated with E2-regulated genes on TN-IBC
The Enrichr tool was used to identify the enriched Gene Ontology (GO) related to the list of genes that were significantly (Adj. p-value < 0.05) regulated by E2 treatment compared to the control (DMSO). The bar graph represents the top 10 detected terms of molecular functions associated with E2-regulated genes in time points of 45 min (A), 90 min (B), and 180 min (C). The values at the X-axis represent the number of genes associated with a term, and the bars are colored based on the p-values.

Below are the top ten enriched terms for GO Cellular components per gene list (E2-treated group per time points) with statistical significance (adj. p-value < 0.05) are listed below. Visualization via graph plot is provided in **Fig. 9**. The number of genes per enriched term is provided as an overlap.

GO term: Cellular components, E2 45 min	Overlap	log10pValue
nucleus (GO:0005634)	92/4484	14.27
intracellular membrane-bounded organelle (GO:0043231)	94/5192	11.23
cytoplasmic side of plasma membrane (GO:0009898)	41/1955	2.72
CD40 receptor complex (GO:0035631)	211/2022	2.32
P-body (GO:0000932)	41/1980	2.13
keratin filament (GO:0045095)	215/2022	2.05
clathrin-coated endocytic vesicle membrane (GO:0030669)	31/1969	1.54
clathrin-coated endocytic vesicle (GO:0045334)	31/1985	1.31
tight junction (GO:0070160)	31/1985	1.31

GO term: Cellular components, E2 90 min	Overlap	log10pValue
nucleus (GO:0005634)	443/4484	25.21
intracellular membrane-bounded organelle (GO:0043231)	480/5192	21.27
nucleolus (GO:0005730)	74/733	4.30
nuclear lumen (GO:0031981)	74/745	4.08
prespliceosome (GO:0071010)	515/2022	2.75
U2-type prespliceosome (GO:0071004)	515/2022	2.75
intracellular non-membrane-bounded organelle (GO:0043232)	97/1158	2.54
cell-substrate junction (GO:0030055)	39/394	2.40
cell-cell junction (GO:0005911)	29/271	2.38
focal adhesion (GO:0005925)	38/387	2.30

GO term: Cellular components, E2 180 min	Overlap	log10pValue
intracellular membrane-bounded organelle (GO:0043231)	1346/5192	19.93
nucleus (GO:0005634)	1177/4484	18.79
focal adhesion (GO:0005925)	155/387	16.55
cell-substrate junction (GO:0030055)	157/394	16.51
intracellular non-membrane-bounded organelle (GO:0043232)	348/1158	12.36
mitochondrial inner membrane (GO:0005743)	118/328	9.22
organelle inner membrane (GO:0019866)	123/346	9.21
nucleolus (GO:0005730)	220/733	7.93
nuclear lumen (GO:0031981)	221/745	7.50
mitochondrial membrane (GO:0031966)	149/469	7.20
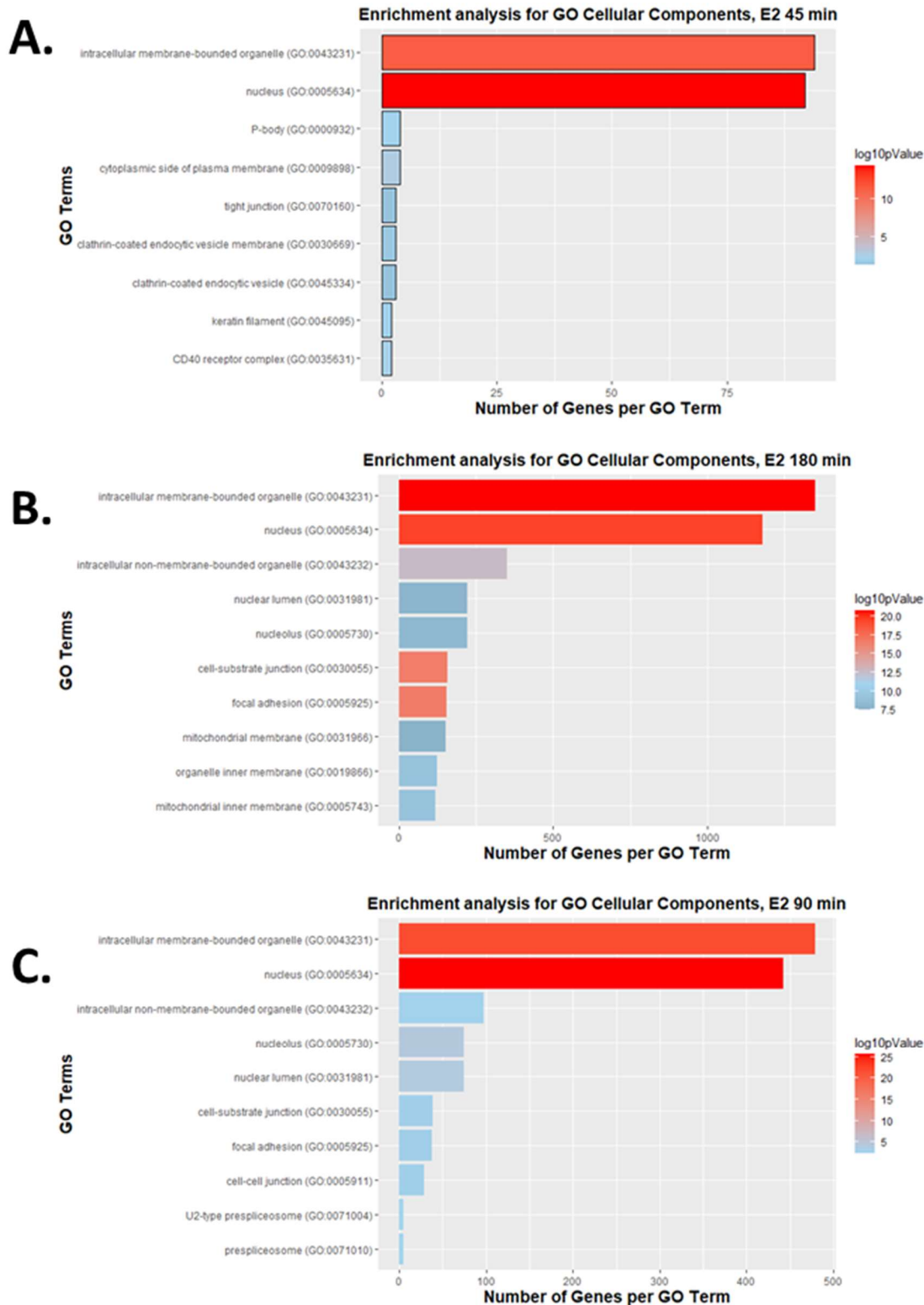
Figure 9. Top 10 GO cellular component terms associated with E2-regulated genes on TN-IBC
The EnrichR tool was used to identify the enriched Gene Ontology (GO) terms associated with the list of genes that were significantly (Adj. p-value < 0.05) regulated by E2 treatment compared to the control (DMSO). The bar graph represents the top 10 detected terms of cellular components associated with E2-regulated genes in time points of 45 min (A), 90 min (B), and 180 min (C). The values at the X-axis represent the number of genes associated with a term, and the bars are colored based on the p-values.

We also search KEGG pathways databases to identify the most significant E2-regulated pathways at each time point. Top ten KEGG pathways per gene list (E2-treated group per time points) with statistical significance (adj. p-value < 0.05) are listed below. Visualization via graph plot is provided in **Fig. 10**. The number of genes per enriched term is provided as an overlap.

GO term: KEGG pathways, E2 45 min	Overlap	log10pValue
IL-17 signaling pathway	13/94	11.22
Colorectal cancer	10/86	8.00
MAPK signaling pathway	16/294	7.57
TNF signaling pathway	10/112	6.89
C-type lectin receptor signaling pathway	9/104	6.14
Pathways in cancer	19/531	6.03
Apoptosis	10/142	5.93
Human T-cell leukemia virus 1 infection	12/219	5.84
Hepatitis B	10/162	5.41
FoxO signaling pathway	9/131	5.30

GO term: KEGG pathways, E2 90 min	Overlap	log10pValue
Herpes simplex virus 1 infection	84/498	15.91
TNF signaling pathway	25/112	7.58
NF-kappa B signaling pathway	22/104	6.32
IL-17 signaling pathway	20/94	5.85
C-type lectin receptor signaling pathway	21/104	5.71
FoxO signaling pathway	24/131	5.64
Colorectal cancer	18/86	5.22
Legionellosis	14/57	5.03
p53 signaling pathway	16/73	4.97
AGE-RAGE signaling pathway in diabetic complications	19/100	4.83

GO term: KEGG pathways, E2 180 min	Overlap	log10pValue
Pathogenic Escherichia coli infection	79/197	8.80
Chronic myeloid leukemia	40/76	8.72
Salmonella infection	92/249	7.99
Alzheimer disease	122/369	7.05
Adherent junction	35/71	6.78
Yersinia infection	56/137	6.77
Pancreatic cancer	35/76	5.89
Non-alcoholic fatty liver disease	59/155	5.86
Endometrial cancer	28/58	5.33
Kaposi sarcoma-associated herpesvirus infection	68/193	5.25
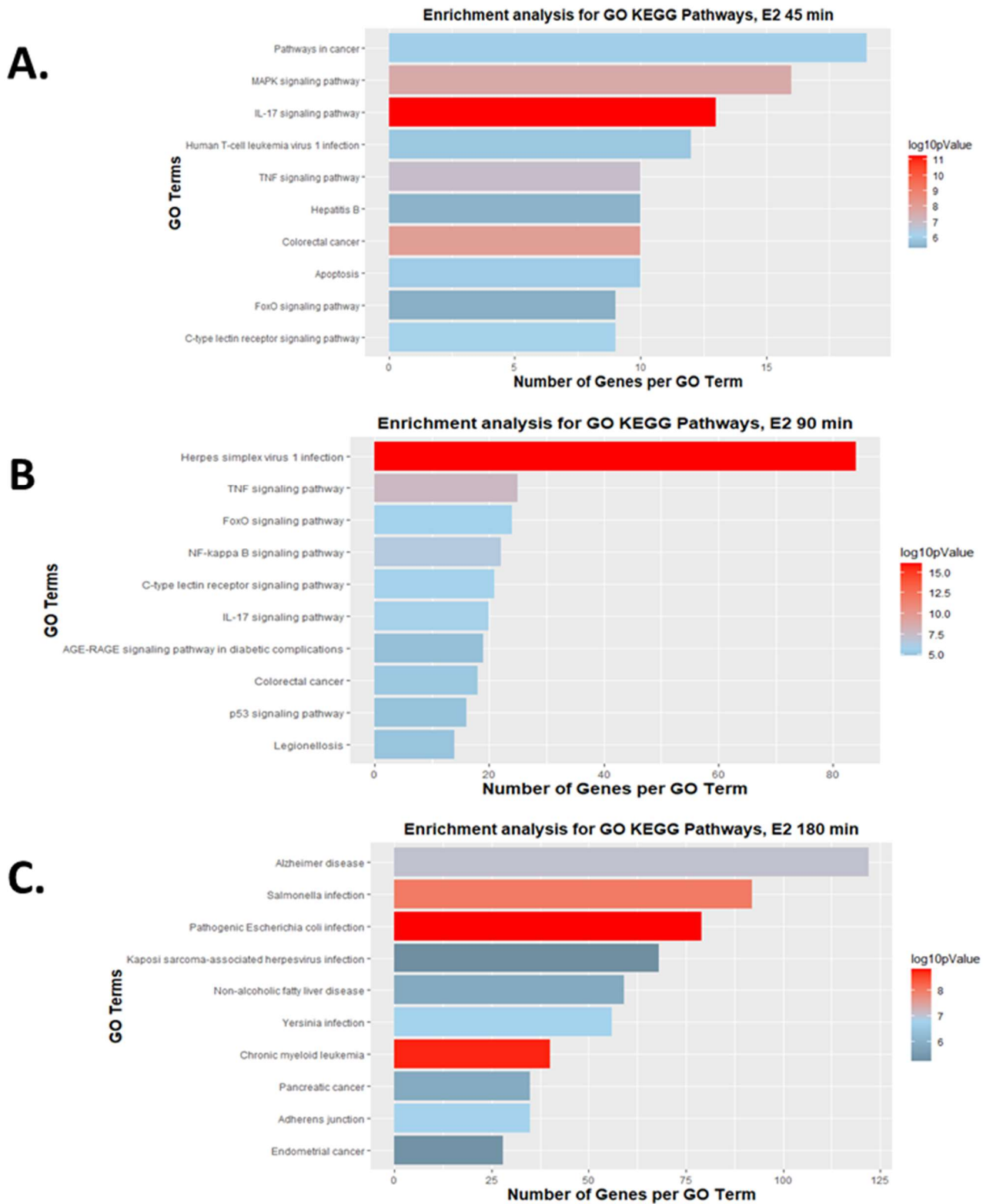
Figure 10. Top 10 KEGG pathways associated with E2-regulated genes on TN-IBC. The EnrichR tool was used to identify the enriched Gene Ontology (GO) terms related to the list of genes that were significantly (Adj. p-value < 0.05) regulated by E2 treatment compared to the control (DMSO). The bar graph represents the top 10 detected terms of KEGG Pathways associated with E2-regulated genes in time points of 45 min (A), 90 min (B), and 180 min (C). The values at the X-axis represent the number of genes associated with a term, and the bars are colored based on the p-values.

II.   **Aim #2: Characterize the effects of G15 on the estrogen genomic and non-genomic signaling pathway in TN-IBC**

A. G15 dysregulates the expression of genes upregulated by estrogen

E2 stimulus has been shown to up-regulate the expression of the early growth response-1 (*EGR1*) gene through the GPER/ERK1/2 signaling in various breast cancer cell lines [144]. Here, E2 treatment up-regulated the expression of *EGR1* on our RNA-seq and was further validated by RT-qPCR analysis—with a fold change of 1.7 $\pm$ 0.1 (Adj. p-Value 0.003) at 45 min, 1.4 $\pm$ 0.0 (Adj. p-Value 0.02) at 90 min, and 1.2 $\pm$ 0.1 at 180 min when measured by RT-qPCR (**Fig. 11A**). However, after cells were pre-treated with G15 (10μM; 1hr) and further stimulated with E2 (10nM) for 90 min, the fold changes on *EGR1* expression compared with control (DMSO) were: 1.2 $\pm$ 0.28 on E2, 1.5 + 0.07 on G15 alone, and 4.3 $\pm$ 1.48 (Adj. p-Value 0.005) on E2 + G15 (**Fig. 11B**).

Furthermore, a previous research study on TNBC cell line MDA-MB-231 showed that the activation of some estrogen-induced non-genomic signaling cascades (e.g., MAPK/ERK1/2 signaling) required the expression of GPER and transactivation of the epidermal growth factor receptor (*EGFR*) by Heparin-binding epidermal growth factor-like growth factor (HB-EGF) [145-147]. Interestingly, our RNA-seq analysis reported an E2-induced upregulation of the HB-EGF mRNA expression in TN-IBC SUM149 cells, which was further validated by RT-qPCR with a fold change of 2.1 $\pm$ 0.3 (Adj. p-Value 0.003) at 45 min, 3.2 $\pm$ 0.2 (Adj. p-Value 0.0001) at 90 min, and 1.3 $\pm$ 0.2 at 180 min (**Fig. 11C**) when compared to control. However, after cells were pre-treated with G15 (10 μM; 1hr) and further stimulated with E2 (10 nM) on time points, the fold changes on HB-EGF expression compared with control (DMSO) were: 1.7 $\pm$ 0.13 (Adj. p-Value 0.0281) at

45 min, 3.7 ± 0.10 (Adj. p-Value 0.0002) at 90 min, and 4.5 ± 0.26 (Adj. p-Value <0.0001) at 180 min (**Fig. 11D**).

Moreover, since the ERK1/2 signaling activation is dictated by the coordinated activities of protein kinases and phosphatases, we sought to identify the effect of G15 on the expression of the known MAPK phosphatase DUSP6—which acts as a feedback regulator attenuating the MAPK/ERK1/2 signaling [148]. On TN-IBC SUM149, we identified an E2-induced upregulation of DUSP6 expression on our RNA-seq analysis which RT-qPCR further validated—with fold changes of 1.5 ± 0.02 at 45 min, 1.9 ± 0.06 at 90 min, and 0.6 ± 0.01 at 180 min when measured by RT-qPCR (**Fig. 11E**). However, after cells were pre-treated with G15 (10μM; 1hr before E2) and further stimulated with E2 (10nM) on time points, the fold changes on DUSP6 expression compared with control (DMSO) were: 0.9 ± 0.05 at 45 min, 0.9 ± 0.03 on 90 min, and 1.4 ± 0.07 at 180 min (**Fig. 11F**).
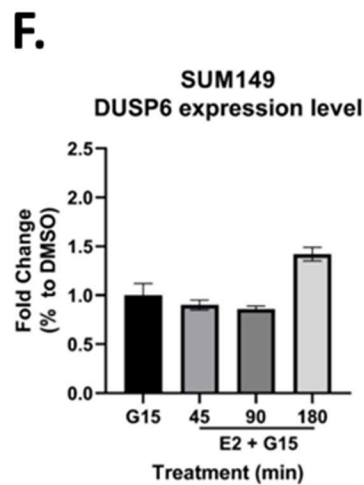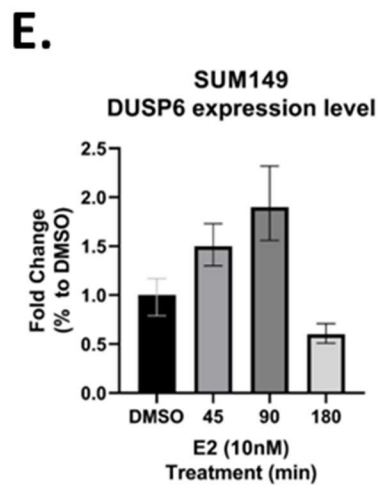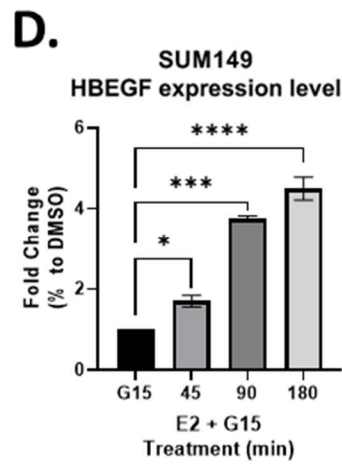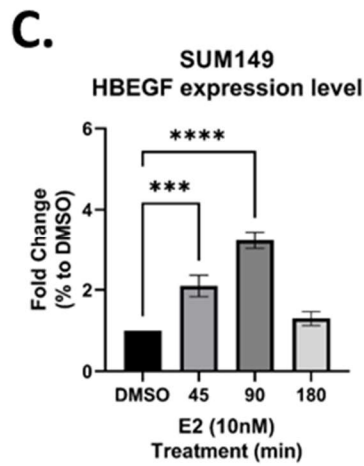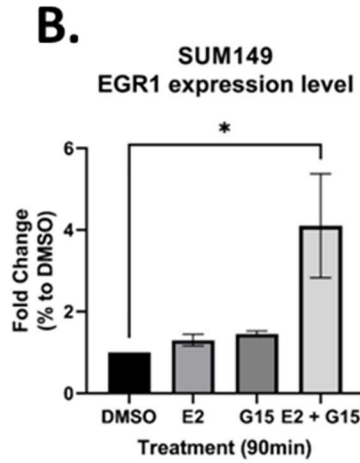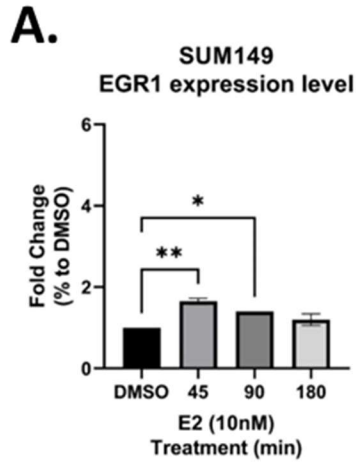
Figure 11. Effect of G15 on the expression of EGR1, HB-EGF, and DUSP6 on TN-IBC
The relative mRNA expression levels of EGR1, HB-EGF, and DUSP6 on TN-IBC SUM149 cells were significantly upregulated after 45 min of E2 treatment (10 nM), followed by a reduction to basal levels after 180 min (A, C, E)—measured by qPCR. G15 (10 µM for 1 h) treatment followed by E2 (10nM for 90 min) upregulated the expression of EGR1 (D) and HB-EGF (F) compared with the E2 group. G15 also inhibited the E2-induced expression of DUSP6 (B). Results are mean + SD of three independent experiments. Ordinary one-way ANOVA analysis followed by Dunnett's multiple comparison test was performed for statistical significant., represented as *$P < 0.05$; **$P < 0.01$; ***$P < 0.001$; ****$P < 0.0001$.

B. G15 disrupts the regulation of estrogen-induced nongenomic signals on TN-IBC

It is known that E2 and G1 (GPER-specific agonists) trigger the ERK1/2 and AKT activation via non-genomic signaling on IBC and non-IBC TNBC [92]. Here, we measured the E2-induced activation of the ERK1/2 and AKT signaling on TN-IBC SUM149 and HER2-amplified IBC SUM190. In brief, cells were treated with E2 (10 nM) at time points of 5-, 15-, and 30-min to further measure the phosphorylation levels of ERK1/2 (p-ERK1/21/2) and AKT (p-AKT) (**Fig. 12A**). After a short period exposure (5, 15, and 30 min) of E2 (10 nM) treatment, fold change values for ERK1/2 phosphorylation levels were 1.7 + 0.54 (Adj. p-value 0.04) at 5 min, 1.3 + 0.09 at 15 min, and 0.6 + 0.20 at 30 min on TN-IBC SUM149, and 1.5 + 0.23 (Adj. p-value 0.02) at 5 min, 0.8 + 0.2 at 15 min, and 0.5 + 0.04 at 30 min (Adj. p-value 0.03) for HER2-amplified IBC SUM190 (**Fig. 12B**). For p-AKT expression, the fold change values of AKT phosphorylation triggered by E2 were 0.8 + 0.11 (Adj. p-value 0.01) at 5 min, 1.1 + 0.04 at 15 min, and 1.3 + 0.08 (Adj. p-value 0.003) at 30 min on TN-IBC SUM149, and 1.1 + 0.15 at 5 min, 1.0 + 0.11 at 15 min, and 0.9 + 0.04 at 30 min for HER2-amplified SUM190.

To investigate the effect of G15 in the E2-induced non-genomic signaling pathway on TN-IBC SUM149, we measured the phosphorylation levels of ERK1/2 and AKT after E2 (10 nM) treatment alone and in combination with G15 (10 µM; 1h before E2) at time points of 5, 15, and 30 min (**Fig. 12C**). Fold change values for ERK1/2 phosphorylation levels in the E2 treated group were 0.9 $\pm$ 0.24 at 5 min, 0.8 $\pm$ 0.092 at 15 min, 0.6 $\pm$ 0.22 at 30 min, and on the E2 + G15 group were 1.5 $\pm$ 0.38 at 5min, 1.4 $\pm$ 0.24 at 15min, and 1.4 $\pm$ 0.04 at 30min. After a one-way ANOVA analysis, we identified a significant increase (Adj. p-value 0.02) in p-ERK1/2 levels in the E2 + G15 group at

30min compared with the E2 group at 30min (**Fig. 12F**). Furthermore, relative expression values for AKT phosphorylation levels in the E2-treated group were 0.6 ± 0.21 at 5min, 0.8 ± 0.25 at 15min, and 1.0 ± 0.27 at 30min, and in the E2+G15 group was 1.4 ± 0.46 at 5min, 1.6 ± 0.39 at 15min, and 1.6 ± 0.43 at 30min.
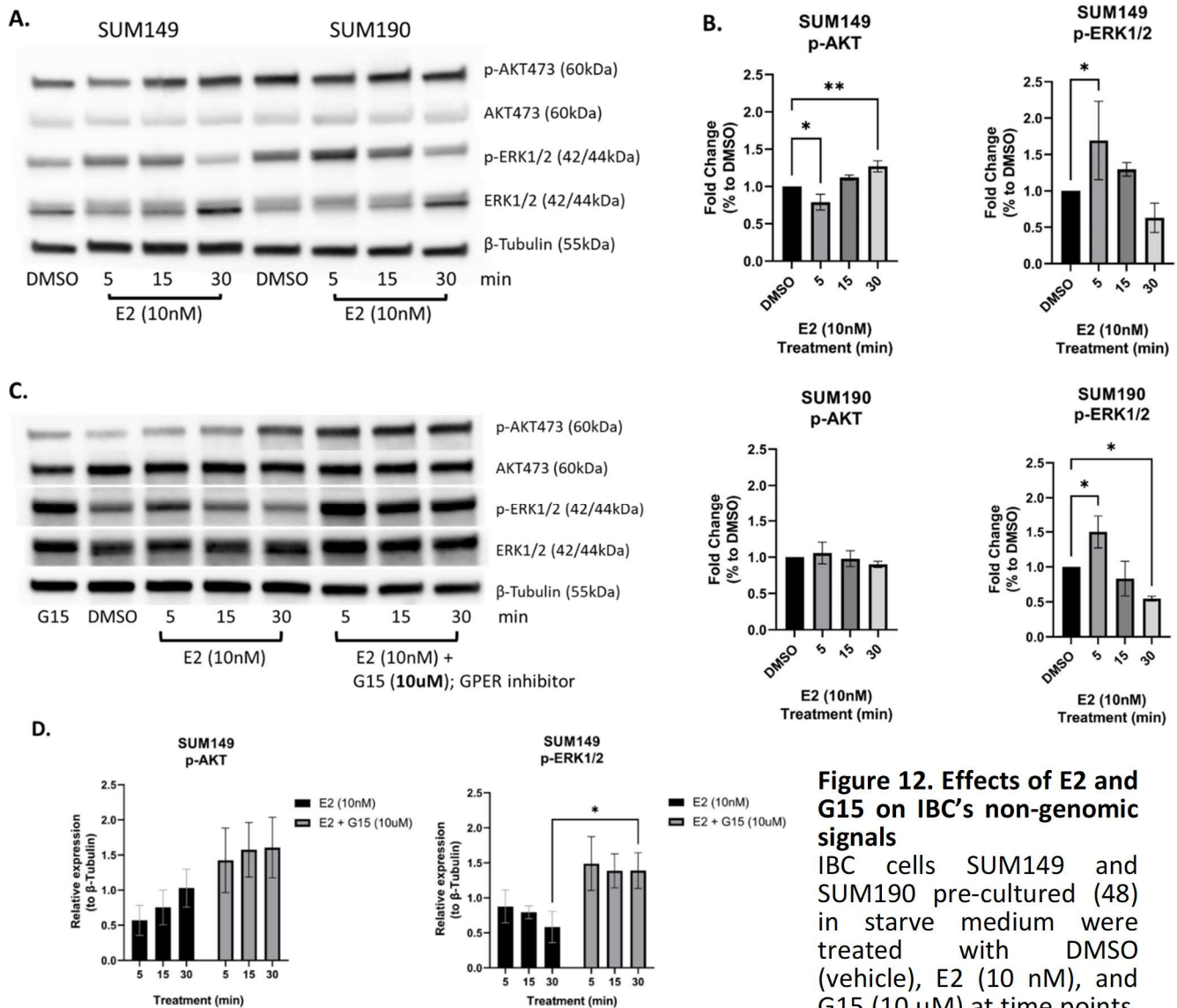
Figure 12. Effects of E2 and G15 on IBC's non-genomic signals

IBC cells SUM149 and SUM190 pre-cultured (48) in starve medium were treated with DMSO (vehicle), E2 (10 nM), and G15 (10 µM) at time points. (A) ERK1/2 and AKT phosphorylation levels after E2 stimulus, identified by western blot. Both IBC cell lines showed a transient regulation of ERK1/2 activation upon E2 treatment, while only SUM149 reported AKT signal regulation (B). Furthermore, TN-IBC SUM149 cells were pretreated with DMSO (control) or G15 (10 µM) for 1h before E2 (10 nM) administration at time points (C). β-tubulin ensures equal loading. The bar graph shows Fold changes against the control (DMSO, with the value set arbitrarily as 1. Results are mean + SD of three independent experiments Adj. P-values were calculated after an ordinary one-way ANOVA analysis with a Dunnett's multiple comparison test, represented as *P < 0.05; **P < 0.01; ***P < 0.001; ****P < 0.0001.

III. Aim #3: Identify the effects of G15 on IBC's oncogenic phenotypes

A. GPER expression in IBC and non-IBC cell lines

To characterize the expression of GPER across many breast cancer cell lines, we measured GPER mRNA expression levels in BC cell lines MCF-7 (ER+), MDA-MB-231 (TNBC), SUM149 (TN-IBC), and SUM190 (IBC HER2-amplified) (**Fig. 13)** Relative expression values for each cell lines were MCF-7: 5.8E-04 (+ 1.6E-04), MDA-MB-231: 2.5E-04 (+0.3E-04), SUM149: 0.3E-04 (+0.06E-04), and SUM190: 0.35E-04 (+0.09E-04) (**Fig. 13A)**. Ordinary one-way ANOVA analysis followed by a Tukey's multiple comparison tests reported significant differences in GPER mRNA expression between MFC-7, SUM149, and SUM190 (Adj. p-value 0.001), MCF-7 and MDA-MB-231 (Adj. p-value 0.004), and between MDA-MB-231 with SUM149 (Adj. p-value 0.04) and SUM190 (Adj. p-value 0.04). There was no significant difference in GPER mRNA expression between IBC cell lines SUM149 and SUM190 (Fig 1 A). The expected RT-qPCR products were observed in a 3% agarose gel: GAPDH (124bps), ESR1 (122bps), ERα36 (91bps), GPR30 (169bps), and EGFR (167bps)—seen in **Fig. S2.**

Western blot was performed to analyze GPER protein abundance between different BC cell lines (**Fig. 13**). A GPER protein band was detected at 55 kDa in all cell lines (as directed by the antibody's instructions), while another band was observed around 50 kDa in TNBC MDA-MB-231 and TN-IBC SUM149. After normalization with β-tubulin (house-keeping gene), relative protein abundance for both GPER protein variants across cell lines were: MCF-7: 0.76 $\pm$ 0.3, MDA-MB-231: 0.84 $\pm$ 0.11, SUM149: 0.60 $\pm$ 0.24, and SUM190: 2.07 $\pm$ 0.7. The relative protein abundance for the 50 kDa variant of the GPER protein present in TNBC MDA-MB-231 and TN-IBC SUM149

were 0.72 $\pm$ 0.3 and 0.36 $\pm$ 0.4 after normalization with β-tubulin, respectively. After an Ordinary one-way ANOVA analysis followed by Tukey's multiple comparison tests, we identify significant differences in GPER protein abundance between SUM190 with MCF-7 (Adj. p-value 0.01), MDA-MB-231 (Adj. p-value 0.02), and SUM149 (Adj. p-value 0.006). We also performed Immunofluorescence microscopy (IF) to identify GPER protein expression and localization on TN-IBC cells SUM149 **(Fig. 13 C).** Protein overexpression and localization are critical events in breast cancer progression. Our results showed GPER abundance in the plasma membrane, but predominantly in the endoplasmic reticulum on TN-IBC cells SIM149.
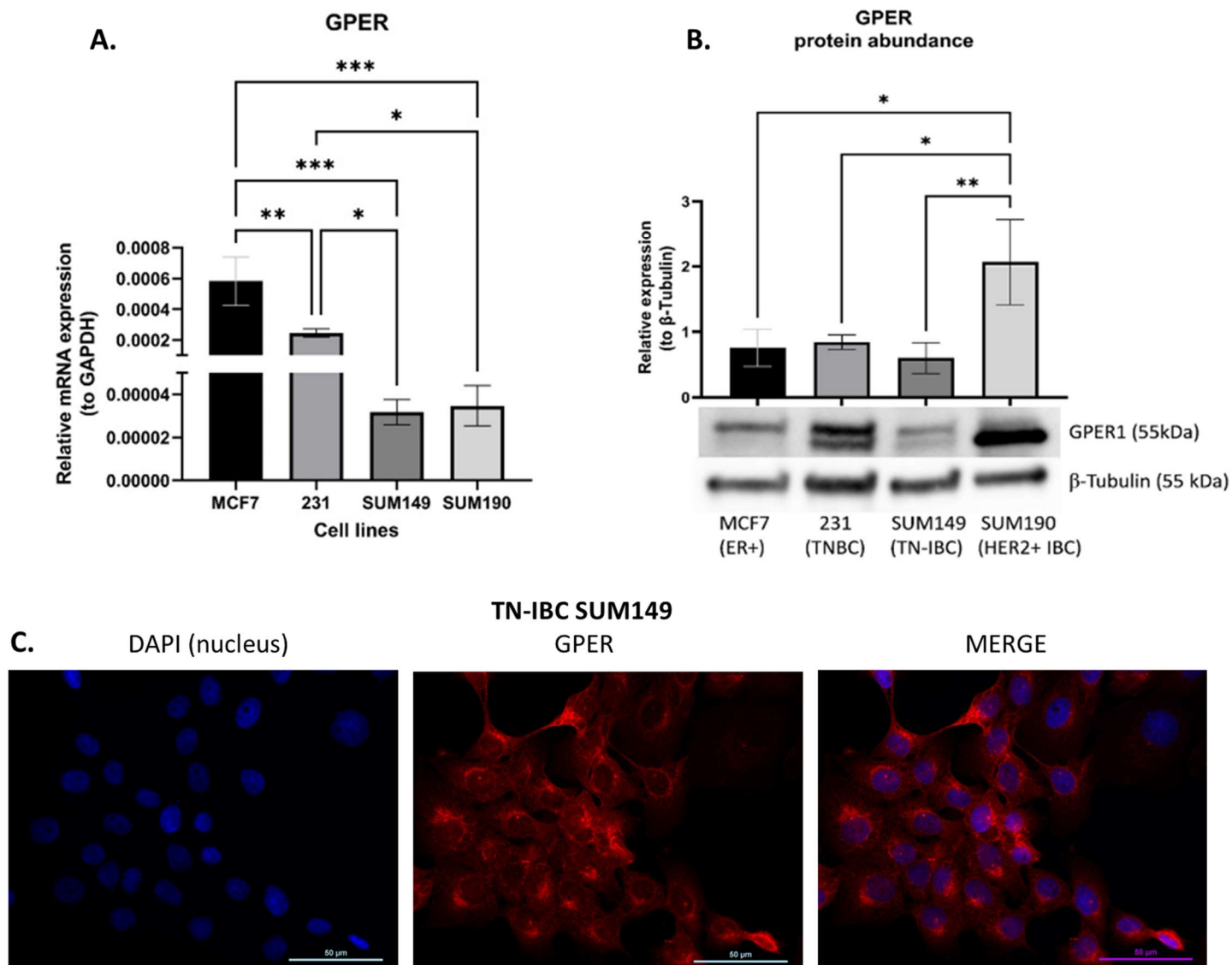
Figure 13. GPER expression across breast cancer cell lines

GPER gene expression (A) and protein abundance (B) were measured across breast cancer cell lines MCF-7 (ER+), MDA-MB-231 (TNBC), SUM149 (TN-IBC), and SUM190 (IBC HER2-amplified). GAPDH and β-tubulin were used as loading control and reference gene. Ordinary One-way ANOVA analysis was performed for statistical significance. Results are shown as mean + SD of three independent experiments, each performed in triplicates. *$P < 0.05$; **$P < 0.01$; ***$P < 0.001$; ****$P < 0.0001$. (C) By immunofluorescence, GPER receptor (red) was seen localized in the cytoplasm and in the periphery of the nucleus on TN-IBC SUM149. Pictures are shown at a magnitude of 400X. DAPI staining (blue) identifies the cell nucleus.

B. G15 reduces cell viability on triple-negative and HER2+ IBC

A dose-response curve was performed to identify the effects of G15 on TN-IBC SUM149 (**Fig. 14A**) and HER2-amplified IBC SUM190 (**Fig. 14B**) cell viability and growth rate. After three days of treatment with G15 at the indicated concentrations (2-fold serial dilutions from 30 μM-0.47 μM), a 50% reduction (IC50 value) in relative cell viability compared with control was reached for TN-IBC SUM149 at 24h: 10 μM, 48h: 12.5 μM, and 72h: 19.5 μM, and 48h: 19.5 μM, and 72h: 11.5 μM for SUM190. On the other hand, SUM190 cells did not reach IC50 values at 24hrs, although the relative cell viability reached 55% at 30 μM G15 compared with the control group (DMSO). In addition, we treated TN-IBC SUM149 cells with E2 (10 nM) alone and in combination with G15 (10 μM) for three days to determine if E2 could stimulate cell viability and whether GPER was involved in the process. The relative cell viability after E2 treatment was: 24h: 105% $\pm$ 8.6, 48h: 106% $\pm$ 5.4, and 72h: 105% $\pm$ 7.6, compared to control DMSO: 100%. However, relative expression values for G15 and E2 + G15 treatment groups were: 24h: 62% $\pm$ 3.3, 57% $\pm$ 2.2, 48h: 67% $\pm$ 6.5, 65% $\pm$ 5.3, and 72h: 75% $\pm$ 10.3, 70% $\pm$ 6.6. After a 2-way ANOVA analysis, G15 and E2 + G15 groups reported a significant ($p < 0.05$) reduction in their relative cell viability compared to the E2 group (**Fig. 14C**).
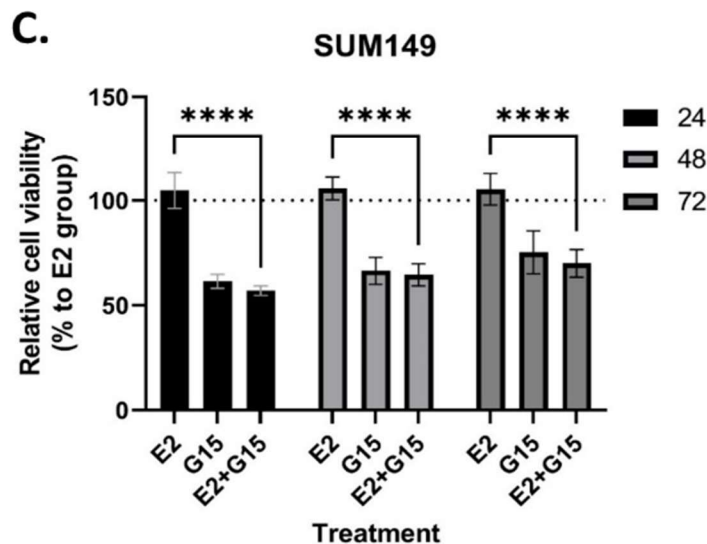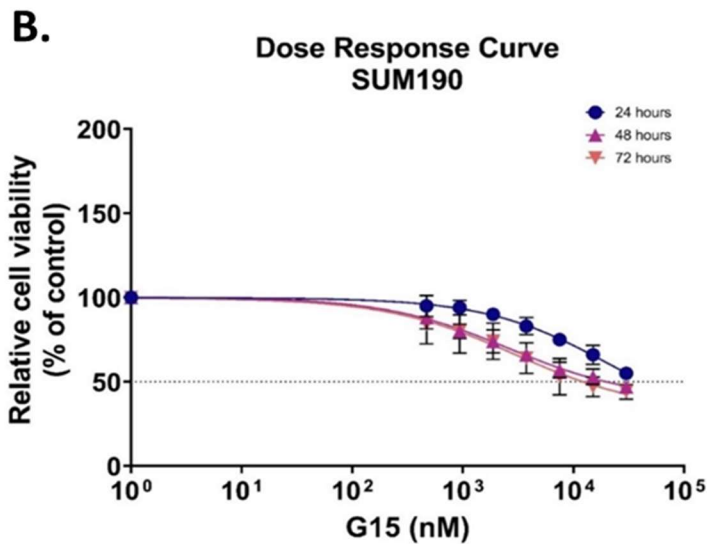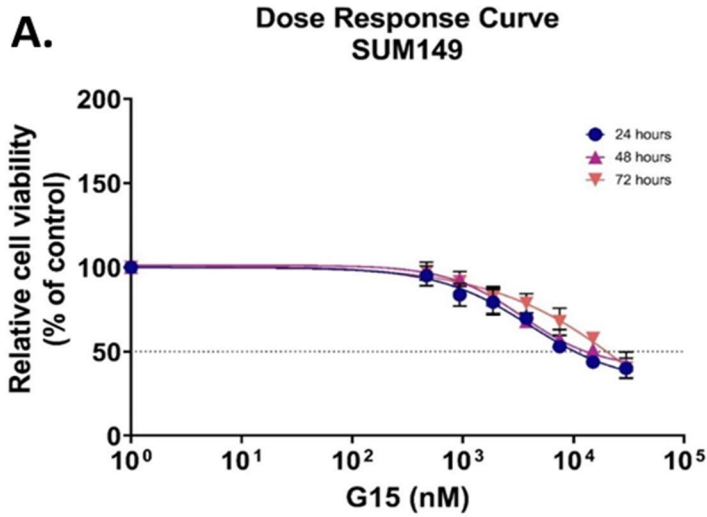
Figure 14. Effects of E2 and G15 treatment on IBC cell viability

Dose-response curve on IBC cell lines SUM149 (A) and SUM190 (B) precultured (48hrs) in starving media, followed by a three-day treatment with DMSO (Control), and G15 (2-fold serial dilutions from 30 μM-0.47μM) alone and in combination with E2 (C). IC:50 values for TN- SUM149 were 10 μM at 24hr, 12.5 μM at 48hr, and 19.5 μM at 72hrs, and HER2+ SUM190 19.5 μM at 48hr, and 11.5 μM at 72hrs. Results represent mean values $\pm$ SE of three independent experiments performed in triplicates. *P<0.05, **P<0.01 and ***P<0.001 versus control.

C. G15 reduces triple-negative and HER2+ IBC cell's growth rate

For growth rate (GR) measurements, we used the same data generated in the dose-response curve and calculated GR values using the GR calculator program from Dr. Sorger's Lab at Harvard Medical School [149]. This approach was performed to identify if the G15-induced cell viability reduction was associated with cell cycle arrest or cell death. GR values are presented on a scale from -1 to 1, where cell growth is GR > 1, partial cell growth inhibition is 1 > GR >0, cytostatic or cell cycle arrest is GR = 0, and cytotoxic or cell death is GR < 0 (**Fig. 15**). After 3-day treatment with G15, TN-IBC SUM149 cells reported GR values for G15 0.47 µM: 2.06 (%CV 4.82), 0.94 µM: 0.07 (%CV 4.93), 1.88 µM: -0.8 (%CV 9.42), 3.75 µM: -0.91 (%CV 11.21), 7.5 µM: -0.99 (%CV 19.5), 15 µM: -1 (%CV 9.73), and 30 µM: -1 (%CV 36.38) compared with untreated cells (**Fig. 15A**). DMSO group reported GR: 3.71 (%CV 2.1) compared with untreated cells.

For HER2-amplified IBC SUM190 cells, the GR values after G15 treatment were: 0.47 µM: -1 (%CV 15.96), 0.94 µM: -1 (%CV 14.87), 1.88 µM: -1 (%CV 13.21), 3.75 µM: -1 (%CV 11.33), 7.5 µM: -1 (%CV 17.92), 15 µM: -1 (%CV 8.62), and 30 µM: -1 (%CV 9.70) compared with untreated cells (**Fig. 15B**). DMSO group reported a GR of 1.15 (%CV 6.90) compared with untreated cells. In addition, we treated TN-IBC SUM149 cells with E2 (10nM) alone and in combination with G15 (10µM) for three days to determine if E2 could stimulate cell growth and whether GPER is necessary for the E2-dependent cell proliferation. GR values were E2: 0.7 $\pm$ 0.28, G15: -0.1 $\pm$ 0.07, and E2 + G15: -1 $\pm$ 0.07; presented in **Fig. 15C**. Fluorescence values measured in the non-stimulated wells (Control; non-treated) were set to 100%. The absorbance values estimated in the stimulated wells were divided by the values of the control wells to give the relative cell number in % achieved under the indicated conditions.

A.

SUM149
Growth Rate (GR) value
(72h)

B.

SUM190
Growth Rate (GR) value
(72h)

C.

SUM149
Growth Rate (GR) value
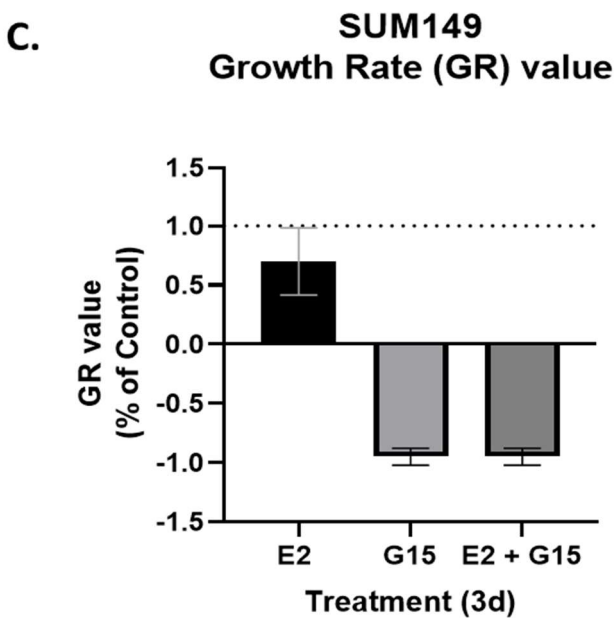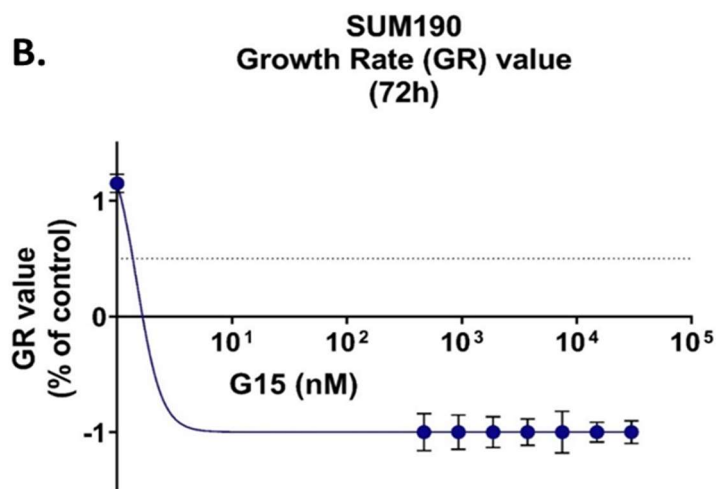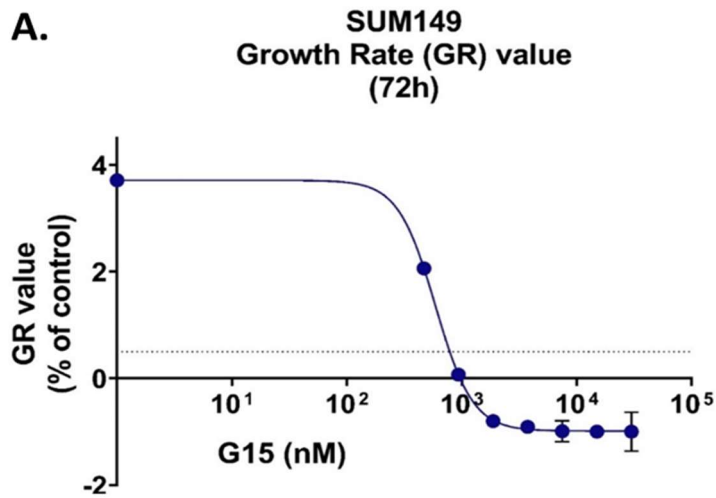
Figure 15. Effects of E2 and G15 treatment on IBC growth rate

Data from the dose-response curve on SUM149 (A) and SUM190 (B) were used to measure the effects of G15 on cell growth rate (GR). In brief, IBC cells precultured (48hrs) in starving media were treated with DMSO (Control) and G15 (2-serial dilution from 30 µM-0.04 µM) for 3 days. GR:0 values (cytostatic stage) after 3 days of G15 treatment were 1 µM for TN-IBC SUM149 and less than 0.47 µM for HER2-amplified IBC SUM190 cells. A colorimetric assay using alamarBlue evaluated the cells in microwell plates. GR values were calculated using the GR calculator program from Dr. Sorger's Lab at Harvard Medical School [149]. GR values are presented as growth (GR > 1), partial inhibition (1 > GR >0), cytostatic (GR = 0), and cytotoxic (GR < 0). Results represent mean values and SD of three independent experiments performed in triplicates.

D. G15 inhibits the E2-induced upregulation of the cell cycle and apoptotic-related markers

We next sought to address whether G15-reduction on IBC cell survival and growth rate were associated with changes in the expression of the cell cycle progression marker Cyclin E1 and the anti-apoptotic molecule BCL-2. To this end, we determined the protein abundance of Cyclin E1 and BCL-2 on IBC cells TN-IBC SUM149 and HER2-amplified SUM190 after E2 (10 nM) treatment alone and in combination with G15 (10 µM; 1h before E2 treatment) for 12h. As shown in **Fig. 16**, we detected a specific band of Bcl-2 and Cyclin E1 of around 26 kDa and 48 kDa, respectively. After normalizing to β-tubulin (house-keeping gene), relative expression values for BCL-2 on TN-IBC SUM149 were: DMSO; 1.0 $\pm$ 0.12, E2; 1.3 $\pm$ 0.02, G15; 0.9 $\pm$ 0.21, and E2 + G15; 0.9 $\pm$ 0.11 (**Fig. 16A**). After an unpaired t-test, E2 group reported a significant increase in BCL-2 protein expression compared to DMSO group (p-values of 0.01), and the E2 + G15 group reported a significant BCL-2 reduction when compared with E2 group (p-values of 0.0026). G15 treated group did not show any significant difference when compared with the DMSO group.

For HER2-amplified SUM190, Bcl-2 protein relative expression values were DMSO: 1.0 ($\pm$ 0.08), E2: 1.1 $\pm$ 0.01, G15: 1.0 $\pm$ 0.01, and E2+G15: 0.9 + 0.04 (**Fig. 16B)**. After an unpaired t-test, E2 group reported no significant increase in BCL-2 protein expression compared to DMSO group, however, the E2 + G15 group reported a significant BCL-2 reduction when compared with E2 group (p-values of 0.01). G15 treated group did not show any significant difference when compared with the DMSO group.

For Cyclin E1, protein relative expression values for TN-IBC SUM149 after normalization to β-tubulin (loading control) were: DMSO 0.9 + 0.10, E2 1.3 $\pm$ 0.13, G15 1.1 $\pm$ 0.12, and E2 + G15 0.8 $\pm$ 0.17 (**Fig. 16C**). After an Ordinary one-way ANOVA analysis and Tukey's multiple comparison tests, the E2 group had a significant increase (Adj. p-value 0.005) in Cyclin E1 protein expression values compared to DMSO and a statistically significant reduction (Adj. p-value 0.001) with the E2 + G15 group. There was also a significant reduction in Cyclin E1 protein expression (Adj. p-value 0.04) reported in the E2+G15 group compared to G15. For HER2-amplified SUM190, Cyclin E1 protein relative expression values were DMSO: 1.0 $\pm$ 0.08, E2: 1.1 $\pm$ 0.03, G15: 1.1 $\pm$ 0.07, and E2 + G15: 0.8 $\pm$ 0.05. After an Ordinary one-way ANOVA analysis and a Tukey's for multiple comparison test, the E2 + G15 group reported a significant protein expression reduction compared to E2 and G15 group, with an Adj. p-value of 0.03 and 0.004, respectively.
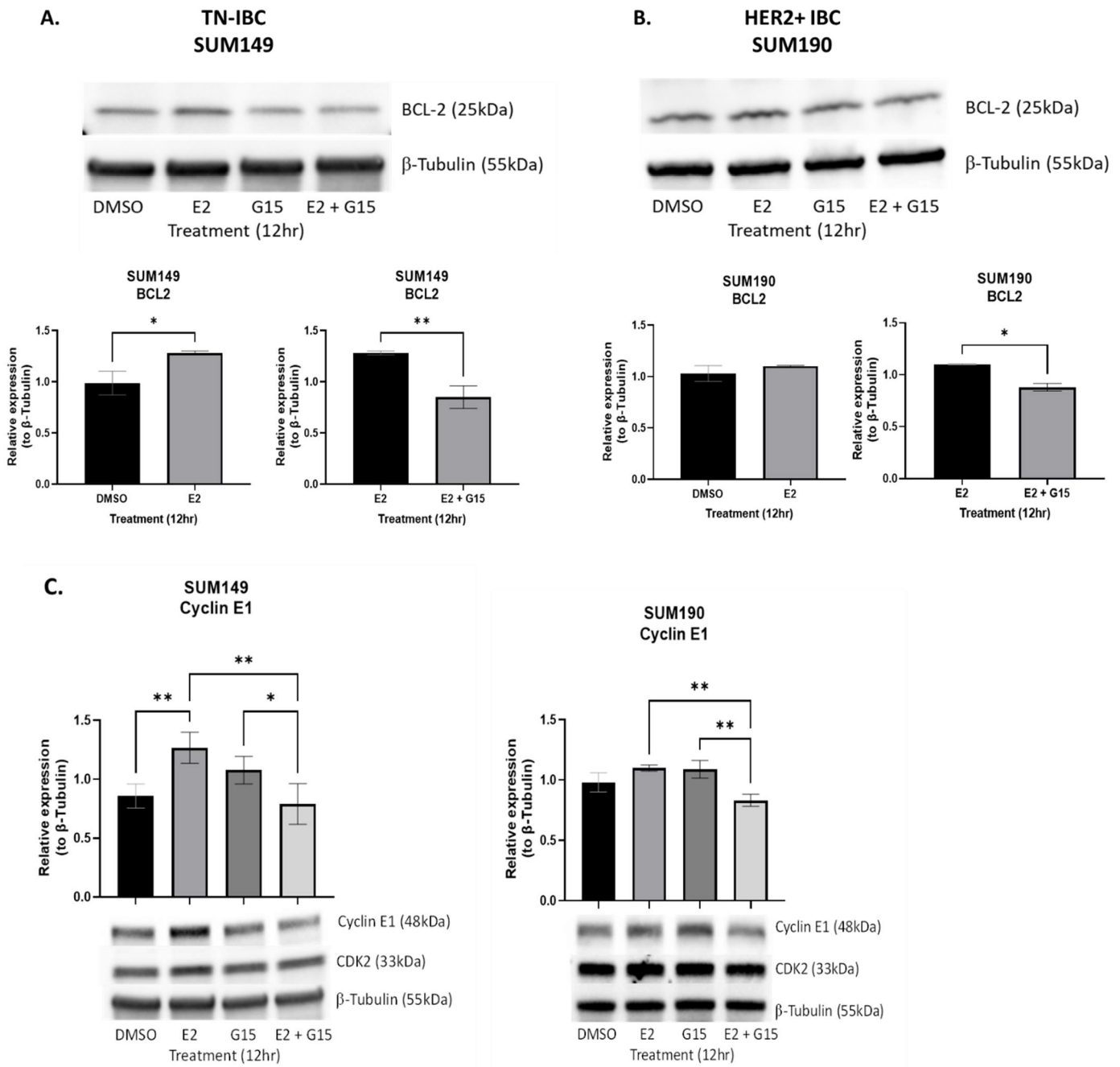
Figure 16. Effect of E2 and G15 treatment on cell cycle and apoptosis-related markers
    TN-IBC SUM149 and HER2-amplified SUM190 IBC cells pre-cultured in starving media for 48 h were treated with DMSO (control) and indicated concentrations of E2 (10 nM), and G15 (10 µM: 1 h after E2) alone and in combination (E2 + G15) for indicated time points. Cell lysates were subjected to Western blot analysis with antibodies for BCL-2 (A-B), Cyclin E1, and CDK2 (C) as described in the Materials and Methods section. β-tubulin ensured equal loading. The bar graph shows the treatment-induced relative expression of the assayed markers against the reference gene. Results are shown as mean + SD of three independent experiments performed in triplicates. *P < 0.05; **P < 0.01; ***P < 0.001; ****P < 0.0001.

G15 inhibits the E2-induced upregulation of the apoptotic-related cleaved caspase-3

We also investigated whether the G15-induced reduction in cell survival and growth rate on IBC cells was associated with changes in the expression of caspase 3—a crucial enzyme for initiating and executing apoptosis within a cell [186]. Cleaved caspase 3, the active form of the enzyme, is a strong indicator of cell death induction since it propagates apoptotic signals. In glioblastoma C6 cells, G15 exposure has been shown to increase the percentage of caspases-3 levels, reporting a reduction in cell proliferation and viability, and favoring apoptosis. In this study, we measured the cytotoxic strength of G15 in TN-IBC SUM149 by measuring and comparing the number of cells positive for cleaved caspase-3 staining (by immunofluorescence) after G15 and DMSO treatment (**Fig. 17)**. Our results showed that the number of cells positive of cleaved caspase-3 increased significantly after G15 treatment (p-value <0.0001) compared to the control group—with a mean of 43.06 and 23.73 percent of cleaved caspase-3 per nucleus, respectively (**Fig. 17B-C**). Additionally, the G15 treated group presented a significant (p-value <0.0001) lower count of cells per image size compared with DMSO groups—with means of 105 and 207 nuclei per image size, respectively. An unpaired t-test was performed for statistical analysis.
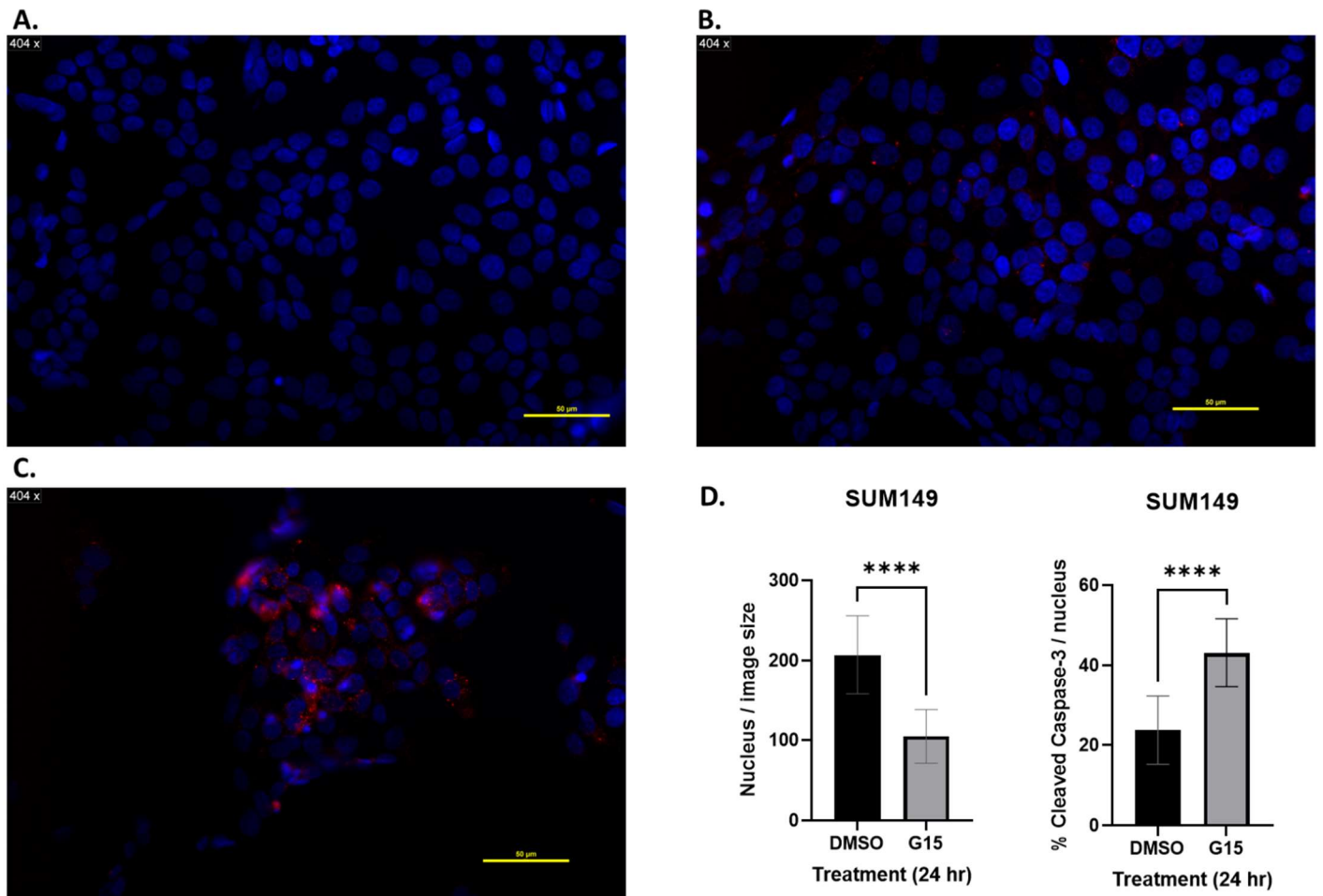
Figure 17. Immunocytochemical detection of Cleaved Caspase-3 in TNBC SUM149 after G15 treatment. The cells were starved for 48 h and stimulated with the corresponding treatment for 24 h. After treatment, the cells were fixed with 4% paraformaldehyde, permeabilized with 0.1% PBS-Tween-20, blocked with 10% normal goat serum in 0.1% PBS-Tween, and incubated overnight with anti-cleaved caspase-3 antibody. The cleaved caspase 3 (red fluorescence) levels increased significantly after G15 treatment (**C**) (p-value <0.0001) compared to DMSO group (**B**)— with a mean of 43.06 and 23.73 percent of cleaved caspase 3 per nucleus. No staining was found in control (**A**). Additionally, the G15 treated group presented a significantly (p-value <0.0001) lower count of cells per image size compared with DMSO groups—with a mean count of 104.5 and 206.7 nuclei (blue fluorescence) per image size, respectively. Pictures are shown at a magnitude of 400X. An unpaired t-test was performed for statistical analysis (**D**). Results are shown as mean + SD of two independent experiments—six pictures on each group per experiment. *P < 0.05; **P < 0.01; ***P < 0.001; ****P < 0.0001.

E. G15 disrupts colony formation on TN-IBC SUM149

One of the unique characteristics of IBC cancers is the high frequency of small clusters of cancer cells leading to obstruction of milk ducts and lymphatic vessels—causing its unique clinical classification. A 3D colony formation assay was performed on TN-IBC SUM149 cells to study the effects of G15 administration on cell proliferation in tumor colonies. After 10 days of G15 treatment, the colonies from the G15-treated cells reported an area/size mean of 12×10^4 square pixels compared to 44×10^4 square pixels in the control group (**Fig. 18**). T-test analysis reported a statistically significant (p-value < 0.0001) reduction in area/size compared with the control (B).

TN-IBC
SUM149

A.

Control

G15

B.

3D Colony formation assay
SUM149

****

Colony Size

1.5×10^6

1×10^6

5×10^5

0
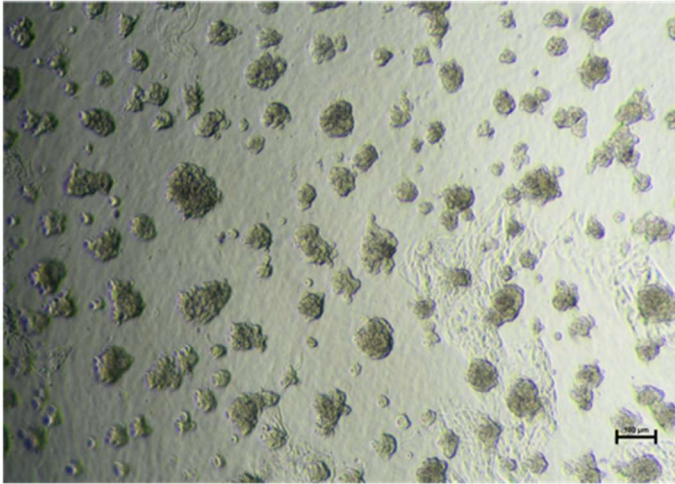
control   G15
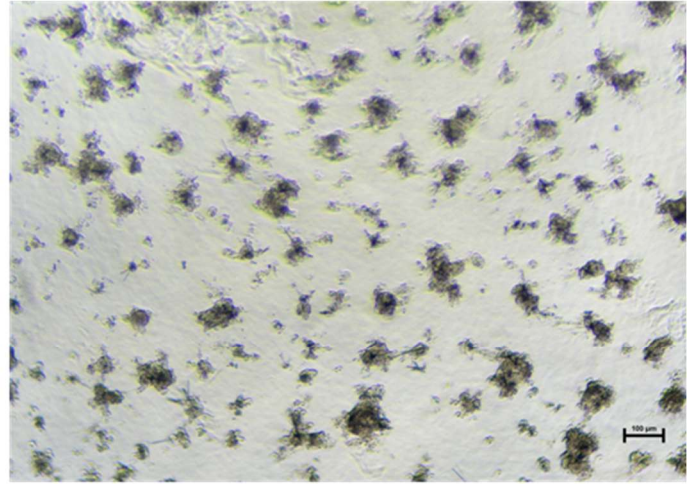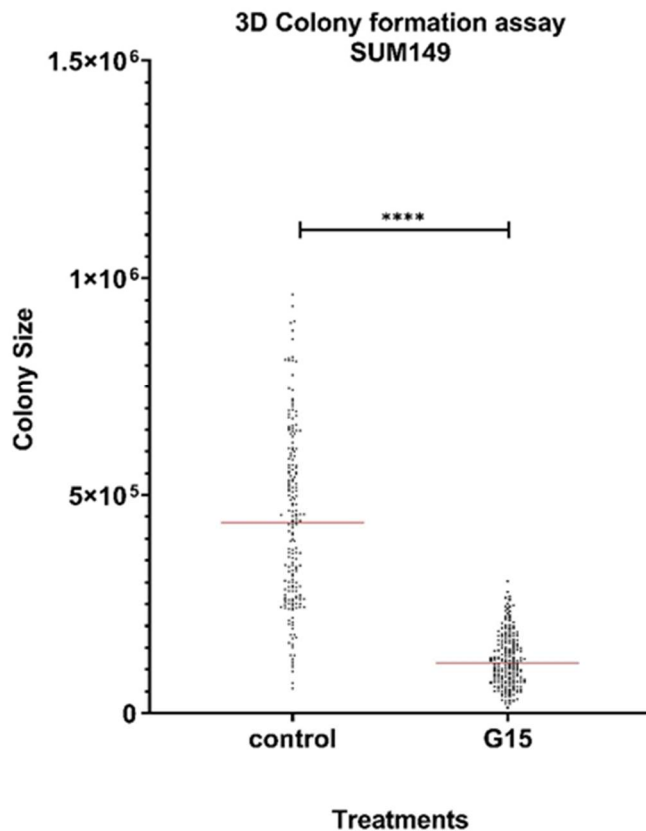
Treatments

Figure 18. Effects of G15 treatment on colony formation of TN-IBC cells. G15 treatment reduces colony formation on TN-IBC cell SUM149 cells treated with G15 (10 µM) for 10 days produce colonies with significantly (p-value <0.0001) smaller area per pixel as compared to DMSO (A). Pictures are shown at a magnitude of 40X. Illustration of colonies under DMSO and G15 treatment (B). Results are means of three independent biological replicates; n=200 colonies for each treatment. p-values of <0.05 were considered statistically significant and presented as *P < 0.05; **P < 0.01; ***P < 0.001; ****P < 0.0001.

F. G15 inhibits the E2-induced cell migration enhancement on TN-IBC SUM149

The aggressive characteristic of IBC enables its malignant cells to invade the dermal lymphatics of the breast, causing the accumulation of fluids within lymphatic vessels and the subsequent edematous red swelling of the breast [150]. Ohshiro et al., reported that E2 and G1 (GPER-specific agonist) stimulus on IBC cells was able to induce the activation of the extracellular-signal-regulated kinases (ERK1/2), enhancing cell migration and invasion behaviors [151]. Here, we validated the E2-induced migratory enhancement of TN-IBC cells SUM149 and further measured the effects of G15 treatment on this behavior (**Fig. 19A**). After 19 h of treatment, the percentage of wound-closure coverage for each group was: DMSO 26% $\pm$ 1.7, E2 47% $\pm$ 8.86, G15 21% $\pm$ 5.92, and E2 + G15 24% $\pm$ 4.9. As seen in **Fig. 19B**, Ordinary one-way ANOVA analysis with Tukey's for multiple comparisons reported a statistically significant enhancement (Adj. P-value 0.0115) in cell migration when TN-IBC SUM149 cells were treated with E2 compared to control (DMSO). Additionally, G15 treatment significantly reduced (Adj. p-value 0.0057) the E2-induced cell migration enhancement when cells were treated in a combination of E2 and G15.

A.
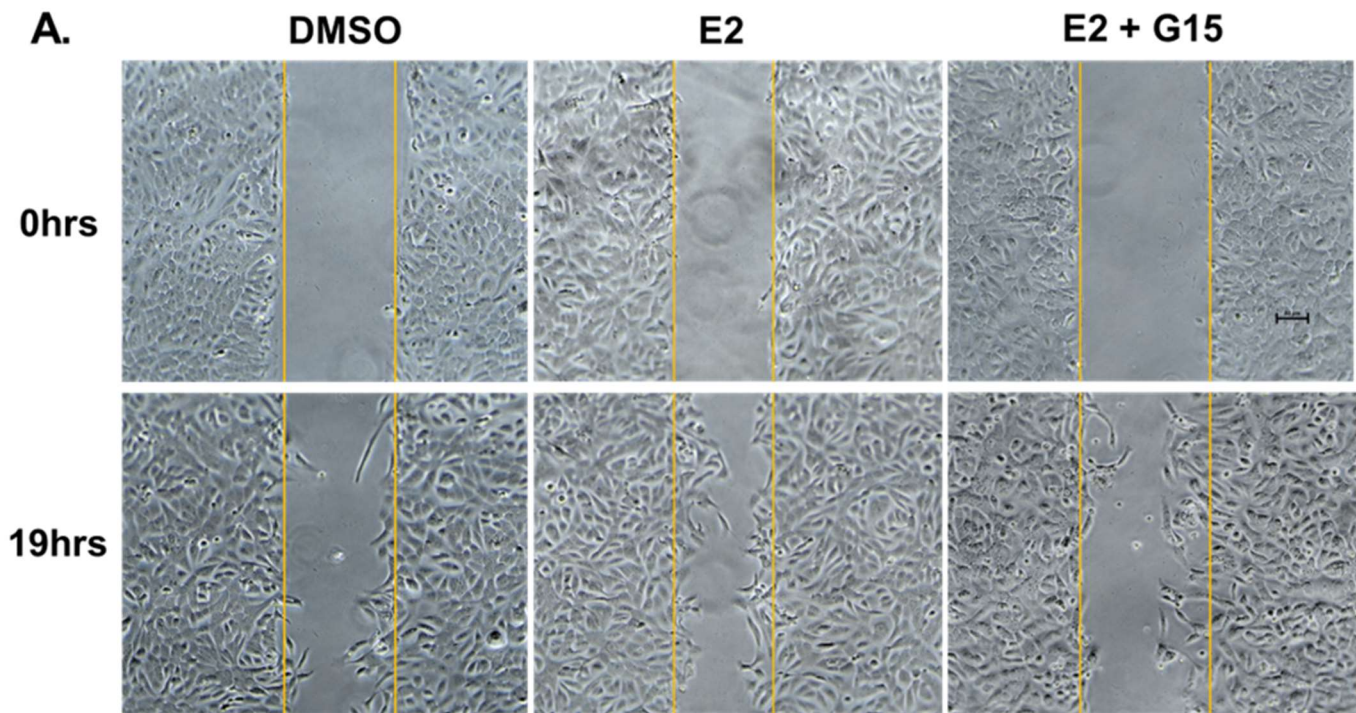
B.
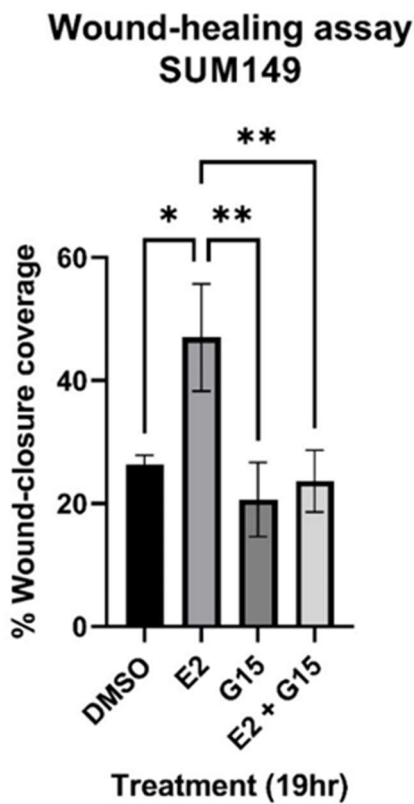
Figure 19. G15 treatment on TN-IBC cells reduces cell migration. In brief, TN-IBC SUM149 cells were cultured in their corresponding medium to 50-60% confluency, then transferred to starving media for 48h until cells reached 100% confluency. (A) Cells were further treated with E2 (10 nM) alone and in combination with G15 (6 µM), and DMSO (vehicle) for 19 h. The wound-closure area was measured using ImageJ, with three pictures per group. The E2-treated group reported higher migration activity than the E2 + G15, G15, and DMSO-treated groups (B). An inverted microscope captured the closure of the wound area (200 x magnification). (B) Wound-closure area measurements were analyzed using ImageJ software and GraphPad. Statistical analysis was performed by Anova using Graph Pad Prism9. Results are shown as mean + SD of three independent experiments performed in triplicates. *P < 0.05; **P < 0.01; ***P < 0.001.

Chapter 4: Discussion

I.   Aim #1: Characterize the transcriptional signature induced by estrogen on TN-IBC

The rapid progression of Inflammatory Breast Cancer can largely be attributed to the aggressive invasive and metastatic behavior of the disease—known to be enhanced by estrogen stimulation [151]. However, transcriptional regulations and molecular pathways by which estrogen signals regulate IBC's carcinogenesis are only partially understood. The presence of alternate estrogen receptors on IBC cells and the prevalence of the disease in younger women bring the rationale of why it is essential to study estrogen signals in IBC cells. Here, RNA-seq was performed on TN-IBC SUM149 to carry out a comprehensive global analysis of the transcriptome induced by estrogen stimulation at time points. Differential RNA-seq analysis revealed gene regulations induced by estrogen signaling on TN-IBC cells, where 73% of the genes with differential expression statistically significant were regulated after three hours of estrogen exposure.

At the earliest stage of estrogen stimulus, the top ten regulated genes were associated with transcription factors and growth factor ligands, while the top ten regulated genes in the last time point were more associated with structural functioning. These results imply that TN-IBC SUM149 cells conserve estrogen-regulated transcription networks, which could be common to other estrogen-responsive ER-negative breast cancers [152, 153]. In addition, this observation suggests that TN-IBC cells may undergo estrogen-response signals similar to the canonical estrogen signaling pathway and could possibly be related to the presence of alternate estrogen receptors like GPER and ERα36.

Some of the most statistically significant E2-upregulated genes included immediate-early response transcription genes (e.g., EGR1, ATF3, KLF6, and JUN/FOS), growth factor ligands (e.g., HB-EGF, EREG, and AREG), cell-cycle progression regulators (e.g., CDKN1A/p1Cip1, MYC), MAPK signaling cascade phosphatases (e.g., DUSP1-DUSP6), and intercellular cell-cell-junction regulators (e.g., CLDN1). Along this line, a study using biopsy specimens obtained from women with clinical IBC identified a list of genes that were significantly upregulated in IBC compared with non-IBC; defined as specimens of noninflammatory locally advanced breast cancers [154]. The upregulated genes in IBC cases included transcription factors (JUN, EGR1, JUNB, FOS, SNAIL1) and growth factors (HB-EGF, EREG, IL6)—all of which were reported upregulated after E2 stimulus on TN-IBC, according to our RNA-Seq analysis. Therefore, our study provides strong evidence that E2 may contribute to IBCs' unique characteristics by inducing gene transcription associated with carcinogenesis and cancer progression.

Furthermore, two genes that remained in the top ten E2-upregulated genes throughout the assay were NR4A1 and NR4A3—transcription factors and members of the NR4A family of orphan nuclear receptors—known to regulate the expression of genes involved in basal breast cancer progression and metastasis [155]. In addition, two genes from the CCN extracellular protein family (CCN1 and CCN2) were also detected as part of the top ten most upregulated genes induced by E2. The CCN1 (cysteine-rich 61/Cyr61) and the connective tissue growth factor (CTGF/CCN2) are the two main CCN proteins that have oncogenic functions in breast cancer. High CCN1 expression is associated with lymph node metastasis and worse prognosis in breast cancer patients [156], which are clinical characteristics also present in IBC patients, giving the impression that these CCN proteins could be involved in the aggressive phenotypes of IBCs. CCN2 is

associated with extracellular matrix remodeling and over-expression is associated with enhanced tumor growth and metastasis [189]. Additionally, CCN2 has been identified as one of the most significant genes induced by GPER signaling in TNBC SkBr3 [157]—providing the rationale of why we hypothesize that GPER is involved in gene transcription in TN-IBC cells and why it is reasonable to study the GPER signaling on TN-IBC SUM149.

Moreover, prostaglandin-endoperoxide synthase 2 (PTGS2; or cyclooxygenase-2/COX-2) and prostaglandin E2 receptor 4 (EP4) were reported as E2-upregulated at an early timepoint (45min). A recent study on IBC cells SUM149 and SUM190 revealed high levels of PTGS2 in both IBC cell lines and associated the EP4's role with the aggressive invasiveness phenotype of this lethal variant of breast cancer [158]. PTGS2 and EP4 could also be suggested as significant genes behind the invasive phenotypes induced by E2 on IBC cells and with possibilities of being considered as alternative markers for treatment options. Furthermore, the EZR gene, which encodes the Ezrin protein from the ERM (Ezrin/Radixin/Moesin) family of actin filament binding proteins, was identified as the most statistically significant E2-upregulated gene after 3 h exposure to E2 treatment. Elevated Ezrin expression has been associated with an increased risk of relapse in node-positive and high-risk node-negative breast cancer patients [159].

Ghaffari et al. reported that pharmacological inhibition of Ezrin has significantly reduced breast cancer cell migration and invasion into the lymph nodes and lungs *in vivo* [160]. In addition, a recent study showed that treatment with E2 on TNBC MDA-MB-231 cells resulted in Ezrin-dependent cytoskeleton rearrangement and elicited a stimulatory effect on cell migration and invasion. Importantly, they observed that Ezrin phosphorylation and the E2-induced enhancement of cell migration and invasion phenotypes were significantly inhibited by silencing

GPER signaling [161]—indicating that E2 induces the phosphorylation of Ezrin protein by GPER to mediate important cellular activities in TNBC cells. This approach could also be considered an alternative signaling pathway for therapeutic purposes for IBC patients. Altogether, this study provides a distinct group of genes that were upregulated by E2 stimulation on TN-IBC cells with the possibility of being essential factors behind the aggressive phenotypes of TN-IBC cancers. These genes can also be further studied as potential biomarkers for IBC cancer progression and prognosis predictions. In addition, some ER-regulated genes in TN-IBC are known to be regulated by GPER signaling in other breast cancers, which makes it reasonable to study the E2/GPER signaling route in more depth in TN-IBC.

Conclusions about acquired biological capabilities (e.g., hallmarks) can be reached by associating gene regulations with biological pathways or functional properties. Here, our list of the E2-regulated genes at an early stage of treatment (45 min) identified significantly enriched terms for molecular functions associated with transcriptional regulation—mainly transcription cis-regulatory region binding, RNA polymerase II transcription regulatory sequence-specific DNA binding, and DNA binding. The DNA binding term includes any molecular process by which proteins interact with DNA. Furthermore, some significantly enriched terms for molecular functions on the delayed E2-regulated genes included cadherin binding, protein kinase binding, and ATP binding. In addition, the E2-regulated genes were also highly enriched in the cellular component terms nucleus, focal adhesion, tight junction, and intracellular membrane-bounded organelle—which corresponded well with the recognized role of some of these genes (e.g., nuclear proteins, and cell adhesion molecules). These observations provide strong evidence of

an estrogen-regulated transcription network of early or primary response genes (rapidly activated in response to cellular stimuli) and delayed or secondary response genes in TN-IBC cells.

In addition, while many of these genes are associated with a wide range of biological processes, the most enriched GO terms for biological processes among the E2-treated groups included the regulation of the apoptotic process, regulation of cell differentiation, regulation of epithelial to mesenchymal transition, MAPK cascade, and cellular responses to cytokine stimulus. Interestingly, the most statistically significant terms for biological processes were associated with gene transcription, which indicates that the signaling cascades in response to estrogen stimulation on TN-IBC are primarily related to modulations in the frequency, rate, or extent of gene transcription. These observations imply that our hypothesis regarding the assumption that estrogen affects the transcription of genes essential for the progression of IBC tumorigenesis is not rejected and shows the complexity of the estrogen signaling in IBC cells despite being classified as an estrogen receptor-negative breast cancer.

In brief, our data provides a comprehensive analysis of the effects induced by estrogen stimulus on TN-IBC SUM149 cells, not only emphasizing the transcription of genes over periods of time but also identifying biological processes and functions properties relevant for understanding the progression of TN-IBC cancers under estrogen stimulation. The content of our study could help identify potential biomarkers involved in estrogen-induced carcinogenesis on IBC cells and possibly therapeutic targets for IBC patients.

II.   Aim #2: Characterize the effects of G15 on the estrogen signaling pathways on TN-IBC

Ohshiro et al., reported that E2 and G1 (GPER-specific agonist) stimulus was able to induce the activation of the extracellular-signal-regulated kinase (ERK1/2) on IBC cells, enhancing cell migration and invasion behaviors [151]—believed to be mediated by ERα36 and GPER. However, G-1 has been shown to induce the phosphorylation of ERK1/2 in GPER-negative HEK293 cells stably transfected with ERα36 [162-163]—suggesting that G-1 can also stimulate ERα36. Therefore, the exact role of ERα36 and GPER on the estrogen-induced ERK1/2 signal activation in triple-negative and HER2-amplified IBC models remains elusive. In this study, the GPER-specific antagonist G15 was used to identify the effects of GPER on the estrogen-induced signaling cascades, and the transcriptional changes reported after E2 treatment in our RNA-seq data. The results from these experiments may guide elucidate the role of GPER on IBC cells and on estrogen signaling. G15 was used since it has been shown to inhibit GPER-mediated proliferation stimulated by E2 and G-1 in other cancer cells— including A549 and H1793 cancer cell lines [164]. We aim to test our hypothesis that GPER has a direct role in mediating estrogen signals in IBC cells by measuring the effects of G15 and associating the results with the inhibition of the receptor.

KEGG pathway mapping on our RNA-seq analysis identified the IL-17 and the MAPK signaling pathways as two of the most statistically significant enriched terms associated with gene regulation at an early stage of E2 stimulus. Notably, the IL-17 signaling pathway is known to promote BC cells' proliferation, migration, invasion, and drug resistance through the ERK1/2 pathway [165]. The MAPK/ERK1/2 signaling pathway is known to lead to the activation and

regulation of many different genes associated with cancer progression [167], including the immediate-early response gene EGR1, Cyclin E, and the MAPK signaling cascade phosphatases DUSP6 (**Fig. 20A**). It is also known that GPER mediates the MAPK/ERK1/2 signaling pathway in ER-positive breast cancer, ER-negative breast cancer, and other estrogen-related carcinomas [168]. Therefore, there is the possibility that GPER could mediate the IL-17 signaling pathway and other signaling cascades by regulating the activation of the MAPK/ERK1/2 signal after the E2 stimulus. However, there is still a lack of evidence that GPER plays a significant role in mediating estrogen action on IBC cells.
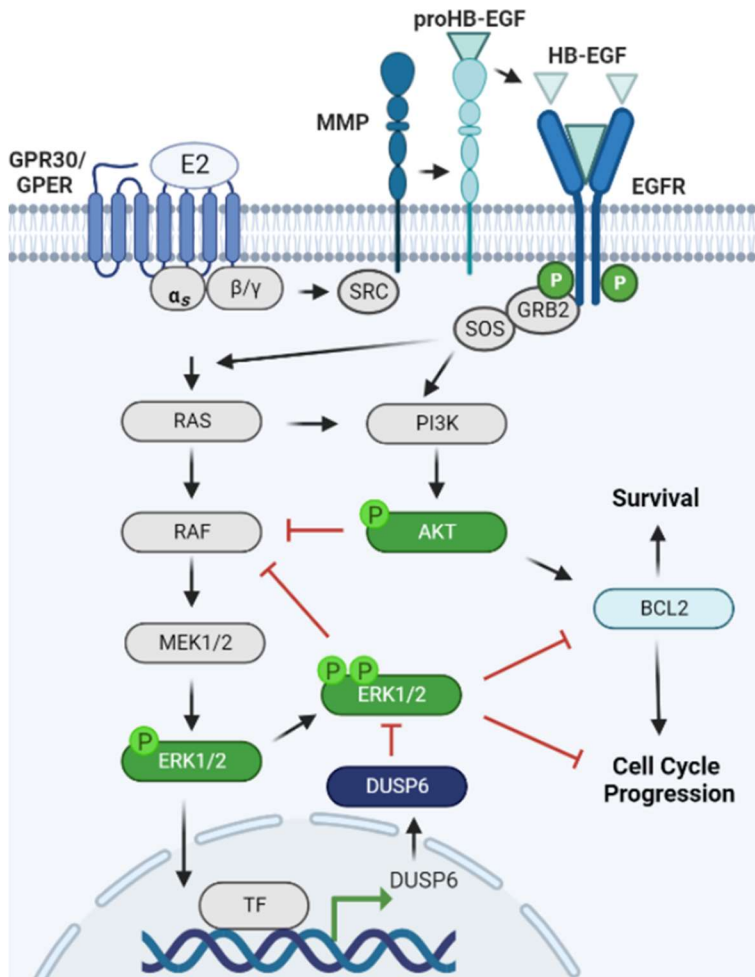
Figure 20. **Model of GPER signaling in breast cancer**

GPER activation in the plasma membrane stimulates steroid receptor coactivator (SRC) through a Gβγ-subunit protein pathway. The β and γ subunits of the G protein activate the SRC tyrosine kinase, which binds to the matrix metalloproteinase (MMP), which then cleaves the pro-heparin-binding EGF-like growth factor (proHB-EGF) and releases the heparin-binding EGF-like growth factor (HB-EGF) into the extracellular space. The free HB-EGF then transactivates the epidermal growth factor receptor (EGFR). Phosphorylation of EGFR activates the downstream pathways, which can induce rapid non-genomic effects, or genomic effects regulating the transcription of different genes involved in cell survival and proliferation. DUSP6 is a key negative feedback regulator of the member of the RAS-ERK MAPK signaling pathway—emanating from EGFR—associated with cellular proliferation. This molecular signaling mechanism is proposed on TN-IBC SUM149.

Here, the E2-induced activation of the ERK1/2 signaling pathway on two IBC cell models was confirmed under hormone-deprived conditions. Interestingly, G15 administration disrupted the E2-induced transient activation of the ERK1/2 signaling on TN-IBC cells, reporting a sustained level of ERK1/2 phosphorylation after E2 treatment. Sustained ERK1/2 activation induced by the GPER signaling has also been reported in hepatocellular carcinoma (e.g., HCCLM3 and SMMC-7721)—promoting apoptosis and inhibiting cell growth by blocking cell cycle progression [169]. However, this observation was seen after GPER activation by G-1—which contradicts our findings. Nonetheless, the biological functions of GPER have been inconsistent between different cell lines and organs for the past decade, and researchers have suggested that the biological effects of GPER may be specific to each cell line. Previous studies have also demonstrated that transient activation of ERK plays a pivotal role in cell proliferation and that sustained ERK activation induces cell cycle arrest and differentiation in mammalian cells [170]. Thus, our results suggest that GPER may play a tumor-promoting role in TN-IBC, and its inhibition may cause a decrease in cell viability by a sustained ERK1/2 signaling activation mechanism.

Furthermore, persistent activation of the ERK1/2 signaling has been associated with E2-mediated apoptosis in endocrine-resistant breast cancers as well as with negative regulation of the anti-apoptotic protein BCL-2 in other breast cancers [171, 172]. By western blot, a reduction in the expression of the BCL-2 protein was identified after TN-IBC cells were treated with E2 in combination with G15—supporting the BCL-2 reduction effect by persistent ERK1/2 activation. Interestingly, the IL-17 signaling pathway induces ERK1/2 activation to inhibit apoptosis and to upregulate BCL-2 expression—triggering the growth, proliferation, and migration of breast tumor cells [173]. Our RNA-seq results suggest that the estrogen signaling could crosstalk with the IL-

17 signaling pathway to promote oncogenic behaviors in TN-IBC—since E2 significantly upregulated genes involved in the IL-17 pathway. G15 administration could be disrupting not only the estrogen signaling pathway, but other signaling mechanisms that use ERK1/2 as an effector to carry out their signals—like the IL-17 pathway—through sustaining ERK1/2 activation. Thus, GPER may be an essential regulator of the ERK1/2 signaling cascade, and sustained activation of the ERK1/2 signaling may be a crucial mechanism behind the effects observed after G15 administration on TN-IBC cells. G15 treatment on TN-IBC SUM149 also showed to delay the E2-induced upregulation of DUSP6 phosphatase, which may be disrupting the DUSP6/ERK1/2 negative feedback-regulated loop—resulting in sustained phosphorylated levels of ERK1/2 (**Fig. 20**). However, more studies on the DUSP6/ERK1/2 regulatory loop are suggested in TN-IBC cells since we did not perform an experiment where we tested the suggested conclusions through the inhibition of the DUSP6/ERK1/2 signaling pathway.

Moreover, a previous research study with TNBC cell line MDA-MB-231 showed that estrogen-induced ERK1/2 activation required the expression of GPER—which transactivates the EGFR signaling pathway through HB-EGF [145-147]. HB-EGF—as well as one of its transcription regulators EGR1—are known to be mediated by the GPER/MEK/ERK1/2 signaling pathway, creating a positive feedback loop (**Fig. 21**). In addition, EGR1 upregulation has been shown to increase the transcription of the HB-EGF gene—resulting in autocrine activation of EGFR, and downstream MEK/ERK1/2 cascade [39]. This EGR1/HB-EGF/ERK1/2 signaling is known to be responsible for tumor development and progression in breast and prostate cancer [144, 174]. However, some studies have related EGR1 upregulation with cell proliferation inhibition in breast

cancer cells—promoting cell cycle arrest via downregulating Cyclin D [175]. Therefore, a deeper understanding of the EGR1 signaling networks in breast cancer cells is needed.
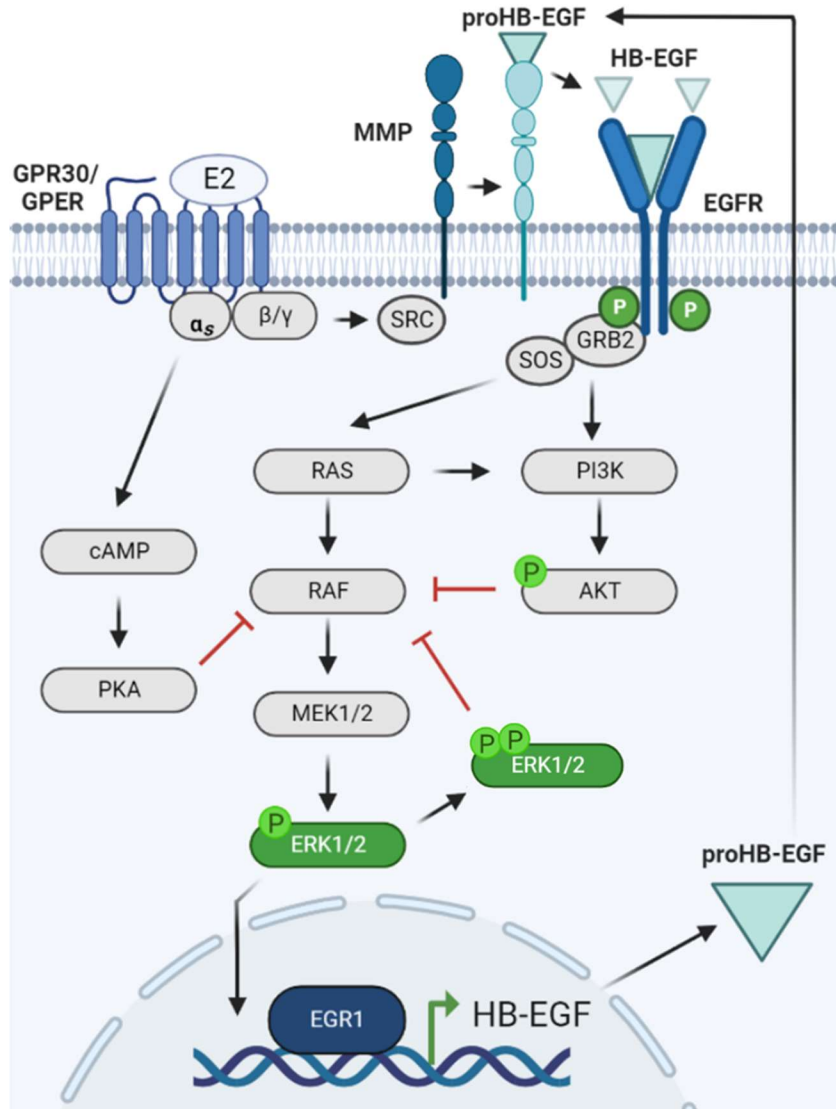
Figure 21. GPER signaling induced the upregulation of HB-EGF through EGRF/ERK signaling

The early growth response-1 (EGR1) transcription factor is induced downstream of EGFR signaling through the MEK/ERK pathway. EGR1 regulates the expression of several growth factors involved in tumor growth and spread—including the Heparin-binding EGF-like growth factor (HB-EGF) [183]. HB-EGF is a member of the EGF family of growth factors and is synthesized as a membrane-associated precursor molecule (proHB-EGF). ProHB-EGF is proteolytically cleaved to release a soluble ligand (Shb-EGF) that activates the EGF receptor [184]. GPER signaling uses HB-EGF to transactivate the EGFR signaling pathway. This is the proposed molecular mechanism behind the GPER signaling pathway on TN-IBC cells SUM149.

Our RNA-seq analysis—further validated through RT-qPCR—reported EGR1 and HB-EGF as two of the most statistically significant E2-upregulated genes in TN-IBC cells after E2 treatment. Interestingly, TN-IBC SUM149 previously treated with G15 and further exposed to E2 reported a sustained upregulation of EGR1, and HB-EGF mRNA expression—suggesting that G15 administration disrupted the mechanism that regulates the expression of these genes. This observation can be the result of two possible outcomes: (1) the E2/GPER/ERK1/2 signaling may be the route in which E2 regulates the expression of these genes and G15 inhibits this reaction, and (2) that the G15-induced upregulation of EGR1 and HB-EGF could lead to the activation of HB-EGF/EGFR signaling and thus sustaining the activation of the ERK1/2 signal. However, more studies are suggested on this manner. We also identified the E2-induced upregulation of the CCN1 gene on our RNA-seq data—a cell-adhesive substrate reported to be involved in the sustained activation of MAPK/ERK1/2 signaling [176]. However, we did not test whether G15 influenced the CCN1 expression.

Altogether, our results suggest that G15 administration may not necessarily inhibit the activation of the estrogen-induced ERK1/2 signal on TN-IBC cells but rather alter complex mechanisms involved in regulating these intracellular signaling cascades—possibly disrupting the estrogen non-genomic signaling and downstream effectors. In addition, the GPER/ERK1/2 signaling could be considered an essential mechanism behind E2-mediated signals, and GPER inhibition could be an effective therapeutic strategy for disrupting these estrogen signal cascades. These findings bring new insights into the possible regulatory role of GPER in estrogen-mediated signaling pathways and gene regulations in TN-IBC cells. However, the unspecific effects of the drug cannot be disregarded. Further studies conducting a GPER knockdown are

suggested to associate the observations provided in this study with the absence of the GPER. This approach can provide a better understanding of the regulatory role of the E2/GPER/ERK1/2 signaling pathway on triple-negative and HER2-amplified IBC cells.

III. Aim #3: Identify the effects of G15 on IBC's oncogenic phenotypes

GPER is a G protein-coupled estrogen receptor known to be expressed on the surface of various cell types, including breast cancer cells. Here, the presence of GPER protein was detected in all the assayed breast cancer cell lines, with a protein abundance statistically significant in TNBC MDA-MB-231 and HER2-amplified IBC SUM190 breast cancer cell lines. This observation goes in agreement with previous studies reporting strong GPER expression in triple-negative breast cancer cells (MDA-MB-231 and MDA-MB-436) and HER2-amplified breast tumors [177-178]. In addition, a possible variant of the GPER protein was identified on TNBC MDA-MB-231, TN-IBC SUM149, and HER2+ SUM190, reported as a smaller band on the western blot assay. This variant may be the result of the lack of post-translational modifications such as cleavage or attachment of small peptides. This variant could be in the cytoplasm, while the canonical version of the receptor is found in the plasma membrane and in the periphery of the nucleus—as seen in our immunofluorescence images. Furthermore, GPER mRNA levels varied significantly between the assayed breast cancer cell lines—suggesting individual post-transcriptional modifications regulating the protein steady state of GPER between each cell line.

Moreover, GPER is thought to be involved in the regulation of cancer cell proliferation and survival on IBC. Studies have shown that GPER activation can promote the growth and survival of IBC cells, and targeting GPER showed a reduction on IBC cell proliferation and induction of cell

death [136]. Here, administration of the GPER-specific antagonist G15 on triple-negative and HER2-amplified IBC cell lines significantly reduced the cell viability and growth rate in a dose-dependent matter. This observation suggests a protective role of GPER on both IBC cell lines against a starved environment—also reported in TNBC MDA-MB-468 [179-180]. Additionally, G15 administration reduced the cell viability and growth rate of triple-negative IBC SUM149 cells in the presence of estrogen—suggesting that G15 exerts its inhibitory effects even in the presence of estrogen. From a therapeutic perspective, this observation is relevant since G15 could be considered a candidate drug to inhibit cell growth on GPER-positive IBC patients even with normal levels of estrogen circulating in their bloodstream.

Along this line, previous studies have shown that TNBC cells that had cell viability reduction associated with the GPER signaling pathway also reported reduced levels of the cycle progression markers CDK2 and Cyclin E1 [179]. Here, we identify an estrogen-induced upregulation of Cyclin E1 after 12 h of E2 exposure on TN-IBC cells, which was significantly inhibited by G15 administration. This observation suggests that E2 may induce the cell cycle progression through an E2/GPER signaling pathway and that G15 administration may reduce the effects of E2 by inhibiting the E2/GPER signal. G15 administration also reduced the abundance of Cyclin E1 in HER2+ IBC SUM190 cells, but only when compared with the E2 group, suggesting that G15 may inhibit the E2-induced enhancement of Cyclin E1 on HER2+ IBC SUM190 cells.

Moreover, the E2/GPER/ERK1/2 signaling pathway has been associated with a high abundance of the anti-apoptotic BCL-2 protein and cell survival enhancement on TNBC [181]. **(Fig. 17A).** Here, TN-IBC cells SUM149 showed a slight E2-induced upregulation of BCL-2 protein abundance—which was significantly inhibited by the presence of G15 administration.

Similar results were seen in HER2-amplified IBC SUM190 cells, where G15 treatment significantly reduced the abundance of BCL-2 protein in the presence of E2. Furthermore, cleaved caspase-3 in SUM149 cells increased significantly after G15 treatment. These observations indicate that G15 treatment can activate apoptotic signaling in TN-IBC cell SUM149 and induce cell death—as the number of cells and cell viability was significantly reduced in our experiments.

The inhibitory effects of G15 on the expression of BCL-2 and Cyclin E1 after E2 treatment may be the result of the sustained ERK1/2 signaling activation induced by G15 treatment—since sustained p-ERK1/2 signaling has been associated with an induced cell cycle arrest in breast cancer cells [182]. Additionally, the inhibitory effects of G15 on the E2-induced protein expression of Cyclin E1 in IBC cells suggest that G15 administration may arrest the cell cycle at a specific phase in IBC cells. However, more studies are suggested to fully understand the effects of G15 on the expression of cell cycle-related markers on TN- and HER2-amplified IBC cells. Furthermore, G15 administration in Triple-negative IBC SUM149 was able to reduce the migratory enhancement induced by E2 treatment and the area/size of colony formation (measured in 3D culture), suggesting a possible involvement of GPER in this oncogenic behavior and the possibility of GPER to be a therapeutic candidate for reducing these aggressive behaviors on TN-IBC cancers.

Altogether, we have shown that G15 administration on triple-negative and HER2-amplified IBC cells can disrupt many regulated mechanisms induced by estrogen signaling—providing a rationale that the G15-induced disruption in the regulation of molecular pathways and gene expression previously described may be essential factors behind the reduced oncogenic characteristics seen on IBC cells after G15 administration. These observations may indicate a

tumor-promoting role for GPER in IBC cells, and its inhibition could be an effective strategy for IBC treatment purposes. However, more studies are suggested to fully understand the GPER's role on IBC cells since the non-specific effects of the G15 administration cannot be outlook in this study.

Chapter 5: Conclusions and future directions

In summary, this study characterizes the effects induced by estrogen stimulation on TN-IBC cells SUM149—emphasizing gene regulations, biological processes, molecular functions, and signaling pathways. To date, no other scientific study has published the transcriptome induced by estrogen on triple-negative IBC cell SUM149, making this study an essential resource for understanding the molecular mechanisms behind the estrogen-induced enhancement of TN-IBC's aggressive phenotypes. Moreover, alternate estrogen receptors remain the most active area in the estrogen signaling research field. However, the role of alternate ERs in breast cancer remains a matter of debate despite the increased scientific publications on the subject in the past decade. Here, we are interested in characterizing the role of GPER on TN-IBC cells and highlighting G15 as an essential inhibitory drug for key biological processes associated with cancer progression on triple-negative and HER2-amplified IBC cell lines.

We have demonstrated for the first time that G15 administration on triple-negative and HER2-amplified IBC cells reduces cell survival and growth rate in a dose-dependent manner, although HER2-amplified IBC cells were more resistant to G15 treatment. G15 also disrupts estrogen-mediated signals on triple-negative IBC, providing the rationale of why it is reasonable to consider GPER as a novel therapeutic target and to support G15-based studies on GPER-

positive IBC patients. Here, sustained activation of the ERK1/2 signal pathway was identified as one of the possible mechanisms behind the inhibitory effects of G15 administration on estrogen signals on triple-negative IBC. In addition, G15 disrupts the expression of genes that were identified as downstream targets of estrogen signal on our RNA-seq data, suggesting that GPER may also be involved in regulatory mechanisms behind estrogen genomic signals on triple-negative IBC. Thus, our data is not only functionally relevant to understand many biological processes mediated by estrogen signaling on triple-negative IBC cells, but also provides novel knowledge to continue unraveling the discrepancy in the role of GPER on triple-negative IBC cells.

However, although G15 is known to act as a specific GPER antagonist, the possibility of unspecific effects by the drug cannot be disregarded. Therefore, it is essential to perform a GPER protein expression inhibition (protein knockdown) on both IBC cell lines. The results obtained from this strategy should be compared with the results presented in this study to directly associate the inhibitory effects observed after G15 treatment with the inhibition of the GPER signaling pathway. This approach will validate our results and give a much more precise knowledge of the role of GPER in IBC cells. In addition, identifying crosstalk reactions between GPER and other signaling pathways can contribute to a better understanding of the molecular mechanism behind GPER signaling and guide the design of adjunctive therapies with G15. As an example, it is essential to conduct a study using a specific ERK1/2 (e.g., U0126) or EGFR signaling (e.g., gefitinib) inhibitory drug in combination with G15 on IBC cells. These would test whether there is a crosstalk between GPER and the EGFR signaling pathway and if the G15-induced sustained ERK1/2 activation is a crucial mechanism behind the inhibitory effects of G15.

Along this line, a previous study reported that Icaritin, a prenyflavonoid known to bind to ERα36, inhibited cell growth in MDA-MB-453 and MCF7 breast cancer cells through sustained activation of ERK1/2 signal—an effect further abrogated by the ERK1/2 phosphorylation inhibitory drug U0126 [185]. Since G15 treatment also induces sustain ERK1/2 activation on TN-IBC cells, it is reasonable to investigate possible crosstalk reaction between GPER and ERα36 with the primary goal of elucidating the complexity of the estrogen non-genomic signaling pathway in IBC cells. In addition, a crosstalk reaction between GPER and ERα36 has been reported in human monocytes [187], which supports why crosstalk reaction between these two alternate estrogen receptors is not ruled out on IBC cells. Combination therapy using Icaritin and G15 in the presence or absence of estrogen would be an excellent strategy to address the crosstalk hypothesis.

Furthermore, a phospho-kinase array after GPER inhibition (either by G15 treatment or protein knockdown) will provide a broad spectrum of possible GPER-signaling downstream targets that could be considered as druggable markers for novel therapeutic approaches against GPER-positive IBC patients. Likewise, RNA sequencing analysis after GPER inhibition would allow a deeper understanding of the transcriptome mediated by the GPER signal, and how it may reflect or contribute to the aggressiveness of IBC cells. We performed RNA-seq on TN-IBC cells after treatment with G15 alone and in combination with estrogen, but unfortunately, high variability was identified between the triplicates in each group and the assay was discontinued. Further studies on the transcriptional signature induced by GPER signaling are needed to fully elucidate the GPER signaling pathway. In brief, an extensive understanding of the expression and function of GPER, as well as other alternate estrogen receptors, and their target genes could shed light on how estrogen stimulates the initiation and promotion of cancer—providing a new approach to

diagnose and treat estrogen-responsive IBC cancers. Overall, GPER appears to play a significant

role in the pathogenesis of IBC and may represent a potential therapeutic target for the disease.

Reference

1. Breast cancer statistics: How common is breast cancer? [Internet]. Breast Cancer Statistics | How Common Is Breast Cancer? 2023 [cited 2023Mar29]. Available from: https://www.cancer.org/cancer/breast-cancer/about/how-common-is-breast-cancer.html.
2. Waks AG, Winer EP. Breast cancer treatment: a review. Jama. 2019 Jan 22;321(3):288-300.
3. Breast cancer - statistics [Internet]. Cancer.Net. 2023 [cited 2023Mar29]. Available from: https://www.cancer.net/cancer-types/breast-cancer/statistics
4. Fitzgibbons PL, Page DL, Weaver D, Thor AD, Allred DC, Clark GM, Ruby SG, O'Malley F, Simpson JF, Connolly JL, Hayes DF. Prognostic factors in breast cancer: College of American Pathologists consensus statement 1999. Archives of pathology & laboratory medicine. 2000 Jun;124(7):966-78.
5. Caughran J, Braun TM, Breslin TM, Smith DR, Kreinbrink JL, Parish GK, Davis AT, Bacon-Baguley TA, Silver SM, Henry NL. The Effect of the 2009 USPSTF breast cancer screening recommendations on breast cancer in Michigan: A longitudinal study. The breast journal. 2018 Sep;24(5):730-7.
6. Harris JR, Lippman ME, Osborne CK, Morrow M. Diseases of the Breast. Lippincott Williams & Wilkins; 2012 Mar 28.
7. Stebbing J, Delaney G, Thompson A. Breast cancer (non-metastatic). BMJ clinical evidence. 2011;2011.
8. The ACS medical and editorial content team (2022). Inflammatory Breast Cancer. cancer.org.https://www.cancer.org/cancer/breast-cancer/about/types-of-breast-cancer/inflammatory-breast-cancer.html
9. Hammond ME, Hayes DF, Dowsett M, Allred DC, Hagerty KL, Badve S, Fitzgibbons PL, Francis G, Goldstein NS, Hayes M, Hicks DG. American Society of Clinical Oncology/College of American Pathologists guideline recommendations for immunohistochemical testing of estrogen and progesterone receptors in breast cancer (unabridged version). Archives of pathology & laboratory medicine. 2010 Jul;134(7):e48-72.
10. Yersal O, Barutca S. Biological subtypes of breast cancer: Prognostic and therapeutic implications. World journal of clinical oncology. 2014 Aug 8;5(3):412.
11. Joshi H, Press MF. Molecular oncology of breast cancer. InThe Breast 2018 Jan 1 (pp. 282-307). Elsevier.
12. Chavez-MacGregor M, Mittendorf EA, Clarke CA, Lichtensztajn DY, Hunt KK, Giordano SH. Incorporating tumor characteristics to the American Joint Committee on Cancer breast cancer staging system. The oncologist. 2017 Nov;22(11):1292-300.

13. Bardia A, Mayer IA, Diamond JR, Moroose RL, Isakoff SJ, Starodub AN, Shah NC, O'Shaughnessy J, Kalinsky K, Guarino M, Abramson V. Efficacy and safety of anti-trop-2 antibody drug conjugate sacituzumab govitecan (IMMU-132) in heavily pretreated patients with metastatic triple-negative breast cancer. Journal of Clinical Oncology. 2017 Jul 7;35(19):2141.

14. Swain SM, Baselga J, Kim SB, Ro J, Semiglazov V, Campone M, Ciruelos E, Ferrero JM, Schneeweiss A, Heeson S, Clark E. Pertuzumab, trastuzumab, and docetaxel in HER2-positive metastatic breast cancer. New England journal of medicine. 2015 Feb 19;372(8):724-34.

15. Robertson JF, Llombart-Cussac A, Feltl D, Dewar J, Jasiowka M, Hewson N, Rukazenkov Y, Ellis M. Fulvestrant 500 mg versus anastrozole as first-line treatment for advanced breast cancer: overall survival from the phase II 'first'study. Cancer Res. 2015 May 1;75(suppl 9).

16. Carey LA, Perou CM, Livasy CA, Dressler LG, Cowan D, Conway K, Karaca G, Troester MA, Tse CK, Edmiston S, Deming SL. Race, breast cancer subtypes, and survival in the Carolina Breast Cancer Study. Jama. 2006 Jun 7;295(21):2492-502.

17. Denkert C, Liedtke C, Tutt A, von Minckwitz G. Molecular alterations in triple-negative breast cancer—the road to new treatment strategies. The Lancet. 2017 Jun 17;389(10087):2430-42.

18. Morris GJ, Naidu S, Topham AK, Guiles F, Xu Y, McCue P, Schwartz GF, Park PK, Rosenberg AL, Brill K, Mitchell EP. Differences in breast carcinoma characteristics in newly diagnosed African–American and Caucasian patients: A single-institution compilation compared with the National Cancer Institute's Surveillance, Epidemiology, and end results database. Cancer: Interdisciplinary International Journal of the American Cancer Society. 2007 Aug 15;110(4):876-84.

19. Foulkes WD, Smith IE, Reis-Filho JS. Triple-negative breast cancer. New England journal of medicine. 2010 Nov 11;363(20):1938-48

20. Dent R, Trudeau M, Pritchard KI, Hanna WM, Kahn HK, Sawka CA, Lickley LA, Rawlinson E, Sun P, Narod SA. Triple-negative breast cancer: clinical features and patterns of recurrence. Clinical cancer research. 2007 Aug 1;13(15):4429-34.

21. Haffty BG, Yang Q, Reiss M, Kearney T, Higgins SA, Weidhaas J, Harris L, Hait W, Toppmeyer D. Locoregional relapse and distant metastasis in conservatively managed triple negative early-stage breast cancer. Journal of clinical oncology. 2006 Dec 20;24(36):5652-7.

22. Foulkes WD, Smith IE, Reis-Filho JS. Triple-negative breast cancer. New England journal of medicine. 2010 Nov 11;363(20):1938-48.

23. Nofech-Mozes S, Trudeau M, Kahn HK, Dent R, Rawlinson E, Sun P, Narod SA, Hanna WM. Patterns of recurrence in the basal and non-basal subtypes of triple-negative breast cancers. Breast cancer research and treatment. 2009 Nov;118(1):131-7

24. Linderholm BK, Klintman M, Grabau D, Bendahl P, Ferno M, Per M. Significantly higher expression of vascular endothelial growth factor (VEGF) and shorter survival after recurrences in premenopausal node negative patients with triple negative breast cancer. Cancer Research. 2009 Jan 15;69(2_Supplement):1077.

25. Anders CK, Winer EP, Ford JM, Dent R, Silver DP, Sledge GW, Carey LA. Poly (ADP-Ribose) polymerase inhibition:"targeted" therapy for triple-negative breast cancer. Clinical Cancer Research. 2010 Oct 1;16(19):4702-10.

26. Zimmer AS, Gillard M, Lipkowitz S, Lee JM. Update on PARP inhibitors in breast cancer. Current treatment options in oncology. 2018 May;19(5):1-9.

27. Siziopikou KP, Ariga R, Proussaloglou KE, Gattuso P, Cobleigh M. The challenging estrogen receptor-negative/progesterone receptor-negative/HER-2-negative patient: a promising candidate for epidermal growth factor receptor-targeted therapy? The breast journal. 2006 Jul;12(4):360-2.

28. Van Uden DJ, Van Laarhoven HW, Westenberg AH, de Wilt JH, Blanken-Peeters CF. Inflammatory breast cancer: an overview. Critical reviews in oncology/hematology. 2015 Feb 1;93(2):116-26.

29. The ACS medical and editorial content team (2022). Inflammatory Breast Cancer. cancer.org.https://www.cancer.org/cancer/breast-cancer/about/types-of-breast-cancer/inflammatory-breast-cancer.html

30. Sartorius CA, Hanna CT, Gril B, Cruz H, Serkova NJ, Huber KM, Kabos P, Schedin TB, Borges VF, Steeg PS, Cittelly DM. Estrogen promotes the brain metastatic colonization of triple negative breast cancer cells via an astrocyte-mediated paracrine mechanism. Oncogene. 2016 Jun;35(22):2881-92.

31. Levine PH, Veneroso C. The epidemiology of inflammatory breast cancer. InSeminars in oncology 2008 Feb 1 (Vol. 35, No. 1, pp. 11-16). WB Saunders.

32. Yang WT, Le-Petross HT, Macapinlac H, Carkaci S, Gonzalez-Angulo AM, Dawood S, Resetkova E, Hortobagyi GN, Cristofanilli M. Inflammatory breast cancer: PET/CT, MRI, mammography, and sonography findings. Breast cancer research and treatment. 2008 Jun;109(3):417-26.

33. Hance KW, Anderson WF, Devesa SS, Young HA, Levine PH. Trends in inflammatory breast carcinoma incidence and survival: the surveillance, epidemiology, and end results program at the National Cancer Institute. Journal of the National Cancer Institute. 2005 Jul 6;97(13):966-75.

34. Chevallier B, Roche H, Olivier JP, Chollet P, Hurteloup P. Inflammatory breast cancer: pilot study of intensive induction chemotherapy (FEC-HD) results in a high histologic response rate. American journal of clinical oncology. 1993 Jun 1;16(3):223-8.

35. Ueno NT, Buzdar AU, Singletary SE, Ames FC, McNeese MD, Holmes FA, Theriault RL, Strom EA, Wasaff BJ, Asmar L, Frye D. Combined-modality treatment of inflammatory breast carcinoma: twenty years of experience at MD Anderson Cancer Center. Cancer chemotherapy and pharmacology. 1997 Jun;40(4):321-9.

36. Gianni L, Eiermann W, Semiglazov V, Manikhas A, Lluch A, Tjulandin S, Zambetti M, Vazquez F, Byakhow M, Lichinitser M, Climent MA. Neoadjuvant chemotherapy with trastuzumab followed by adjuvant trastuzumab versus neoadjuvant chemotherapy alone, in patients with HER2-positive locally advanced breast cancer (the NOAH trial): a randomised controlled superiority trial with a parallel HER2-negative cohort. The Lancet. 2010 Jan 30;375(9712):377-84.

37. Kleer CG, van Golen KL, Merajver SD. Molecular biology of breast cancer metastasis Inflammatory breast cancer: clinical syndrome and molecular determinants. Breast Cancer Research. 2000 Dec;2(6):1-7.

38. Zell JA, Tsang WY, Taylor TH, Mehta RS, Anton-Culver H. Prognostic impact of human epidermal growth factor-like receptor 2 and hormone receptor status in inflammatory breast cancer (IBC): analysis of 2,014 IBC patient cases from the California Cancer Registry. Breast Cancer Research. 2009 Jun;11(1):1-0.

39. Cabioglu N, Gong Y, Islam R, Broglio KR, Sneige N, Sahin A, Gonzalez-Angulo AM, Morandi P, Bucana C, Hortobagyi GN, Cristofanilli M. Expression of growth factor and chemokine receptors: new insights in the biology of inflammatory breast cancer. Annals of oncology. 2007 Jun 1;18(6):1021-9.

40. Woodward WA, Cristofanilli M. Inflammatory breast cancer. InSeminars in radiation oncology 2009 Oct 1 (Vol. 19, No. 4, pp. 256-265). WB Saunders.

41. Bennink HJ. Are all estrogens the same?. Maturitas. 2004 Apr 15;47(4):269-75.

42. Burgess AW. Growth factors and their receptors: specific roles in development. BioEssays. 1987 Feb;6(2):79-81.

43. Cabioglu N, Gong Y, Islam R, Broglio KR, Sneige N, Sahin A, Gonzalez-Angulo AM, Morandi P, Bucana C, Hortobagyi GN, Cristofanilli M. Expression of growth factor and chemokine receptors: new insights in the biology of inflammatory breast cancer. Annals of oncology. 2007 Jun 1;18(6):1021-9.

44. Zell JA, Tsang WY, Taylor TH, Mehta RS, Anton-Culver H. Prognostic impact of human epidermal growth factor-like receptor 2 and hormone receptor status in inflammatory breast cancer (IBC): analysis of 2,014 IBC patient cases from the California Cancer Registry. Breast Cancer Research. 2009 Jun;11(1):1-0.

45. Rusnak DW, Affleck K, Cockerill SG, Stubberfield C, Harris R, Page M, Smith KJ, Guntrip SB, Carter MC, Shaw RJ, Jowett A. The characterization of novel, dual ErbB-2/EGFR, tyrosine kinase inhibitors: potential therapy for cancer. Cancer research. 2001 Oct 1;61(19):7196-203.

46. Dawood S, Ueno NT, Valero V, Andreopoulou E, Hsu L, Lara J, Woodward W, Buchholz TA, Hortobagyi GN, Cristofanilli M. Incidence of and survival following brain metastases among women with inflammatory breast cancer. Annals of oncology. 2010 Dec 1;21(12):2348-55.

47. Dawood S, Ueno NT, Valero V, Woodward WA, Buchholz TA, Hortobagyi GN, Gonzalez-Angulo AM, Cristofanilli M. Differences in survival among women with stage III inflammatory and noninflammatory locally advanced breast cancer appear early: a large population-based study. Cancer. 2011 May 1;117(9):1819-26.

48. Chaher N, Arias-Pulido H, Terki N, Qualls C, Bouzid K, Verschraegen C, Wallace AM, Royce M. Molecular and epidemiological characteristics of inflammatory breast cancer in Algerian patients. Breast cancer research and treatment. 2012 Jan;131:437-44.

49. Masuda H, Baggerly KA, Wang Y, Iwamoto T, Brewer T, Pusztai L, Kai K, Kogawa T, Finetti P, Birnbaum D, Dirix L. Comparison of molecular subtype distribution in triple-negative inflammatory and non-inflammatory breast cancers. Breast Cancer Research. 2013 Dec;15:1-9.

50. Simpson ER, Davis SR. Minireview: aromatase and the regulation of estrogen biosynthesis—some new perspectives. Endocrinology. 2001 Nov 1;142(11):4589-94.
51. Fuentes N, Silveyra P. Estrogen receptor signaling mechanisms. Advances in protein chemistry and structural biology. 2019 Jan 1;116:135-70.
52. Folkerd EJ, Dowsett M. Influence of sex hormones on cancer progression. Journal of Clinical Oncology. 2010 Sep 10;28(26):4038-44.
53. Urano T, Saito T, Tsukui T, Fujita M, Hosoi T, Muramatsu M, et al. Efp targets 14-3-3 sigma for proteolysis and promotes breast tumour growth. Nature. 2002;417:871–5.
54. Colditz GA, Rosner BA, Chen WY, Holmes MD, Hankinson SE. Risk factors for breast cancer according to estrogen and progesterone receptor status. Journal of the national cancer institute. 2004 Feb 4;96(3):218-28.
55. Ikeda K, Horie-Inoue K, Inoue S. Identification of estrogen-responsive genes based on the DNA binding properties of estrogen receptors using high-throughput sequencing technology. Acta Pharmacologica Sinica. 2015 Jan;36(1):24-31.
56. Wu C, Zhang HF, Gupta N, Alshareef A, Wang Q, Huang YH, et al. A positive feedback loop involving the Wnt/β-catenin/MYC/Sox2 axis defines a highly tumorigenic cell subpopulation in ALK-positive anaplastic large cell lymphoma. J Hematol Oncol. 2016;9:120.
57. Urano T, Saito T, Tsukui T, Fujita M, Hosoi T, Muramatsu M, et al. Efp targets 14-3-3 sigma for proteolysis and promotes breast tumour growth. Nature. 2002;417:871–5.
58. Le Mellay V, Grosse B, Lieberherr M. Phospholipase C β and membrane action of calcitriol and estradiol. Journal of Biological Chemistry. 1997 May 2;272(18):11902-7.
59. Razandi M, et al. Cell membrane and nuclear estrogen receptors (ERs) originate from a single transcript: studies of ERalpha and ERbeta expressed in Chinese hamster ovary cells. Mol Endocrinol. 1999;13(2):307–19.
60. Simoncini T, Genazzani AR. Non-genomic actions of sex steroid hormones. Eur J Endocrinol. 2003;148(3):281–92.
61. Baum M, Budzar AU, Cuzick J, Forbes J, Houghton JH, Klijn JG, Sahmoud TA. ATAC Trialists' Group (2002) Anastrozole alone or in combination with tamoxifen versus tamoxifen alone for adjuvant treatment of postmenopausal women with early breast cancer: first results of the ATAC randomised trial. Lancet. 2002;359(9324):2131-9.
62. Taylor SE, Martin-Hirsch PL, Martin FL. Oestrogen receptor splice variants in the pathogenesis of disease. Cancer letters. 2010 Feb 28;288(2):133-48.
63. Kampa M, Pelekanou V, Notas G, Stathopoulos EN, Castanas E. The estrogen receptor: two or more molecules, multiple variants, diverse localizations, signaling and functions. Are we undergoing a paradigm-shift as regards their significance in breast cancer?. Hormones. 2013 Jan;12(1):69-85.
64. Irsik DL, Carmines PK, Lane PH. Classical estrogen receptors and ERα splice variants in the mouse. PloS one. 2013 Aug 5;8(8):e70926.
65. Adlanmerini M, Solinhac R, Abot A, Fabre A, Raymond-Letron I, Guihot AL, et al. Mutation of the palmitoylation site of estrogen receptor α in vivo reveals tissue-specific roles for membrane versus nuclear actions. Proc Natl Acad Sci USA. 2014;111:E283–90.

66. Omarjee S, Jacquemetton J, Poulard C, Rochel N, Dejaegere A, Chebaro Y, et al. The molecular mechanisms underlying the ERα-36-mediated signaling in breast cancer. Oncogene. 2017;36:2503–14.

67. Sun Q, Liang Y, Zhang T, Wang K, Yang X. ER-α36 mediates estrogen-stimulated MAPK/ERK activation and regulates migration, invasion, proliferation in cervical cancer cells. Biochem Biophys Res Commun. 2017;487:625–32

68. The ACS medical and editorial content team (2022). Inflammatory Breast Cancer. cancer.org. https://www.cancer.org/cancer/breast-cancer/about/types-of-breast-cancer/inflammatory-breast-cancer.html

69. Carmeci C, Thompson DA, Ring HZ, Francke U, Weigel RJ. Identification of a gene (GPR30) with homology to the G-protein-coupled receptor superfamily associated with estrogen receptor expression in breast cancer. Genomics. 1997 Nov 1;45(3):607-17.

70. Takada Y, Kato C, Kondo S, Korenaga R, Ando J. Cloning of cDNAs encoding G protein-coupled receptor expressed in human endothelial cells exposed to fluid shear stress. Biochemical and biophysical research communications. 1997 Nov 26;240(3):737-41.

71. Revankar CM, Cimino DF, Sklar LA, Arterburn JB, Prossnitz ER. A transmembrane intracellular estrogen receptor mediates rapid cell signaling. Science. 2005 Mar 11;307(5715):1625-30.

72. O'Dowd BF, Nguyen T, Marchese A, Cheng R, Lynch KR, Heng HH, Kolakowski Jr LF, George SR. Discovery of three novel G-protein-coupled receptor genes. Genomics. 1998 Jan 15;47(2):310-3.

73. Owman C, Blay P, Nilsson C, Lolait SJ. Cloning of human cDNA encoding a novel heptahelix receptor expressed in Burkitt's lymphoma and widely distributed in brain and peripheral tissues. Biochemical and biophysical research communications. 1996 Nov 12;228(2):285-92.

74. Feng Y, Gregor P. Cloning of a novel member of the G protein-coupled receptor family related to peptide receptors. Biochemical and biophysical research communications. 1997 Feb 24;231(3):651-4.

75. Rae JM, Johnson MD. What does an orphan G-protein-coupled receptor have to do with estrogen?. Breast Cancer Research. 2005 Dec;7:1-2.

76. Thomas P, Pang Y, Filardo EJ, Dong J. Identity of an estrogen membrane receptor coupled to a G protein in human breast cancer cells. Endocrinology. 2005 Feb 1;146(2):624-32.

77. Hsieh YC, Yu HP, Frink M, Suzuki T, Choudhry MA, Schwacha MG, Chaudry IH. G protein-coupled receptor 30-dependent protein kinase A pathway is critical in nongenomic effects of estrogen in attenuating liver injury after trauma-hemorrhage. The American journal of pathology. 2007 Apr 1;170(4):1210-8.

78. Alexander SP, Mathie A, Peters JA. Guide to receptors and channels (GRAC). British journal of pharmacology. 2011 Nov;164:S1-2.

79. Gaudet HM, Cheng SB, Christensen EM, Filardo EJ. The G-protein coupled estrogen receptor, GPER: The inside and inside-out story. Molecular and cellular endocrinology. 2015 Dec 15;418:207-19.

80. Thomas P, Pang Y, Filardo EJ, Dong J. Identity of an estrogen membrane receptor coupled to a G protein in human breast cancer cells. Endocrinology. 2005 Feb 1;146(2):624-32.

81. Revankar CM, Cimino DF, Sklar LA, Arterburn JB, Prossnitz ER. A transmembrane intracellular estrogen receptor mediates rapid cell signaling. Science. 2005 Mar 11;307(5715):1625-30.

82. Kuiper GG, Carlsson BO, Grandien KA, Enmark E, Häggblad J, Nilsson S, Gustafsson JA. Comparison of the ligand binding specificity and transcript tissue distribution of estrogen receptors α and β. Endocrinology. 1997 Mar 1;138(3):863-70.

83. Vivacqua A, Romeo E, De Marco P, De Francesco EM, Abonante S, Maggiolini M. GPER mediates the Egr-1 expression induced by 17β-estradiol and 4-hydroxitamoxifen in breast and endometrial cancer cells. Breast cancer research and treatment. 2012 Jun;133:1025-35.

84. Lappano R, Rosano C, F Santolla M, Pupo M, M De Francesco E, De Marco P, Ponassi M, Spallarossa A, Ranise A, Maggiolini M. Two novel GPER agonists induce gene expression changes and growth effects in cancer cells. Current cancer drug targets. 2012 Jun 1;12(5):531-42.

85. Lappano R, Santolla MF, Pupo M, Sinicropi MS, Caruso A, Rosano C, Maggiolini M. MIBE acts as antagonist ligand of both estrogen receptor α and GPER in breast cancer cells. Breast Cancer Research. 2012 Feb;14:1-3.

86. Prossnitz ER, Barton M. The G-protein-coupled estrogen receptor GPER in health and disease. Nature Reviews Endocrinology. 2011 Dec;7(12):715-26.

87. Molina L, Bustamante FA, Bhoola KD, Figueroa CD, Ehrenfeld P. Possible role of phytoestrogens in breast cancer via GPER-1/GPR30 signaling. Clinical Science. 2018 Dec 13;132(24):2583-98.

88. Gao F, Huang Y, Zhang L, Liu W. Involvement of estrogen receptor and GPER in bisphenol A induced proliferation of vascular smooth muscle cells. Toxicology in Vitro. 2019 Apr 1;56:156-62.

89. Castillo-Sanchez R, Ramirez-Ricardo J, Martinez-Baeza E, Cortes-Reynosa P, Candanedo-Gonzales F, Gomez R, Salazar EP. Bisphenol A induces focal adhesions assembly and activation of FAK, Src and ERK2 via GPER in MDA-MB-231 breast cancer cells. Toxicology in Vitro. 2020 Aug 1;66:104871.

90. Vivacqua A, Bonofiglio D, Recchia AG, Musti AM, Picard D, Andò S, Maggiolini M. The G protein-coupled receptor GPR30 mediates the proliferative effects induced by 17β-estradiol and hydroxytamoxifen in endometrial cancer cells. Molecular endocrinology. 2006 Mar 1;20(3):631-46.

91. Thomas P, Pang Y, Filardo EJ, Dong J. Identity of an estrogen membrane receptor coupled to a G protein in human breast cancer cells. Endocrinology. 2005 Feb 1;146(2):624-32.

92. Bologa CG, Revankar CM, Young SM, Edwards BS, Arterburn JB, Kiselyov AS, Parker MA, Tkachenko SE, Savchuck NP, Sklar LA, Oprea TI. Virtual and biomolecular screening converge on a selective agonist for GPR30. Nature chemical biology. 2006 Apr;2(4):207-12.

93. Dennis MK, Field AS, Burai R, Ramesh C, Petrie WK, Bologa CG, Oprea TI, Yamaguchi Y, Hayashi SI, Sklar LA, Hathaway HJ. Identification of a GPER/GPR30 antagonist with improved estrogen receptor counterselectivity. The Journal of steroid biochemistry and molecular biology. 2011 Nov 1;127(3-5):358-66.

94. Lappano R, Rosano C, F Santolla M, Pupo M, M De Francesco E, De Marco P, Ponassi M, Spallarossa A, Ranise A, Maggiolini M. Two novel GPER agonists induce gene expression changes and growth effects in cancer cells. Current cancer drug targets. 2012 Jun 1;12(5):531-42.

95. Petrie WK, Dennis MK, Hu C, Dai D, Arterburn JB, Smith HO, Hathaway HJ, Prossnitz ER. G protein-coupled estrogen receptor-selective ligands modulate endometrial tumor growth. Obstetrics and gynecology international. 2013 Oct;2013.

96. Chan QK, Lam HM, Ng CF, Lee AY, Chan ES, Ng HK, Ho SM, Lau KM. Activation of GPR30 inhibits the growth of prostate cancer cells through sustained activation of Erk1/2, c-jun/c-fos-dependent upregulation of p21, and induction of G2 cell-cycle arrest. Cell Death & Differentiation. 2010 Sep;17(9):1511-23.

97. Dennis MK, Field AS, Burai R, Ramesh C, Petrie WK, Bologa CG, Oprea TI, Yamaguchi Y, Hayashi SI, Sklar LA, Hathaway HJ. Identification of a GPER/GPR30 antagonist with improved estrogen receptor counterselectivity. The Journal of steroid biochemistry and molecular biology. 2011 Nov 1;127(3-5):358-66.

98. Bai LY, Weng JR, Hu JL, Wang D, Sargeant AM, Chiu CF. G15, a GPR30 antagonist, induces apoptosis and autophagy in human oral squamous carcinoma cells. Chemico-biological interactions. 2013 Nov 25;206(2):375-84.

99. Thomas P, Pang Y, Filardo EJ, Dong J. Identity of an estrogen membrane receptor coupled to a G protein in human breast cancer cells. Endocrinology. 2005 Feb 1;146(2):624-32.

100.   Revankar CM, Cimino DF, Sklar LA, Arterburn JB, Prossnitz ER. A transmembrane intracellular estrogen receptor mediates rapid cell signaling. Science. 2005 Mar 11;307(5715):1625-30.

101.   Cheung CC, Thornton JE, Kuijper JL, Weigle DS, Clifton DK, Steiner RA. Leptin is a metabolic gate for the onset of puberty in the female rat. Endocrinology. 1997 Feb 1;138(2):855-8.

102.   Yin G, Zeng B, Peng Z, Liu Y, Sun L, Liu C. Synthesis and application of 131I-fulvestrant as a targeted radiation drug for endocrine therapy in human breast cancer. Oncology Reports. 2018 Mar 1;39(3):1215-26.

103.   Vivacqua A, Bonofiglio D, Albanito L, Madeo A, Rago V, Carpino A, Musti AM, Picard D, Andò S, Maggiolini M. 17β-Estradiol, genistein, and 4-hydroxytamoxifen induce the proliferation of thyroid cancer cells through the G protein-coupled receptor GPR30. Molecular pharmacology. 2006 Oct 1;70(4):1414-23.

104.   Luo J, Wang A, Zhen W, Wang Y, Si H, Jia Z, Alkhalidy H, Cheng Z, Gilbert E, Xu B, Liu D. Phytonutrient genistein is a survival factor for pancreatic β-cells via GPR30-mediated mechanism. The Journal of nutritional biochemistry. 2018 Aug 1;58:59-70.

105.   Vivacqua A, Bonofiglio D, Albanito L, Madeo A, Rago V, Carpino A, Musti AM, Picard D, Andò S, Maggiolini M. 17β-Estradiol, genistein, and 4-hydroxytamoxifen induce the proliferation of thyroid cancer cells through the G protein-coupled receptor GPR30. Molecular pharmacology. 2006 Oct 1;70(4):1414-23.

106.   Filardo EJ, Quinn JA, Bland KI, Frackelton Jr AR. Estrogen-induced activation of Erk-1 and Erk-2 requires the G protein-coupled receptor homolog, GPR30, and occurs via trans-activation of the epidermal growth factor receptor through release of HB-EGF. Molecular endocrinology. 2000 Oct 1;14(10):1649-60.

107.   Dennis MK, Field AS, Burai R, Ramesh C, Petrie WK, Bologa CG, Oprea TI, Yamaguchi Y, Hayashi SI, Sklar LA, Hathaway HJ. Identification of a GPER/GPR30 antagonist with improved estrogen receptor counterselectivity. The Journal of steroid biochemistry and molecular biology. 2011 Nov 1;127(3-5):358-66.

108.   Lappano R, Rosano C, F Santolla M, Pupo M, M De Francesco E, De Marco P, Ponassi M, Spallarossa A, Ranise A, Maggiolini M. Two novel GPER agonists induce gene expression changes and growth effects in cancer cells. Current cancer drug targets. 2012 Jun 1;12(5):531-42.

109.   Lappano R, Santolla MF, Pupo M, Sinicropi MS, Caruso A, Rosano C, Maggiolini M. MIBE acts as antagonist ligand of both estrogen receptor α and GPER in breast cancer cells. Breast Cancer Research. 2012 Feb;14:1-3.

110.   Smith LC, Ralston-Hooper KJ, Ferguson PL, Sabo-Attwood T. The G protein-coupled estrogen receptor agonist G-1 inhibits nuclear estrogen receptor activity and stimulates novel phosphoproteomic signatures. Toxicological Sciences. 2016 Jun 1;151(2):434-46.

111.   Petrie WK, Dennis MK, Hu C, Dai D, Arterburn JB, Smith HO, Hathaway HJ, Prossnitz ER. G protein-coupled estrogen receptor-selective ligands modulate endometrial tumor growth. Obstetrics and gynecology international. 2013 Oct;2013.

112.   Thomas P, Dong J. Binding and activation of the seven-transmembrane estrogen receptor GPR30 by environmental estrogens: a potential novel mechanism of endocrine disruption. The Journal of steroid biochemistry and molecular biology. 2006 Dec 1;102(1-5):175-9.

113.   Dennis MK, Burai R, Ramesh C, Petrie WK, Alcon SN, Nayak TK, Bologa CG, Leitao A, Brailoiu E, Deliu E, Dun NJ. In vivo effects of a GPR30 antagonist. Nature chemical biology. 2009 Jun;5(6):421-7.

114.   Dennis MK, Burai R, Ramesh C, Petrie WK, Alcon SN, Nayak TK, Bologa CG, Leitao A, Brailoiu E, Deliu E, Dun NJ. In vivo effects of a GPR30 antagonist. Nature chemical biology. 2009 Jun;5(6):421-7.

115.   Prossnitz ER, Barton M. Estrogen biology: new insights into GPER function and clinical opportunities. Molecular and cellular endocrinology. 2014 May 25;389(1-2):71-83.

116.   Barton M, Filardo EJ, Lolait SJ, Thomas P, Maggiolini M, Prossnitz ER. Twenty years of the G protein-coupled estrogen receptor GPER: Historical and personal perspectives. The Journal of steroid biochemistry and molecular biology. 2018 Feb 1;176:4-15.

117.   Lappano R, Mallet C, Rizzuti B, Grande F, Galli GR, Byrne C, Broutin I, Eschalier A, Jacquot Y, Maggiolini M. The peptide ERα17p is a GPER inverse agonist that exerts antiproliferative effects in breast cancer cells. Cells. 2019 Jun 14;8(6):590.

118.   Trichet M, Lappano R, Belnou M, Salazar Vazquez LS, Alves I, Ravault D, Sagan S, Khemtemourian L, Maggiolini M, Jacquot Y. Interaction of the anti-proliferative GPER inverse agonist ERα17p with the breast cancer cell plasma membrane: from biophysics to biology. Cells. 2020 Feb 15;9(2):447.

119.   Lappano R, Mallet C, Rizzuti B, Grande F, Galli GR, Byrne C, Broutin I, Eschalier A, Jacquot Y, Maggiolini M. The peptide ERα17p is a GPER inverse agonist that exerts antiproliferative effects in breast cancer cells. Cells. 2019 Jun 14;8(6):590.

120.   Carnesecchi J, Malbouyres M, de Mets R, Balland M, Beauchef G, Vie K, Chamot C, Lionnet C, Ruggiero F, Vanacker JM. Estrogens induce rapid cytoskeleton re-organization

in human dermal fibroblasts via the non-classical receptor GPR30. PLoS One. 2015 Mar 17;10(3):e0120672.

121.   Vivacqua A, Bonofiglio D, Albanito L, Madeo A, Rago V, Carpino A, Musti AM, Picard D, Andò S, Maggiolini M. 17β-Estradiol, genistein, and 4-hydroxytamoxifen induce the proliferation of thyroid cancer cells through the G protein-coupled receptor GPR30. Molecular pharmacology. 2006 Oct 1;70(4):1414-23.

122.   Vivacqua A, Bonofiglio D, Recchia AG, Musti AM, Picard D, Ando S, Maggiolini M. The G protein-coupled receptor GPR30 mediates the proliferative effects induced by 17b-estradiol and hydroxytamoxifen in endometrial cancer cells. Mol Endocrinol 2005

123.   Mungenast F, Thalhammer T. Estrogen biosynthesis and action in ovarian cancer. Frontiers in endocrinology. 2014 Nov 12;5:192.

124.   Maggiolini M, Vivacqua A, Fasanella G, Recchia AG, Sisci D, Pezzi V, Montanaro D, Musti AM, Picard D, Andò S. The G protein-coupled receptor GPR30 mediates c-fos up-regulation by 17β-estradiol and phytoestrogens in breast cancer cells. Journal of Biological Chemistry. 2004 Jun 25;279(26):27008-16.

125.   Wu W, Warner M, Wang L, He WW, Zhao R, Guan X, Botero C, Huang B, Ion C, Coombes C, Gustafsson JA. Drivers and suppressors of triple-negative breast cancer. Proceedings of the National Academy of Sciences. 2021 Aug 17;118(33):e2104162118.

126.   Vermeulen PB, van Golen KL, Dirix LY. Angiogenesis, lymphangiogenesis, growth pattern, and tumor emboli in inflammatory breast cancer: a review of the current knowledge. Cancer. 2010 Jun 1;116(S11):2748-54.

127.   Wang Z, Zhang X, Shen P, Loggie BW, Chang Y, Deuel TF. Identification, cloning, and expression of human estrogen receptor-alpha36, a novel variant of human estrogen receptor-alpha66. Biochem. Biophys. Res. Commun. 2005;336:1023–1027

128.   Barton M. Position paper: The membrane estrogen receptor GPER--Clues and questions. Steroids. 2012;77:935–942

129.   Pandey DP, Lappano R, Albanito L, Madeo A, Maggiolini M, Picard D. Estrogenic GPR30 signalling induces proliferation and migration of breast cancer cells through CTGF. The EMBO journal. 2009 Mar 4;28(5):523-32.

130.   Vivacqua A, Romeo E, De Marco P, De Francesco EM, Abonante S, Maggiolini M. GPER mediates the Egr-1 expression induced by 17β-estradiol and 4-hydroxitamoxifen in breast and endometrial cancer cells. Breast cancer research and treatment. 2012 Jun;133:1025-35.

131.   Saion E, Gharibshahi E, Naghavi K. Size-controlled and optical properties of monodispersed silver nanoparticles synthesized by the radiolytic reduction method. International journal of molecular sciences. 2013 Apr 11;14(4):7880-96.

132.   Barton M, Filardo EJ, Lolait SJ, Thomas P, Maggiolini M, Prossnitz ER. Twenty years of the G protein-coupled estrogen receptor GPER: Historical and personal perspectives. The Journal of steroid biochemistry and molecular biology. 2018 Feb 1;176:4-15.

133.   Harris JR, Lippman ME, Osborne CK, Morrow M. Diseases of the Breast. Lippincott Williams & Wilkins; 2012 Mar 28.

134.   Luo J, Liu D. Does GPER really function as a G protein-coupled estrogen receptor in vivo?. Frontiers in endocrinology. 2020 Mar 31;11:148.

135.   Xu T, Ma D, Chen S, Tang R, Yang J, Meng C, Feng Y, Liu L, Wang J, Luo H, Yu K. High GPER expression in triple-negative breast cancer is linked to pro-metastatic pathways and predicts poor patient outcomes. NPJ Breast Cancer. 2022 Aug 30;8(1):100.

136.   Hsu LH, Chu NM, Lin YF, Kao SH. G-protein coupled estrogen receptor in breast cancer. International journal of molecular sciences. 2019 Jan 14;20(2):306.

137.   Treeck O, Schüler-Toprak S, Ortmann O. Estrogen actions in triple-negative breast cancer. Cells. 2020 Oct 26;9(11):2358.

138.   Robertson FM, Bondy M, Yang W, Yamauchi H, Wiggins S, Kamrudin S, Krishnamurthy S, Le-Petross H, Bidaut L, Player AN, Barsky SH, Woodward WA, Buchholz T, Lucci A, Ueno NT, Cristofanilli M. (2010) Inflammatory breast cancer: the disease, the biology, the treatment. CA Cancer J Clin. 2010, 60(6):351- 75.

139.   Van Uden DJ, Van Laarhoven HW, Westenberg AH, de Wilt JH, Blanken-Peeters CF. Inflammatory breast cancer: an overview. Critical reviews in oncology/hematology. 2015 Feb 1;93(2):116-26.

140.   Schmitz V, Bauerschmitz G, Gallwas J, Gründker C. Suppression of G Protein-coupled Estrogen Receptor 1 (GPER1) Enhances the Anti-invasive Efficacy of Selective ERβ Agonists. Anticancer Research. 2022 Nov 1;42(11):5187-94.

141.   Kang L, Zhang X, Xie Y, Tu Y, Wang D, Liu Z, Wang ZY. Involvement of estrogen receptor variant ER-α36, not GPR30, in nongenomic estrogen signaling. Molecular Endocrinology. 2010 Apr 1;24(4):709-21.

142.   Kang L, Zhang X, Xie Y, Tu Y, Wang D, Liu Z, Wang ZY. Involvement of estrogen receptor variant ER-α36, not GPR30, in nongenomic estrogen signaling. Molecular Endocrinology. 2010 Apr 1;24(4):709-21.

143.   Marotti JD, Collins LC, Hu R, Tamimi RM. Estrogen receptor-β expression in invasive breast cancer in relation to molecular phenotype: results from the Nurses' Health Study. Modern Pathology. 2010 Feb;23(2):197-204.

144.   Vivacqua A, Romeo E, De Marco P, De Francesco EM, Abonante S, Maggiolini M. GPER mediates the EGR1 expression induced by 17β-estradiol and 4-hydroxitamoxifen in breast and endometrial cancer cells. Breast cancer research and treatment. 2012 Jun;133(3):1025-35.

145.   Yu X, Stallone JN, Heaps CL, Han G. The activation of G protein-coupled estrogen receptor induces relaxation via cAMP as well as potentiates contraction via EGFR transactivation in porcine coronary arteries. PLoS One. 2018 Jan 23;13(1):e0191418.

146.   Filardo EJ, Quinn JA, Bland KI, Frackelton Jr AR. Estrogen-induced activation of Erk-1 and Erk-2 requires the G protein-coupled receptor homolog, GPR30, and occurs via trans-activation of the epidermal growth factor receptor through release of HB-EGF. Molecular endocrinology. 2000 Oct 1;14(10):1649-60.

147.   Lappano R, De Marco P, De Francesco EM, Chimento A, Pezzi V, Maggiolini M. Cross-talk between GPER and growth factor signaling. The Journal of steroid biochemistry and molecular biology. 2013 Sep 1;137:50-6.

148.   Dennis MK, Burai R, Ramesh C, Petrie WK, Alcon SN, Nayak TK, Bologa CG, Leitao A, Brailoiu E, Deliu E, Dun NJ. In vivo effects of a GPR30 antagonist. Nature chemical biology. 2009 Jun;5(6):421-7.

149.   Clark NA, Hafner M, Kouril M, Williams EH, Muhlich JL, Pilarczyk M, Niepel M, Sorger PK, Medvedovic M. GRcalculator: an online tool for calculating and mining dose–response data. BMC cancer. 2017 Dec;17:1-1.

150.   Kleer CG, van Golen KL, Merajver SD (2000) Molecular biology of breast cancer metastasis. Inflammatory breast cancer: clinical syndrome and molecular determinants. Breast Cancer Red 2: 423-429.

151.   Ohshiro K, Schwartz AM, Levine PH, KµMar R. Alternate estrogen receptors promote invasion of inflammatory breast cancer cells via non-genomic signaling. PLoS One. 2012 Jan 25;7(1):e30725.

152.   Gupta PB, Kuperwasser C. Contributions of estrogen to ER-negative breast tumor growth. The Journal of steroid biochemistry and molecular biology. 2006 Dec 1;102(1-5):71-8.

153.   Ali S, Coombes RC. Estrogen receptor alpha in human breast cancer: occurrence and significance. Journal of mammary gland biology and neoplasia. 2000 Jul;5:271-81.

154.   Bièche I, Lerebours F, Tozlu S, Espie M, Marty M, Lidereau R. Molecular profiling of inflammatory breast cancer: identification of a poor-prognosis gene expression signature. Clinical cancer research. 2004 Oct 15;10(20):6789-95.

155.   Llopis S, Singleton B, Duplessis T, Carrier L, Rowan B, Williams C. Dichotomous roles for the orphan nuclear receptor NURR1 in breast cancer. BMC cancer. 2013 Dec;13(1):1-9.

156.   Jiang WG, Watkins G, Fodstad O, Douglas-Jones A, Mokbel K, Mansel RE. Differential expression of the CCN family members Cyr61, CTGF and Nov in Human breast cancer. Endocrine-related cancer. 2004 Dec 1;11(4):781-91.

157.   Recchia, A.G., De Francesco, E.M., Vivacqua, A., Sisci, D., Panno, M.L., Ando, S. and Maggiolini, M., 2011. The G protein-coupled receptor 30 is up-regulated by hypoxia-inducible factor-1α (HIF-1α) in breast cancer cells and cardiomyocytes. Journal of Biological Chemistry, 286(12), pp.10773-10782.

158.   Robertson FM, Simeone AM, Lucci A, McMurray JS, Ghosh S, Cristofanilli M. Differential regulation of the aggressive phenotype of inflammatory breast cancer cells by prostanoid receptors EP3 and EP4. Cancer. 2010 Jun 1;116(S11):2806-14.

159.   Song Y, Ma X, Zhang M, Wang M, Wang G, Ye Y, Xia W. Ezrin mediates invasion and metastasis in tumorigenesis: a review. Frontiers in Cell and Developmental Biology. 2020 Nov 10;8:588801.

160.   Ghaffari A, Hoskin V, Turashvili G, Varma S, Mewburn J, Mullins G, Greer PA, Kiefer F, Day AG, Madarnas Y, SenGupta S. Intravital imaging reveals systemic ezrin inhibition impedes cancer cell migration and lymph node metastasis in breast cancer. Breast Cancer Research. 2019 Dec;21(1):1-1.

161.   Zhou K, Sun P, Zhang Y, You X, Li P, Wang T. Estrogen stimulated migration and invasion of estrogen receptor-negative breast cancer cells involves an ezrin-dependent crosstalk between G protein-coupled receptor 30 and estrogen receptor beta signaling. Steroids. 2016 Jul 1;111:113-20.

162.   Kang L, Zhang X, Xie Y, Tu Y, Wang D, Liu Z, Wang ZY. Involvement of estrogen receptor variant ER-α36, not GPR30, in nongenomic estrogen signaling. Molecular Endocrinology. 2010 Apr 1;24(4):709-21.

163.	Wang Z, Zhang X, Shen P, Loggie BW, Chang Y, Deuel TF. Identification, cloning, and expression of human estrogen receptor-α36, a novel variant of human estrogen receptor-α66. Biochemical and biophysical research communications. 2005 Nov 4;336(4):1023-7.

164.	Liu C, Liao Y, Fan S, Fu X, Xiong J, Zhou S, Zou M, Wang J. G-protein-coupled estrogen receptor antagonist G15 decreases estrogen-induced development of non-small cell lung cancer. Oncology Research. 2019;27(3):283.

165.	Laprevotte E, Cochaud S, Du Manoir S, Lapierre M, Dejou C, Philippe M, Giustiniani J, Frewer KA, Sanders AJ, Jiang WG, Michaud HA. The IL-17B-IL-17 receptor B pathway promotes resistance to paclitaxel in breast tumors through activation of the ERK1/2 pathway. Oncotarget. 2017 Dec 12;8(69):113360.

166.	Bahrami S, Drabløs F. Gene regulation in the immediate-early response process. Advances in biological regulation. 2016 Sep 1;62:37-49.

167.	Guo YJ, Pan WW, Liu SB, Shen ZF, Xu Y, Hu LL. ERK/MAPK signalling pathway and tumorigenesis. Experimental and therapeutic medicine. 2020 Mar 1;19(3):1997-2007.

168.	Qiu YA, Xiong J, Fu Q, Dong Y, Liu M, Peng M, Jin W, Zhou L, Xu X, Huang X, Fu A. GPER-induced ERK signaling decreases cell viability of hepatocellular carcinoma. Frontiers in Oncology. 2021 Mar 9;11:638171.

169.	Guo Y, Zhang X, Meng J, Wang ZY. An anticancer agent icaritin induces sustained activation of the extracellular signal-regulated kinase (ERK) pathway and inhibits growth of breast cancer cells. European journal of pharmacology. 2011 May 11;658(2-3):114-22.

170.	Zhang W, Liu HT. MAPK signal pathways in the regulation of cell proliferation in mammalian cells. Cell research. 2002 Mar;12(1):9-18.

171.	Fan P, Jordan VC. PERK1/2, beyond an unfolded protein response sensor in estrogen-induced apoptosis in endocrine-resistant breast cancer. Molecular Cancer Research. 2022 Feb 1;20(2):193-201.

172.	Alinejad V, Somi MH, Baradaran B, Akbarzadeh P, Atyabi F, Kazerooni H, Kafil HS, Maleki LA, Mansouri HS, Yousefi M. Co-delivery of IL17RB siRNA and doxorubicin by chitosan-based nanoparticles for enhanced anticancer efficacy in breast cancer cells. Biomedicine & Pharmacotherapy. 2016 Oct 1;83:229-40.

173.	Sauer L, Gitenay D, Vo C, Baron VT. Mutant p53 initiates a feedback loop that involves EGR1/EGF receptor/ERK1/2 in prostate cancer cells. Oncogene. 2010 May;29(18):2628-37.

174.	Wei LL, Wu XJ, Gong CC, Pei DS. EGR1 suppresses breast cancer cell proliferation by arresting cell cycle progression via down-regulating CyclinDs. International Journal of Clinical and Experimental Pathology. 2017;10(10):10212.

175.	Chen CC, Mo FE, Lau LF. The angiogenic factor Cyr61 activates a genetic program for wound healing in human skin fibroblasts. Journal of Biological Chemistry. 2001 Dec 14;276(50):47329-37.

176.	Buffet C, Hecale-Perlemoine K, Bricaire L, DµMont F, Baudry C, Tissier F, Bertherat J, Cochand-Priollet B, Raffin-Sanson ML, Cormier F, Groussin L. DUSP5 and DUSP6, two ERK1/2 specific phosphatases, are markers of a higher MAPK signaling activation in BRAF mutated thyroid cancers. PloS one. 2017 Sep 14;12(9):e0184861.

177.   Filardo EJ, Graeber CT, Quinn JA, Resnick MB, Giri D, DeLellis RA, Steinhoff MM, Sabo E. Distribution of GPR30, a seven membrane-spanning estrogen receptor, in primary breast cancer and its association with clinicopathologic determinants of tumor progression. Clinical cancer research. 2006 Nov 1;12(21):6359-66.

178.   Yu T, Liu M, Luo H, Wu C, Tang X, Tang S, Hu P, Yan Y, Wang Z, Tu G. GPER mediates enhanced cell viability and motility via non-genomic signaling induced by 17β-estradiol in triple-negative breast cancer cells. The Journal of Steroid Biochemistry and Molecular Biology. 2014 Sep 1;143:392-403.

179.   Huang R, Li J, Pan F, Zhang B, Yao Y. The activation of GPER inhibits cell proliferation, invasion, and EMT of triple-negative breast cancer via CD151/miR-199a-3p bio-axis. American Journal of Translational Research. 2020;12(1):32.

180.   Steiman J, Peralta EA, Louis S, Kamel O. Biology of the estrogen receptor, GPR30, in triple-negative breast cancer. The American Journal of Surgery. 2013 Nov 1;206(5):698-703.

181.   Kim BW, Lee ER, Min HM, Jeong HS, Ahn JY, Kim JH, Choi HY, Choi H, Kim EY, Park SP, Cho SG. Sustained ERK1/2 activation is involved in the kaempferol-induced apoptosis of breast cancer cells and is more evident under 3-D culture condition. Cancer Biology & Therapy. 2008 Jul 1;7(7):1080-9.

182.   Tarcic G, Avraham R, Pines G, Amit I, Shay T, Lu Y, Zwang Y, Katz M, Ben-Chetrit N, Jacob-Hirsch J, Virgilio L. EGR1 and the ERK-ERF axis drive mammary cell migration in response to EGF. The FASEB Journal. 2012 Apr;26(4):1582.

183.   Nanba D, Higashiyama S. Dual intracellular signaling by proteolytic cleavage of membrane-anchored heparin-binding EGF-like growth factor. Cytokine & growth factor reviews. 2004 Feb 1;15(1):13-9.

184.   Arias-Pulido H, Royce M, Gong Y, Joste N, Lomo L, Lee SJ, Chaher N, Verschraegen C, Lara J, Prossnitz ER, Cristofanilli M. GPR30 and estrogen receptor expression: new insights into hormone dependence of inflammatory breast cancer. Breast cancer research and treatment. 2010 Aug;123:51-8.

185.   Guo Y, Zhang X, Meng J, Wang ZY. An anticancer agent icaritin induces sustained activation of the extracellular signal-regulated kinase (ERK) pathway and inhibits growth of breast cancer cells. European journal of pharmacology. 2011 May 11;658(2-3):114-22.

186.   Strasser A, Cory S, Adams JM. Deciphering the rules of programmed cell death to improve therapy of cancer and other diseases. EMBO J. 2011 Aug 23;30(18):3667-83. doi: 10.1038/emboj.2011.307. PMID: 21863020; PMCID: PMC3173800.

187.   Pelekanou V, Kampa M, Kiagiadaki F, Deli A, Theodoropoulos P, Agrogiannis G, Patsouris E, Tsapis A, Castanas E, Notas G. Estrogen anti-inflammatory activity on human monocytes is mediated through cross-talk between estrogen receptor ERα36 and GPR30/GPER1. Journal of leukocyte biology. 2016 Feb;99(2):333-47.

188.   Horvath E. Molecular subtypes of breast cancer-What breast imaging radiologists need to know. Rev. Chil. Radiol. 2021;27:17-26.

189.   Jia Q, Xu B, Zhang Y, Ali A, Liao X. CCN family proteins in cancer: insight into their structures and coordination role in tumor microenvironment. Frontiers in Genetics. 2021 Mar 23;12:649387

Supplementary data

Table S1. List of RT-qPCR primers

Parameter sets: qPCR

Target type **DNA**, Oligo Conc **0.5μM**, Na+ Conc **50mM**, Mg++ Conc **3mM**, dNTPs Conc **0.8mM**

Gene		Position	Sequence	Length	Start	End	Amplicon length	Tm	GC%	Hairpin ΔG	Self-Dimer	Hetero-Dimer
GAPDH	NM_001256799.3	Forward	ACCCAGAAGACTGTGGATGG	20	727	746	124	56.6	55	-2.56	-5.02	-6.14
		Reverse	TCAGCTCAGGGATGACCTTG	20	850	831		56.6	55	-1.5	-6.34	
ERa36	NM_001328100.2	Forward	GAGGCATGAGGAAGCACTTG	20	4941	4960	91		55	-0.85	-5.38	-6.69
		Reverse	TGCTCTCCGCATTGTTTCAG	20	5031	5012			50	-1.53	-5.09	
GPR30	NM_001039966.2	Forward	TCCTGATCCTGGTGGTGAAC	20	806	825	169	56.6	55	-0.68	-4.62	-8.2
		Reverse	GACATGAAGGTGCACAGGAC	20	974	955		56	55	0.22	-9.73	
EGR1 (ZNF268)	NM_001165887.2	Forward	TCCATGCAATGGAGTCCTGT	20	10479	10498	197	56	50	-3.46	-8.07	-5.09
		Reverse	TGCCCTCTACAAACCGTCAT	20	10675	10656		56	50	0.04	-3.61	
DUSP6	NM_001946.4	Forward	GCTGCTGCTCAAGAAGCTCA	20	810	829	X	58	55	-2.47	-6.34	-6.68
		Reverse	AGGGAGAACTCGGCTTGGAA	20	877	896		58.4	55	1.07	-3.61	
HB-EGF	NM_001945.3	Forward	TATCCTCCAAGCCACAAGCA	20	502	521	X	56.4	50	-1.62	-3.14	-3.54
		Reverse	GTCCCTCTTCTTCCCTAGCC	20	574	593		56.7	60	1.6	-4.16	

Table S2. Top 100 most statistically significant E2-regulated genes at 45 min

Ensemble ID	Gene Symbol	log2 Fold Change	P value	Adjusted P value
ENSG00000118523	CCN2	4.63	7.77E-235	1.30E-230
ENSG00000067082	KLF6	2.23	2.96E-214	2.47E-210
ENSG00000142871	CCN1	2.54	4.90E-193	2.73E-189
ENSG00000177606	JUN	3.52	4.86E-175	2.03E-171
ENSG00000120738	EGR1	3.73	9.96E-169	3.33E-165
ENSG00000170345	FOS	4.97	3.75E-106	1.05E-102
ENSG00000122877	EGR2	4.44	7.60E-88	1.82E-84
ENSG00000123358	NR4A1	3.34	1.13E-85	2.37E-82
ENSG00000124762	CDKN1A	1.77	1.47E-76	2.73E-73
ENSG00000120129	DUSP1	3.14	2.13E-75	3.56E-72
ENSG00000087074	PPP1R15A	1.54	3.69E-67	5.61E-64
ENSG00000137331	IER3	1.94	1.70E-57	2.37E-54
ENSG00000144655	CSRNP1	1.89	4.34E-57	5.58E-54
ENSG00000125740	FOSB	3.80	2.60E-56	3.10E-53
ENSG00000143878	RHOB	1.69	1.51E-55	1.69E-52
ENSG00000162772	ATF3	2.22	1.88E-53	1.97E-50
ENSG00000179388	EGR3	3.41	3.03E-53	2.98E-50
ENSG00000175592	FOSL1	2.26	7.13E-49	6.62E-46
ENSG00000136997	MYC	1.31	5.60E-47	4.93E-44
ENSG00000198142	SOWAHC	1.45	1.74E-43	1.46E-40
ENSG00000160888	IER2	2.32	1.50E-37	1.20E-34
ENSG00000116717	GADD45A	1.82	5.36E-33	4.07E-30
ENSG00000143384	MCL1	0.91	1.95E-32	1.42E-29
ENSG00000162783	IER5	1.23	1.11E-31	7.74E-29
ENSG00000144802	NFKBIZ	1.41	2.56E-30	1.71E-27
ENSG00000013441	CLK1	-1.09	3.00E-29	1.93E-26
ENSG00000128342	LIF	2.32	6.52E-27	4.04E-24
ENSG00000204103	MAFB	1.40	4.47E-25	2.67E-22
ENSG00000138166	DUSP5	1.70	2.40E-24	1.38E-21
ENSG00000139289	PHLDA1	0.85	2.04E-23	1.10E-20
ENSG00000145632	PLK2	1.09	2.10E-23	1.10E-20
ENSG00000181026	AEN	1.57	2.02E-23	1.10E-20
ENSG00000128016	ZFP36	1.52	6.37E-22	3.23E-19
ENSG00000267519	None	1.40	1.69E-21	8.32E-19
ENSG00000136158	SPRY2	0.90	2.68E-20	1.28E-17
ENSG00000148339	SLC25A25	1.10	5.84E-20	2.64E-17
ENSG00000164442	CITED2	1.50	5.77E-20	2.64E-17
ENSG00000134107	BHLHE40	0.81	2.70E-18	1.19E-15

ENSG00000185022	MAFF	1.32	1.58E-17	6.79E-15
ENSG00000232656	IDI2-AS1	1.16	3.36E-17	1.41E-14
ENSG00000118515	SGK1	1.81	1.63E-16	6.65E-14
ENSG00000257671	KRT7-AS	1.25	6.18E-16	2.46E-13
ENSG00000078401	EDN1	1.17	2.76E-15	1.07E-12
ENSG00000141682	PMAIP1	1.11	6.69E-15	2.54E-12
ENSG00000136826	KLF4	0.98	1.22E-13	4.54E-11
ENSG00000073756	PTGS2	1.27	1.27E-13	4.60E-11
ENSG00000114019	AMOTL2	0.80	1.41E-13	5.02E-11
ENSG00000198455	ZXDB	0.78	8.69E-13	3.03E-10
ENSG00000163874	ZC3H12A	1.03	1.34E-12	4.56E-10
ENSG00000132002	DNAJB1	0.54	1.86E-12	6.22E-10
ENSG00000269929	MIRLET7A1HG	1.17	3.52E-12	1.15E-09
ENSG00000136244	IL6	1.38	4.73E-11	1.52E-08
ENSG00000177426	TGIF1	0.52	5.08E-11	1.60E-08
ENSG00000179094	PER1	1.06	5.50E-11	1.70E-08
ENSG00000165312	OTUD1	0.69	6.05E-11	1.84E-08
ENSG00000120875	DUSP4	1.11	8.00E-11	2.39E-08
ENSG00000173812	EIF1	0.55	2.86E-10	8.39E-08
ENSG00000232810	TNF	1.01	3.08E-10	8.87E-08
ENSG00000112245	PTP4A1	0.57	3.36E-10	9.53E-08
ENSG00000003756	RBM5	-0.52	3.43E-10	9.57E-08
ENSG00000153234	NR4A2	1.24	3.77E-10	1.03E-07
ENSG00000159388	BTG2	1.05	5.30E-10	1.43E-07
ENSG00000276107	None	1.86	6.27E-10	1.66E-07
ENSG00000111912	NCOA7	0.66	1.11E-09	2.89E-07
ENSG00000180667	YOD1	0.61	1.16E-09	2.98E-07
ENSG00000259884	NR4A1AS	3.16	1.72E-09	4.37E-07
ENSG00000196449	YRDC	0.69	2.29E-09	5.72E-07
ENSG00000111057	KRT18	0.36	3.01E-09	7.40E-07
ENSG00000081041	CXCL2	1.37	3.75E-09	9.09E-07
ENSG00000114315	HES1	0.82	9.20E-09	2.20E-06
ENSG00000163482	STK36	-0.62	1.02E-08	2.40E-06
ENSG00000158615	PPP1R15B	0.38	1.05E-08	2.43E-06
ENSG00000113070	HB-EGF	1.36	1.74E-08	3.99E-06
ENSG00000127528	KLF2	3.09	1.86E-08	4.21E-06
ENSG00000142867	BCL10	0.62	3.46E-08	7.70E-06
ENSG00000169429	CXCL8	0.85	4.48E-08	9.86E-06
ENSG00000255112	CHMP1B	0.36	5.90E-08	1.28E-05
ENSG00000100219	XBP1	0.42	7.78E-08	1.67E-05
ENSG00000113240	CLK4	-0.76	8.18E-08	1.73E-05
ENSG00000157514	TSC22D3	0.68	1.18E-07	2.46E-05
ENSG00000284669	None	2.72	1.30E-07	2.68E-05

ENSG00000115009	CCL20	1.16	1.68E-07	3.43E-05
ENSG00000186594	MIR22HG	0.57	3.12E-07	6.29E-05
ENSG00000099860	GADD45B	0.98	3.20E-07	6.36E-05
ENSG00000226752	CUTALP	-0.35	3.78E-07	7.43E-05
ENSG00000163435	ELF3	0.42	5.33E-07	1.04E-04
ENSG00000169045	HNRNPH1	-0.44	5.48E-07	1.05E-04
ENSG00000117569	PTBP2	-0.66	6.10E-07	1.16E-04
ENSG00000142627	EPHA2	0.82	7.93E-07	1.49E-04
ENSG00000257379	None	-1.19	1.17E-06	2.17E-04
ENSG00000139318	DUSP6	0.87	1.25E-06	2.29E-04
ENSG00000014914	MTMR11	-0.37	1.65E-06	3.00E-04
ENSG00000185650	ZFP36L1	0.59	1.77E-06	3.18E-04
ENSG00000076604	TRAF4	0.71	2.08E-06	3.71E-04
ENSG00000173559	NABP1	-0.43	2.56E-06	4.51E-04
ENSG00000251474	RPL32P3	-0.86	2.79E-06	4.85E-04
ENSG00000116001	TIA1	-0.33	3.12E-06	5.32E-04
ENSG00000157557	ETS2	0.62	3.11E-06	5.32E-04
ENSG00000116741	RGS2	0.93	3.61E-06	6.09E-04
ENSG00000118961	LDAH	-0.61	3.70E-06	6.19E-04

Table S3. Top 100 most statistically significant E2-regulated genes at 90 min

Ensemble ID	Gene Symbol	log2 Fold Change	P value	Adjusted P value
ENSG00000118523	CCN2	4.67	2.10E-239	3.51E-235
ENSG00000142871	CCN1	2.77	1.73E-229	1.45E-225
ENSG00000067082	KLF6	2.07	2.53E-187	1.41E-183
ENSG00000124762	CDKN1A	1.98	3.72E-96	1.56E-92
ENSG00000175592	FOSL1	3.16	1.06E-94	3.54E-91
ENSG00000123358	NR4A1	3.31	2.34E-84	6.52E-81
ENSG00000119508	NR4A3	3.14	3.06E-78	7.31E-75
ENSG00000162772	ATF3	2.46	3.13E-66	5.90E-63
ENSG00000092820	EZR	0.93	3.18E-66	5.90E-63
ENSG00000198142	SOWAHC	1.7	3.35E-60	5.60E-57
ENSG00000179388	EGR3	3.6	5.18E-60	7.88E-57
ENSG00000185022	MAFF	2.39	1.54E-54	2.15E-51
ENSG00000177606	JUN	1.95	1.93E-53	2.48E-50
ENSG00000159200	RCAN1	2.15	2.08E-50	2.48E-47
ENSG00000130164	LDLR	1.17	6.41E-50	7.14E-47
ENSG00000181467	RAP2B	1.07	1.49E-49	1.56E-46
ENSG00000213694	S1PR3	1.2	5.43E-49	5.34E-46

ENSG00000150457	LATS2	1.25	4.15E-47	3.85E-44
ENSG00000128342	LIF	3.08	3.39E-46	2.98E-43
ENSG00000136997	MYC	1.24	5.25E-43	4.39E-40
ENSG00000124882	EREG	1.74	8.04E-43	6.40E-40
ENSG00000143367	TUFT1	1.36	3.14E-42	2.39E-39
ENSG00000122877	EGR2	3.04	3.03E-41	2.20E-38
ENSG00000111859	NEDD9	2.11	3.00E-40	2.09E-37
ENSG00000172818	OVOL1	2.09	4.53E-40	3.03E-37
ENSG00000125266	EFNB2	1.09	8.53E-39	5.48E-36
ENSG00000165312	OTUD1	1.35	1.11E-38	6.86E-36
ENSG00000181026	AEN	2.02	3.82E-38	2.28E-35
ENSG00000157557	ETS2	1.68	5.26E-37	3.03E-34
ENSG00000143322	ABL2	2.11	6.72E-37	3.75E-34
ENSG00000107984	DKK1	1.44	2.08E-36	1.12E-33
ENSG00000144802	NFKBIZ	1.55	2.48E-36	1.29E-33
ENSG00000136244	IL6	2.59	6.42E-36	3.25E-33
ENSG00000136826	KLF4	1.59	4.26E-35	2.09E-32
ENSG00000111912	NCOA7	1.32	7.34E-35	3.51E-32
ENSG00000143384	MCL1	0.95	9.30E-35	4.32E-32
ENSG00000120875	DUSP4	2.08	1.98E-34	8.95E-32
ENSG00000163235	TGFA	1.27	4.21E-34	1.85E-31
ENSG00000137801	THBS1	1.66	5.18E-34	2.22E-31
ENSG00000117525	F3	1.84	1.55E-33	6.47E-31
ENSG00000138166	DUSP5	1.97	2.78E-33	1.13E-30
ENSG00000109321	AREG	1.85	4.05E-33	1.61E-30
ENSG00000125740	FOSB	2.88	1.01E-32	3.92E-30
ENSG00000135679	MDM2	1.63	5.62E-31	2.14E-28
ENSG00000138623	SEMA7A	2.12	6.23E-31	2.29E-28
ENSG00000087074	PPP1R15A	1.03	6.31E-31	2.29E-28
ENSG00000116717	GADD45A	1.74	8.43E-31	3.00E-28
ENSG00000134107	BHLHE40	1.07	2.37E-30	8.25E-28
ENSG00000115009	CCL20	2.5	2.53E-30	8.64E-28
ENSG00000165997	ARL5B	1.23	2.83E-30	9.46E-28
ENSG00000136158	SPRY2	1.1	4.60E-30	1.51E-27
ENSG00000100219	XBP1	0.87	1.47E-29	4.72E-27
ENSG00000073756	PTGS2	1.94	1.57E-29	4.95E-27
ENSG00000075426	FOSL2	0.97	7.61E-29	2.36E-26
ENSG00000013441	CLK1	-1.07	1.66E-28	5.05E-26
ENSG00000116285	ERRFI1	1.11	8.36E-28	2.50E-25
ENSG00000118503	TNFAIP3	1.37	6.84E-27	2.01E-24
ENSG00000205002	AARD	0.62	7.01E-27	2.02E-24
ENSG00000153234	NR4A2	2.1	7.77E-27	2.20E-24
ENSG00000162702	ZNF281	1.2	1.16E-26	3.23E-24

ENSG00000144655	CSRNP1	1.28	1.36E-26	3.69E-24
ENSG00000145632	PLK2	1.17	1.37E-26	3.69E-24
ENSG00000114019	AMOTL2	1.13	2.66E-25	7.05E-23
ENSG00000171617	ENC1	1	4.57E-25	1.19E-22
ENSG00000169908	TM4SF1	1.14	6.88E-25	1.75E-22
ENSG00000169429	CXCL8	1.59	6.93E-25	1.75E-22
ENSG00000117616	RSRP1	-1.04	7.17E-25	1.79E-22
ENSG00000107968	MAP3K8	1.07	8.27E-25	2.03E-22
ENSG00000113448	PDE4D	1.18	1.40E-24	3.39E-22
ENSG00000171150	SOCS5	0.8	1.45E-24	3.44E-22
ENSG00000197632	SERPINB2	1.39	1.46E-24	3.44E-22
ENSG00000170677	SOCS6	0.86	2.22E-24	5.16E-22
ENSG00000232810	TNF	1.58	2.80E-24	6.40E-22
ENSG00000105971	CAV2	0.72	1.26E-23	2.85E-21
ENSG00000164543	STK17A	1.18	4.59E-23	1.02E-20
ENSG00000177426	TGIF1	0.77	1.81E-22	3.98E-20
ENSG00000253276	CCDC71L	1.56	4.44E-22	9.63E-20
ENSG00000112245	PTP4A1	0.87	1.58E-21	3.38E-19
ENSG00000111266	DUSP16	0.95	3.25E-21	6.88E-19
ENSG00000102554	KLF5	0.99	3.34E-21	6.99E-19
ENSG00000154734	ADAMTS1	0.71	3.45E-21	7.11E-19
ENSG00000179094	PER1	1.51	4.39E-21	8.94E-19
ENSG00000182585	EPGN	1.82	5.55E-21	1.12E-18
ENSG00000170802	FOXN2	0.88	5.62E-21	1.12E-18
ENSG00000149289	ZC3H12C	1.11	6.21E-21	1.22E-18
ENSG00000155850	SLC26A2	0.95	8.23E-21	1.60E-18
ENSG00000124145	SDC4	0.88	8.44E-21	1.62E-18
ENSG00000173281	PPP1R3B	1	1.10E-20	2.09E-18
ENSG00000162783	IER5	0.97	2.44E-20	4.57E-18
ENSG00000081320	STK17B	1.39	2.79E-20	5.18E-18
ENSG00000182795	C1orf116	0.66	8.62E-20	1.58E-17
ENSG00000148339	SLC25A25	1.08	9.50E-20	1.73E-17
ENSG00000185950	IRS2	1.11	1.22E-19	2.19E-17
ENSG00000164951	PDP1	0.85	1.45E-19	2.58E-17
ENSG00000170525	PFKFB3	0.92	3.34E-19	5.89E-17
ENSG00000113369	ARRDC3	-1.38	3.77E-19	6.56E-17
ENSG00000013588	GPRC5A	0.74	6.20E-19	1.07E-16
ENSG00000188215	DCUN1D3	0.97	7.25E-19	1.24E-16
ENSG00000142627	EPHA2	1.46	1.22E-18	2.06E-16
ENSG00000170561	IRX2	0.98	3.04E-18	5.09E-16

Table S4. Top 100 most statistically significant E2-regulated genes at 180 min

Ensemble ID	Gene Symbol	log2 Fold Change	P value	Adjusted P value
ENSG00000120738	EGR1	-2.43	7.41E-66	1.24E-61
ENSG00000092820	EZR	0.87	6.86E-58	5.74E-54
ENSG00000163110	PDLIM5	1.24	5.90E-50	3.29E-46
ENSG00000213694	S1PR3	1.12	5.28E-43	2.21E-39
ENSG00000177614	PGBD5	1.77	1.05E-42	3.51E-39
ENSG00000157654	PALM2AKAP2	1.08	3.83E-42	1.07E-38
ENSG00000163347	CLDN1	1.74	1.38E-39	3.31E-36
ENSG00000020577	SAMD4A	1.83	5.23E-36	1.09E-32
ENSG00000146072	TNFRSF21	0.76	4.47E-34	7.99E-31
ENSG00000154447	SH3RF1	1.07	4.78E-34	7.99E-31
ENSG00000119125	GDA	1.86	7.49E-34	1.14E-30
ENSG00000077238	IL4R	1.24	1.52E-32	2.12E-29
ENSG00000164171	ITGA2	0.92	5.16E-31	6.63E-28
ENSG00000110092	CCND1	1.33	4.64E-29	5.54E-26
ENSG00000188042	ARL4C	1.15	1.74E-28	1.94E-25
ENSG00000178860	MSC	1.18	2.72E-28	2.84E-25
ENSG00000139514	SLC7A1	0.81	2.05E-26	1.91E-23
ENSG00000183579	ZNRF3	1.31	1.95E-26	1.91E-23
ENSG00000083307	GRHL2	-0.71	3.32E-26	2.92E-23
ENSG00000166016	ABTB2	1.03	3.72E-26	2.96E-23
ENSG00000175592	FOSL1	1.64	3.55E-26	2.96E-23
ENSG00000107984	DKK1	1.19	3.15E-25	2.39E-22
ENSG00000073008	PVR	0.75	8.98E-25	6.53E-22
ENSG00000226752	CUTALP	-0.71	1.58E-24	1.10E-21
ENSG00000105971	CAV2	0.73	2.20E-24	1.47E-21
ENSG00000277586	NEFL	0.88	6.59E-24	4.24E-21
ENSG00000205268	PDE7A	-1.11	8.31E-24	5.15E-21
ENSG00000137267	TUBB2A	1.13	9.00E-24	5.37E-21
ENSG00000070961	ATP2B1	0.77	3.93E-23	2.26E-20
ENSG00000160584	SIK3	0.64	5.75E-23	3.21E-20
ENSG00000119280	C1orf198	0.68	6.44E-23	3.47E-20
ENSG00000137460	FHDC1	0.78	6.63E-23	3.47E-20
ENSG00000104635	SLC39A14	0.75	5.03E-22	2.55E-19
ENSG00000138771	SHROOM3	1.09	6.56E-22	3.23E-19
ENSG00000134294	SLC38A2	0.69	7.10E-22	3.39E-19
ENSG00000167767	KRT80	0.88	3.26E-21	1.51E-18
ENSG00000198369	SPRED2	0.75	3.81E-21	1.72E-18
ENSG00000113645	WWC1	1.06	2.13E-20	9.36E-18

ENSG00000075426	FOSL2	0.80	4.74E-20	2.03E-17
ENSG00000144063	MALL	0.91	1.28E-19	5.35E-17
ENSG00000124193	SRSF6	-0.56	1.37E-19	5.59E-17
ENSG00000035403	VCL	0.61	1.82E-19	7.25E-17
ENSG00000223960	CHROMR	-0.76	5.58E-19	2.17E-16
ENSG00000188910	GJB3	0.88	7.24E-19	2.75E-16
ENSG00000179431	FJX1	1.49	9.28E-19	3.45E-16
ENSG00000171729	TMEM51	1.31	9.78E-19	3.56E-16
ENSG00000178075	GRAMD1C	-0.86	1.61E-18	5.74E-16
ENSG00000172818	OVOL1	1.39	2.24E-18	7.81E-16
ENSG00000095383	TBC1D2	1.15	2.30E-18	7.86E-16
ENSG00000109079	TNFAIP1	0.63	2.45E-18	8.20E-16
ENSG00000124225	PMEPA1	0.96	3.74E-18	1.21E-15
ENSG00000276023	DUSP14	0.79	3.77E-18	1.21E-15
ENSG00000197632	SERPINB2	1.18	5.53E-18	1.75E-15
ENSG00000149346	SLX4IP	-0.78	1.02E-17	3.17E-15
ENSG00000168575	SLC20A2	0.87	1.26E-17	3.83E-15
ENSG00000272645	None	-1.05	1.40E-17	4.19E-15
ENSG00000110047	EHD1	1.16	2.43E-17	7.14E-15
ENSG00000171552	BCL2L1	0.66	2.54E-17	7.32E-15
ENSG00000122863	CHST3	0.69	2.92E-17	8.28E-15
ENSG00000108244	KRT23	1.60	3.49E-17	9.73E-15
ENSG00000180229	HERC2P3	-1.01	5.61E-17	1.54E-14
ENSG00000105810	CDK6	0.65	5.81E-17	1.57E-14
ENSG00000110104	CCDC86	1.10	6.40E-17	1.62E-14
ENSG00000130559	CAMSAP1	0.77	6.27E-17	1.62E-14
ENSG00000176971	FIBIN	-0.85	6.26E-17	1.62E-14
ENSG00000276550	HERC2P2	-0.76	6.33E-17	1.62E-14
ENSG00000186814	ZSCAN30	-0.78	7.65E-17	1.91E-14
ENSG00000121039	RDH10	0.98	8.20E-17	2.02E-14
ENSG00000146112	PPP1R18	0.51	8.37E-17	2.03E-14
ENSG00000158966	CACHD1	-0.98	1.11E-16	2.66E-14
ENSG00000034152	MAP2K3	1.06	1.21E-16	2.86E-14
ENSG00000155324	GRAMD2B	0.87	1.95E-16	4.53E-14
ENSG00000124762	CDKN1A	0.78	3.92E-16	8.99E-14
ENSG00000106261	ZKSCAN1	-0.97	4.53E-16	1.02E-13
ENSG00000184292	TACSTD2	0.85	5.54E-16	1.23E-13
ENSG00000104368	PLAT	0.81	9.64E-16	2.12E-13
ENSG00000127328	RAB3IP	0.94	9.82E-16	2.13E-13
ENSG00000103404	USP31	0.81	1.02E-15	2.18E-13
ENSG00000115641	FHL2	1.04	1.14E-15	2.42E-13
ENSG00000144824	PHLDB2	0.88	1.24E-15	2.59E-13
ENSG00000152926	ZNF117	-0.92	1.31E-15	2.71E-13

ENSG00000129474	AJUBA	0.62	1.96E-15	4.00E-13
ENSG00000128422	KRT17	1.12	2.21E-15	4.45E-13
ENSG00000118507	AKAP7	-0.86	2.94E-15	5.86E-13
ENSG00000272668	LOC107985216	-1.54	3.07E-15	6.03E-13
ENSG00000188112	C6orf132	0.67	3.33E-15	6.47E-13
ENSG00000116001	TIA1	-0.55	4.11E-15	7.91E-13
ENSG00000172572	PDE3A	-0.70	4.17E-15	7.93E-13
ENSG00000159840	ZYX	1.15	4.30E-15	8.00E-13
ENSG00000185479	KRT6B	0.76	4.31E-15	8.00E-13
ENSG00000183742	MACC1	1.15	5.11E-15	9.39E-13
ENSG00000004534	RBM6	-0.78	5.37E-15	9.76E-13
ENSG00000185963	BICD2	0.65	5.74E-15	1.03E-12
ENSG00000138271	GPR87	1.05	5.84E-15	1.04E-12
ENSG00000074621	SLC24A1	-0.83	6.21E-15	1.09E-12
ENSG00000103126	AXIN1	1.16	6.69E-15	1.16E-12
ENSG00000184675	AMER1	0.64	6.83E-15	1.18E-12
ENSG00000112578	BYSL	0.75	7.23E-15	1.23E-12
ENSG00000092969	TGFB2	0.76	9.04E-15	1.53E-12
ENSG00000100336	APOL4	-0.96	9.21E-15	1.54E-12

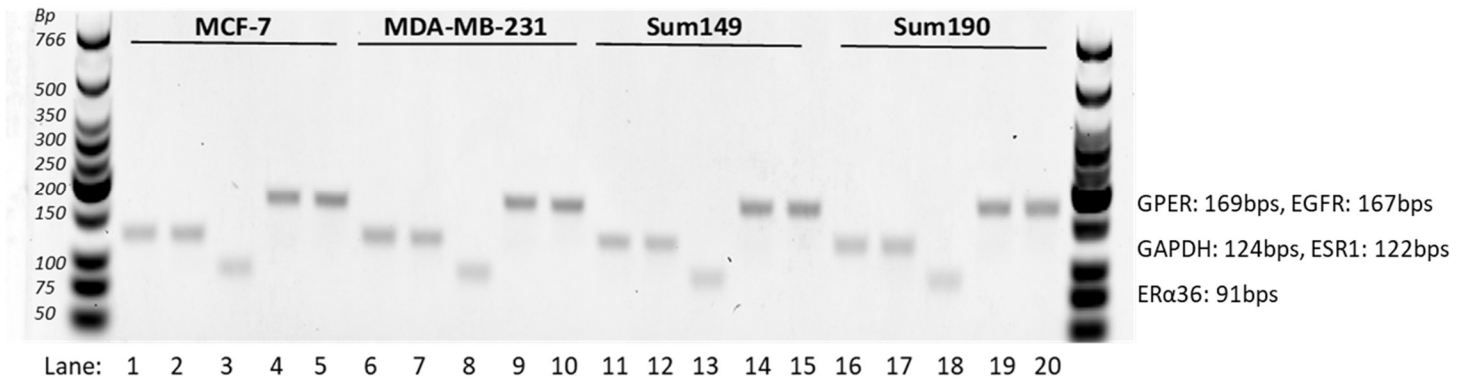**Figure S1**. qPCR products validation by agarose gel

Figure S1, Agarose gel validation of qPCR products

Agarose gel (3%) electrophoresis confirmed RT-qPCR primers' amplicons (B). The base pairs (bps) for each RT-qPCR product are: GAPDH 124bps (1, 6, 11, 16), ESR1 122bps (2, 7, 12, 17), ERα36 91bps (3, 8, 13, 18), GPER 169bps (4, 9, 14, 19), and EGFR 167bps (5, 10, 15, 20).

Figure S2. BCL-2 protein abundance in TN-IBC SUM149 after E2 and G15 treatment
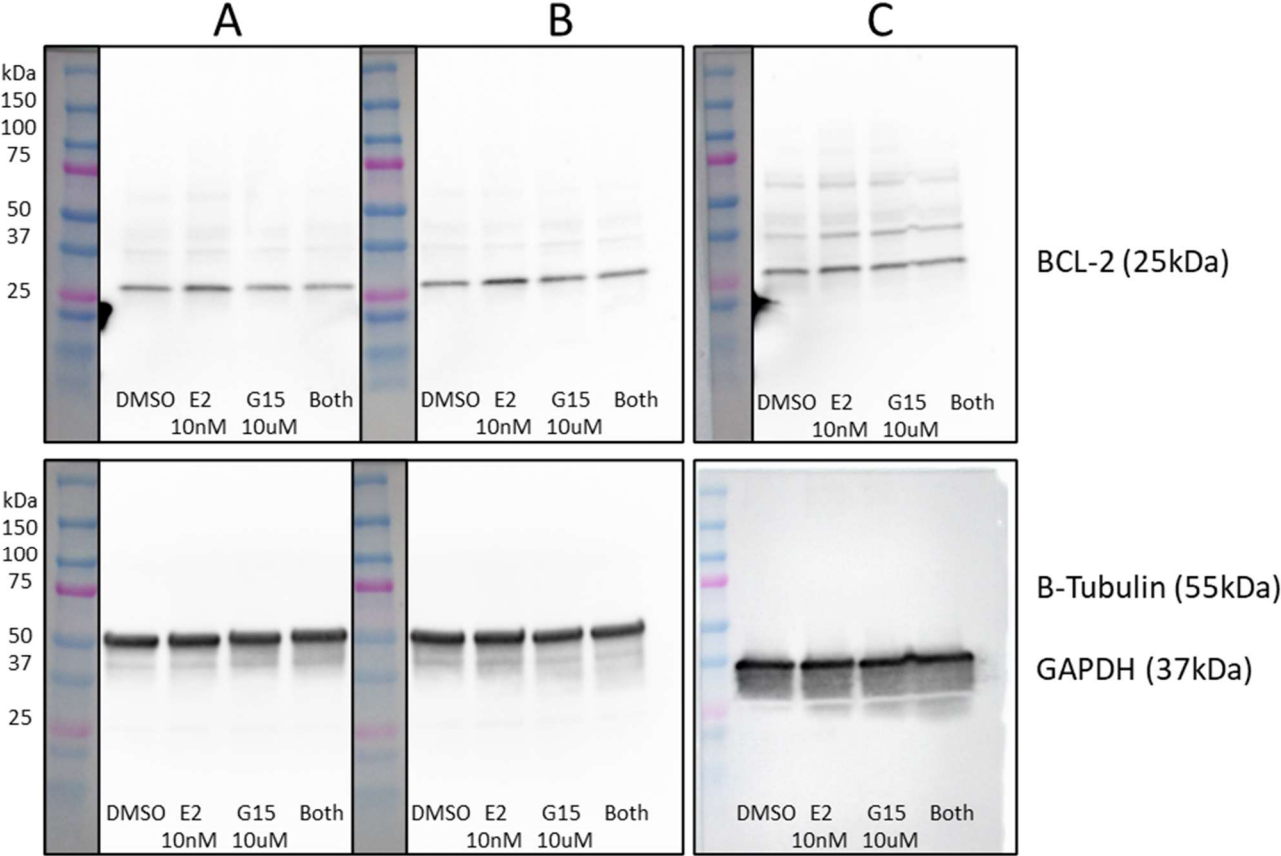
Figure S3. BCL-2 protein abundance in HER2-amplified IBC SUM190 after E2 and G15 treatment
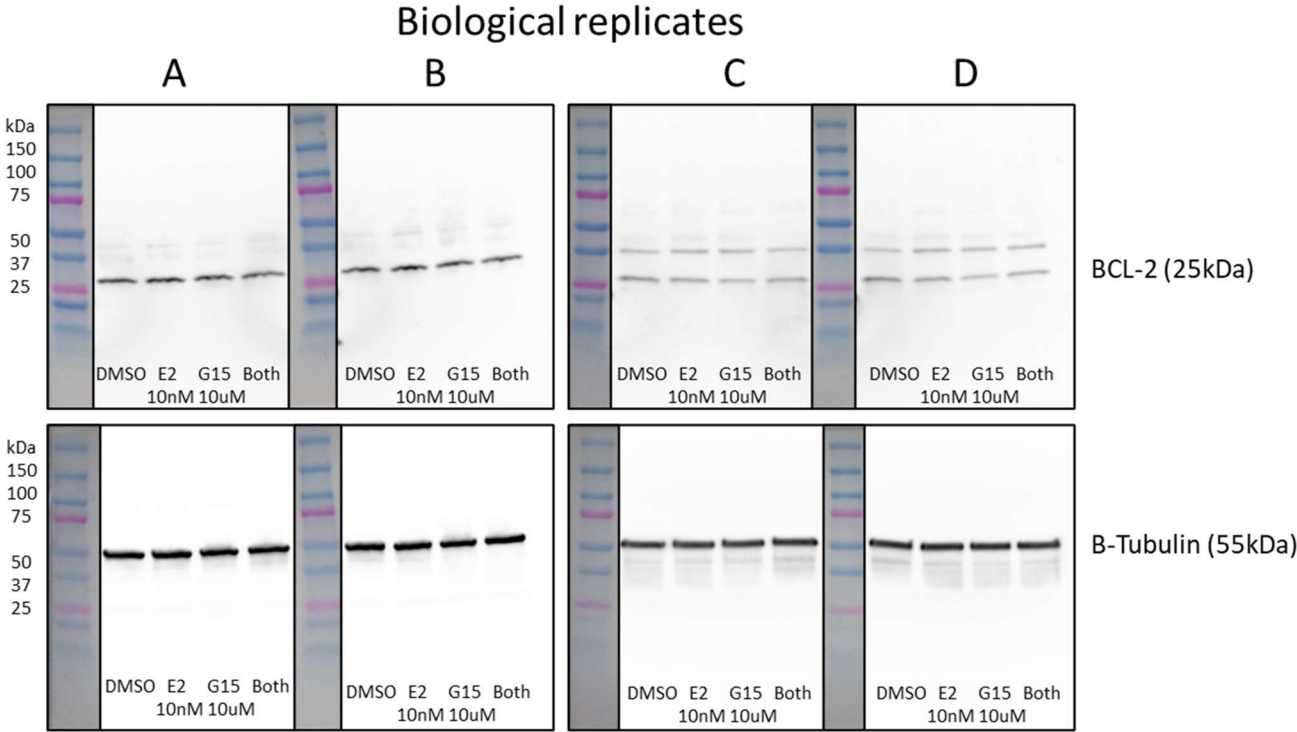
Figure S4. Cyclin E1 and CDK2 protein abundance in TN-IBC SUM149 after E2 + G15 treatment
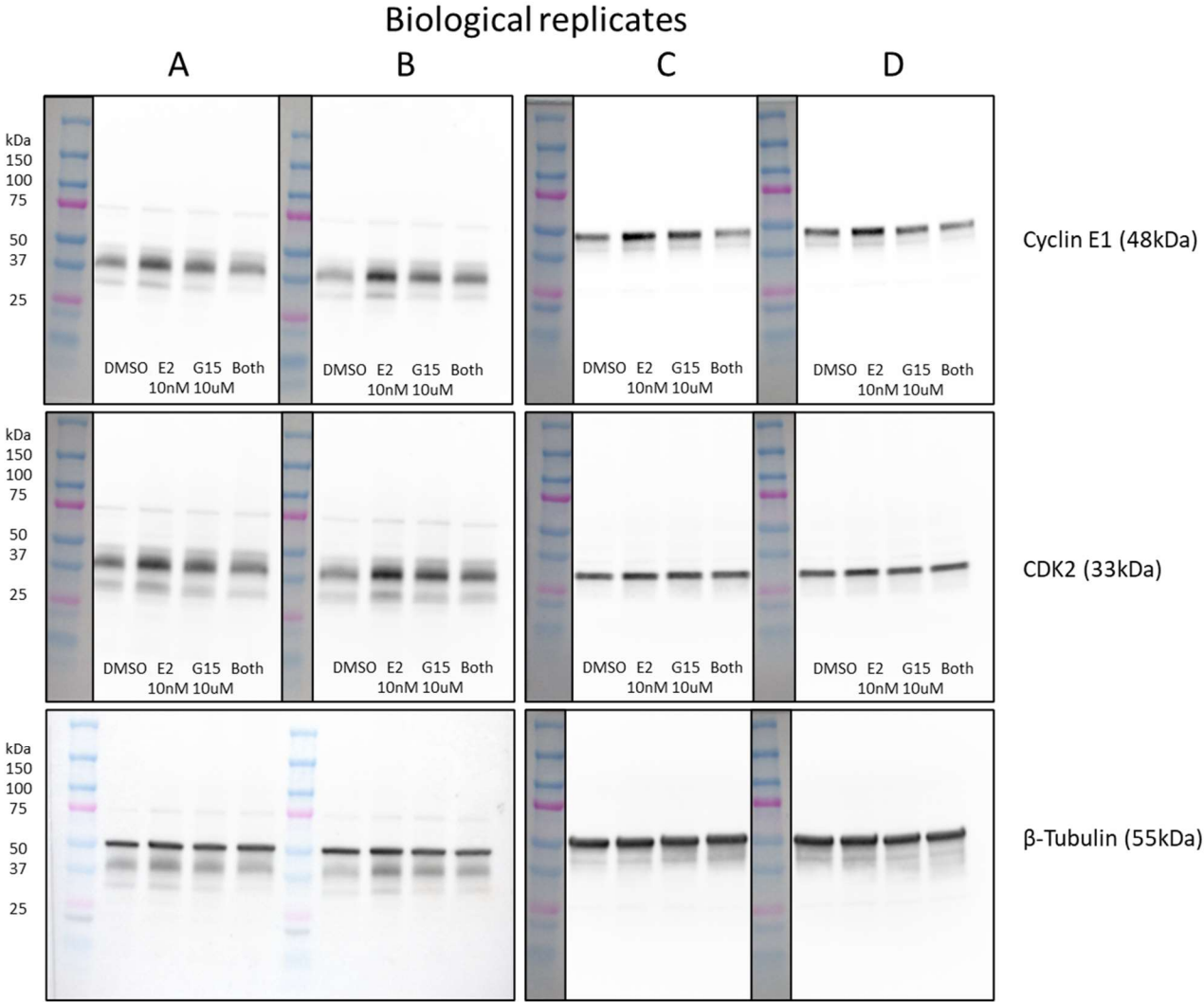
Figure S5. Cyclin E1 and CDK2 protein abundance in HER2-amplified IBC SUM190 after E2 + G15 treatment
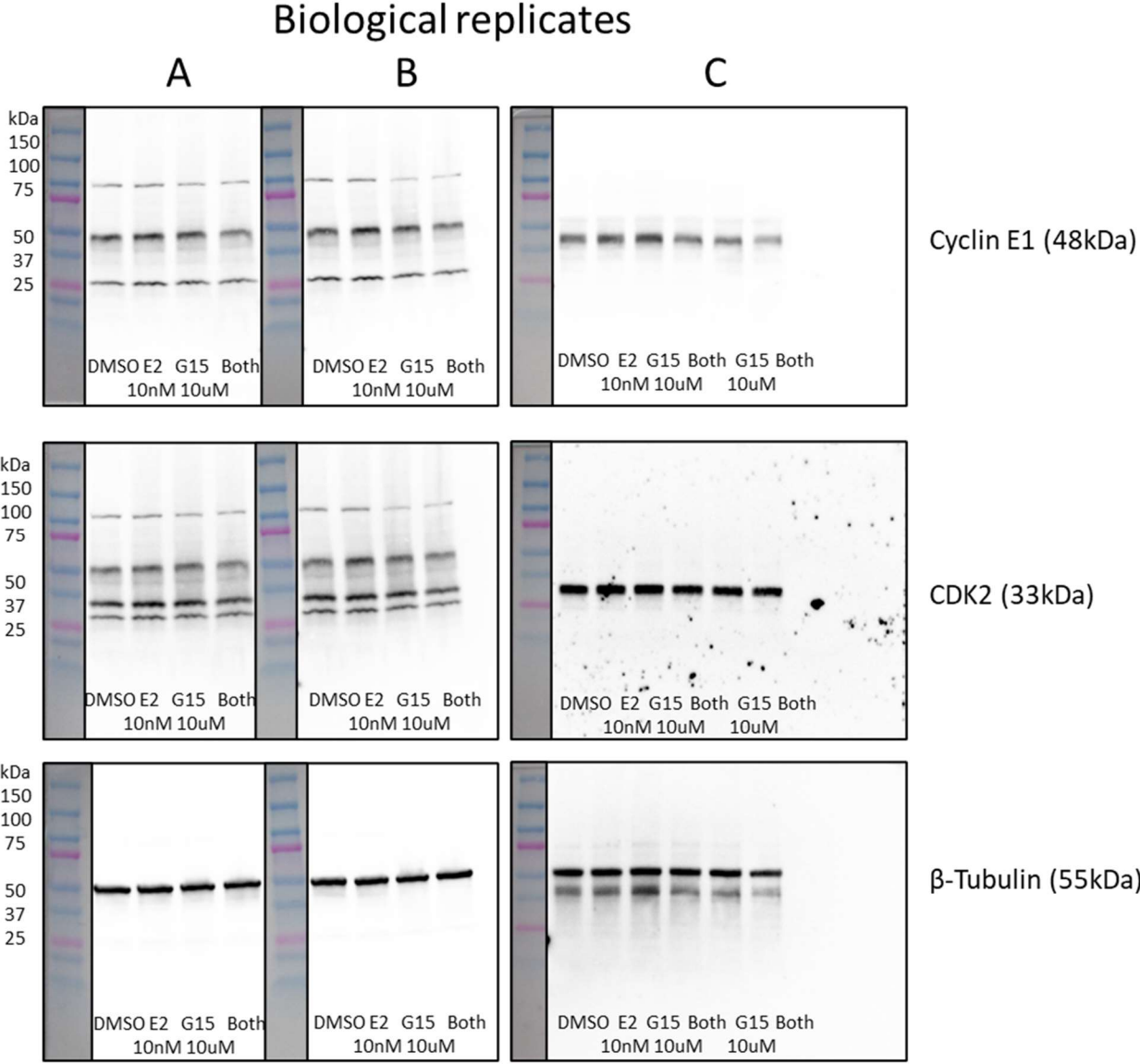
Figure S6. GPER protein abundance across different breast cancer cell lines
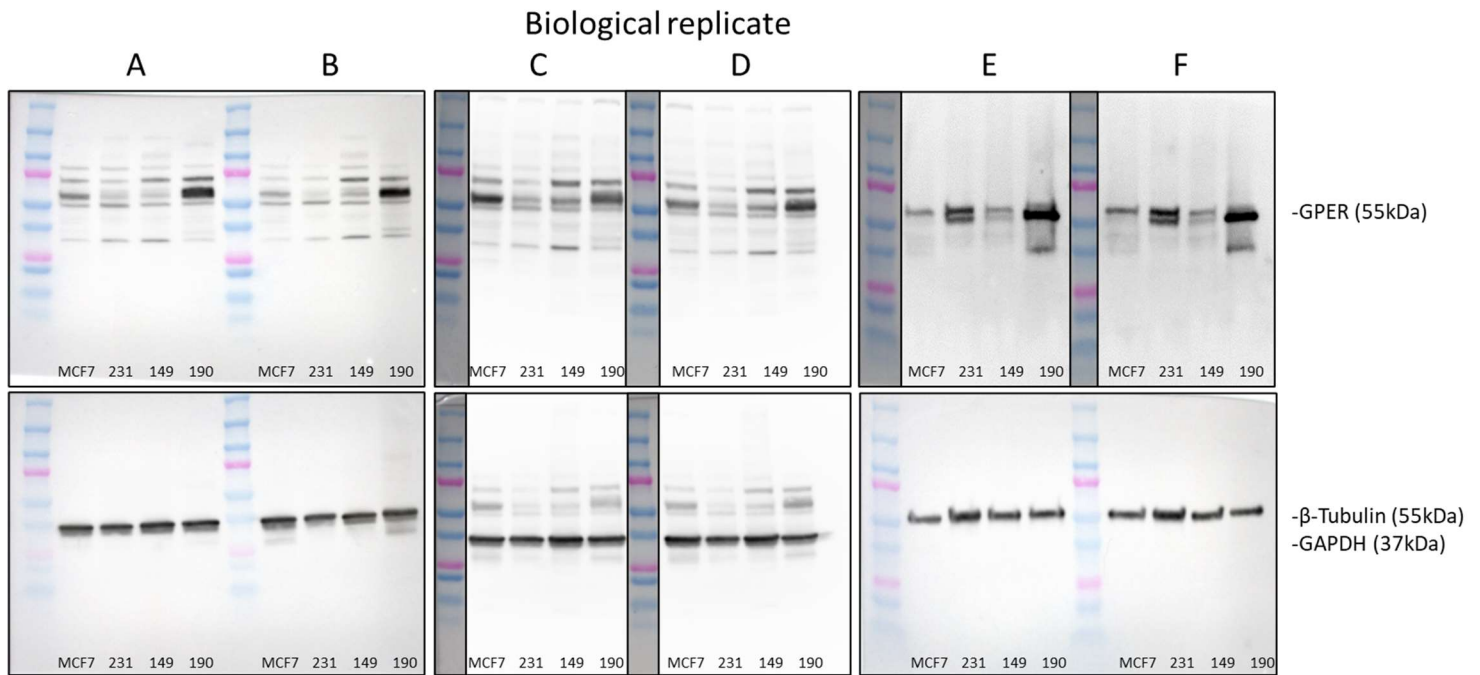
Membranes and antibodies against GPER:

A – B: Anti-G-protein coupled receptor 30 antibody (Abcam, ab39742; 1:50)

C – D: Anti-G-protein coupled receptor 30 antibody (Abcam, ab39742; 1:50)

E – F: anti-GPER (Abcam, #260033; 1:50)

Figure S7. ERK1/2 and AKT phosphorylation levels after E2 treatment in IBC cells
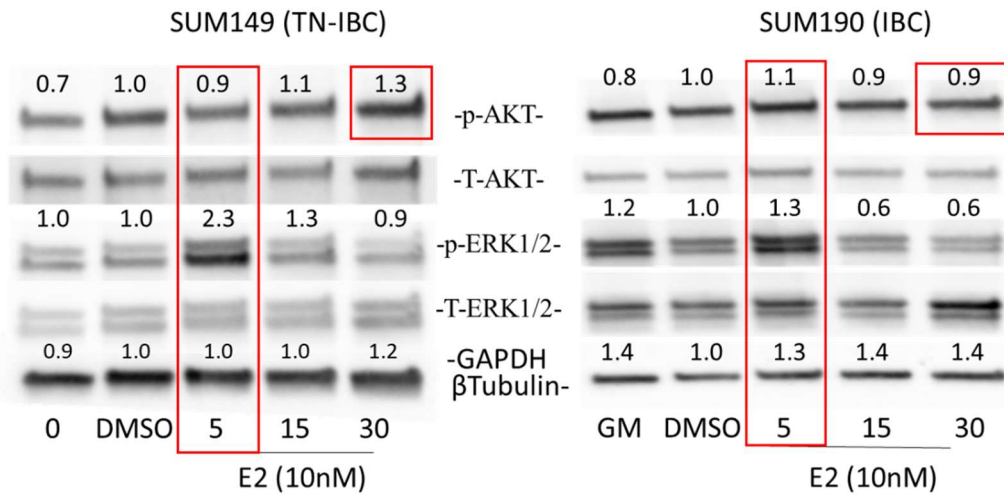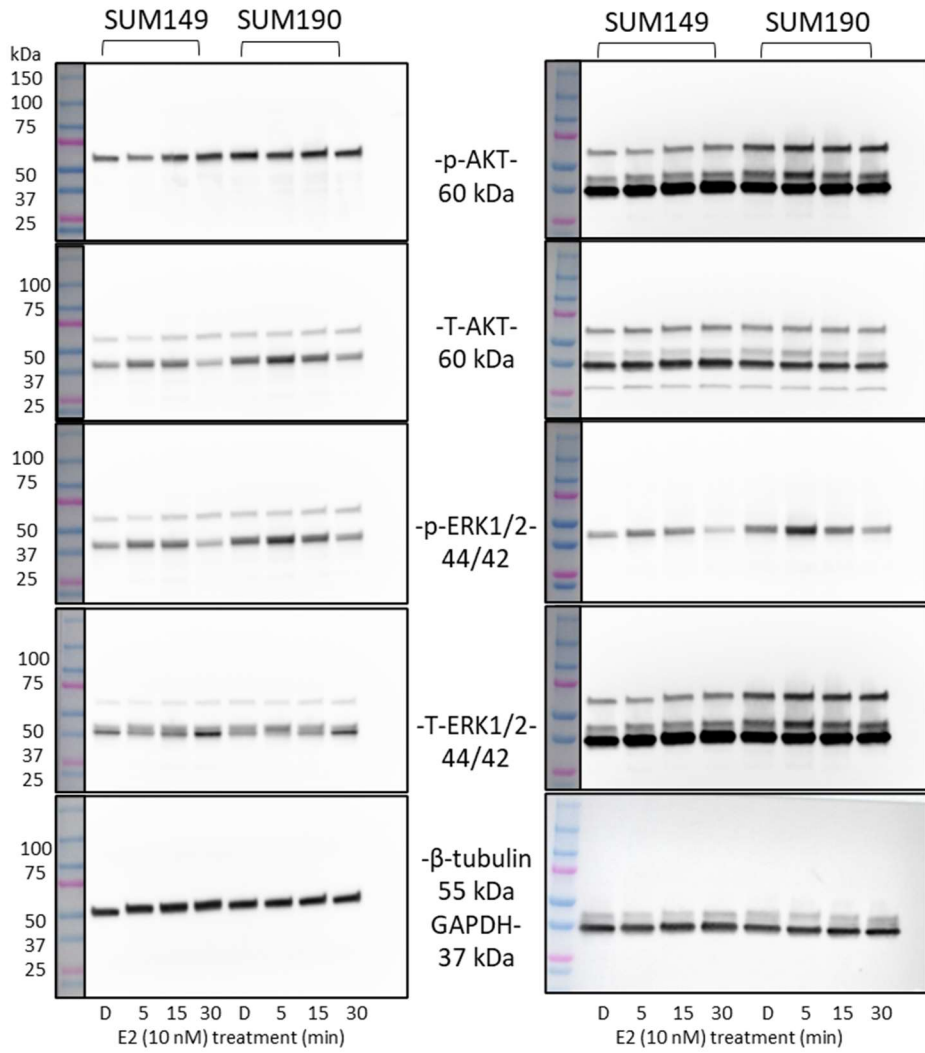
Figure S8. ERK1/2 phosphorylation levels after E2 treatment in IBC cells

SUM149

p-AKT473 (60kDa)
AKT473 (60kDa)
p-ERK1/2 (42/44kDa)
ERK1/2 (42/44kDa)
β-Tubulin (55kDa)

G15 DMSO 5 15 30 5 15 30 min

E2 (10nM)   E2 (10nM) +
                   G15 (**10uM**)

SUM149

p-ERK1/2 (42/44kDa)
ERK1/2 (42/44kDa)
β-Tubulin (55kDa)

G15 DMSO 5 15 30 5 15 30 min

E2 (10 nM)   E2 (10 nM) +
                  G15 (10 μM)

SUM149

p-AKT473 (60kDa)
AKT473 (60kDa)
p-ERK1/2 (42/44kDa)
ERK1/2 (42/44kDa)
β-Tubulin (55kDa)

DMSO 5 15 30 G15 5 15 30 min

E2 (10 nM)   E2 (10 nM) +
                  G15 (10 μM)
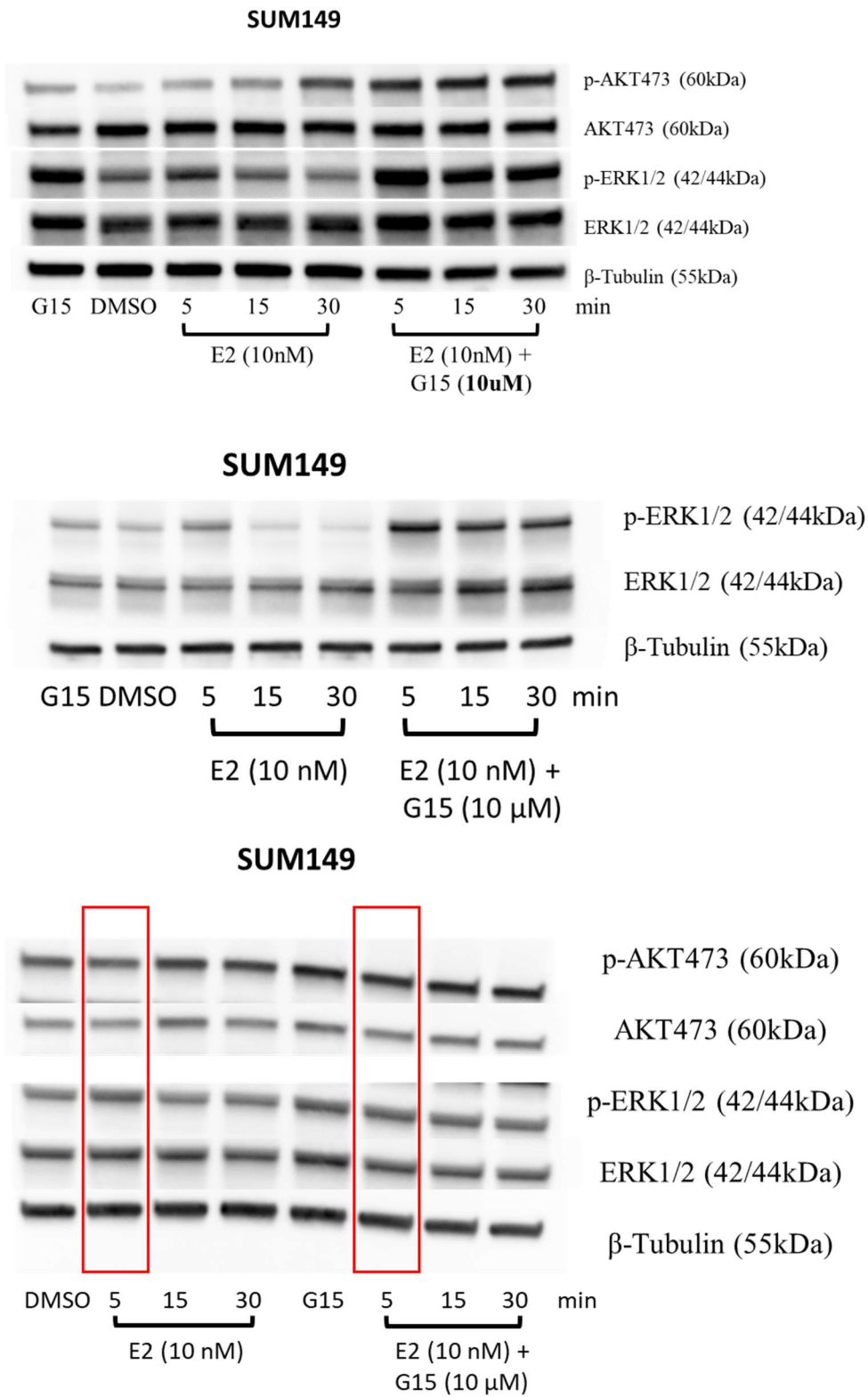
49 Spadina Ave. Suite 200
Toronto ON M5V 2J1 Canada
www.biorender.com

Confirmation of Publication and Licensing Rights

May 2nd, 2023
Science Suite Inc.

Subscription: Student Plan
Agreement number: XO25BGD1KN
Journal name: Repositorio Institucional UPR

To whom this may concern,

This document is to confirm that Xavier Bittman has been granted a license to use the BioRender content, including icons, templates and other original artwork, appearing in the attached completed graphic pursuant to BioRender's Academic License Terms. This license permits BioRender content to be sublicensed for use in journal publications.

All rights and ownership of BioRender content are reserved by BioRender. All completed graphics must be accompanied by the following citation: "Created with BioRender.com".

BioRender content included in the completed graphic is not licensed for any commercial uses beyond publication in a journal. For any commercial use of this figure, users may, if allowed, recreate it in BioRender under an Industry BioRender Plan.

For any questions regarding this document, or other questions about publishing with BioRender refer to our BioRender Publication Guide, or contact BioRender Support at support@biorender.com.

Confirmation of Publication and Licensing Rights

May 2nd, 2023
Science Suite Inc.

Subscription:	*Student Plan*
Agreement number:	*CJ25BGEV6W*
Journal name:	*Repositorio Institicional UPR*

To whom this may concern,

This document is to confirm that Xavier Bittman has been granted a license to use the BioRender content, including icons, templates and other original artwork, appearing in the attached completed graphic pursuant to BioRender's Academic License Terms. This license permits BioRender content to be sublicensed for use in journal publications.

All rights and ownership of BioRender content are reserved by BioRender. All completed graphics must be accompanied by the following citation: "Created with BioRender.com".

BioRender content included in the completed graphic is not licensed for any commercial uses beyond publication in a journal. For any commercial use of this figure, users may, if allowed, recreate it in BioRender under an Industry BioRender Plan.

For any questions regarding this document, or other questions about publishing with BioRender refer to our BioRender Publication Guide, or contact BioRender Support at support@biorender.com.

Protocols

A. Immunocytochemistry and immunofluorescence staining protocol (Abcam)

Fixation:

1. 4% paraformaldehyde in PBS pH 7.4 for 10 min at room temperature.

2. The cells should be washed three times with ice-cold PBS.

Permeabilization:

If the target protein is intracellular, it is essential to permeabilize the cells.

1. Incubate the samples for 10 min with PBS containing either 0.1–0.25% Triton X-100 or Tween-20. Triton X-100 is the most popular detergent for improving the penetration of the antibody. However, it is not appropriate for membrane-associated antigens since it destroys membranes.

2. The optimal percentage of detergent should be determined for each protein of interest.

3. Wash cells in PBS three times for 5 min.

Blocking and immunostaining:

1. Incubate cells with 10% serum in PBST (PBS + 0.1% Tween 20) for 30 min to block unspecific binding. Use serum from the species of the secondary antibody were raised in, typically goat serum or donkey serum. Alternative blocking 1% BSA.

2. Incubate cells in the diluted antibody in 10% serum in PBST in a humidified chamber for 1 h at room temperature or overnight at 4°C.

3. Decant the solution and wash the cells three times in PBS, 5 min each wash.

4. Incubate cells with the secondary antibody in 1% serum for 1 h at room temperature in the dark.

5. Decant the secondary antibody solution and wash three times with PBS for 5 min each in the dark.

Mounting:

1. Mount the coverslip with a drop of mounting medium.

2. Seal the coverslip with nail polish to prevent drying and movement under the microscope.

3. Store in the dark at -20°C or +4°C.

B. RNA extraction and purification

RNeasy® Mini Kit, Part 1 (cat. nos. 74104 and 74106)

The RNeasy Mini Kit can be stored at room temperature (15–25°C) for at least 9 months if not otherwise stated on the label.

Further information

>   RNeasy Mini Handbook: www.qiagen.com/HB-0435

>   Safety Data Sheets: www.qiagen.com/safety

>   Technical assistance: support.qiagen.com

Notes before starting:

- If purifying RNA from cell lines rich in RNases, or tissue, add either 10 µl β-mercaptoethanol (βME), or 20 µl 2 M dithiothreitol (DTT), to 1 ml Buffer RLT. Buffer RLT with β-ME or DTT can be stored at room temperature for up to 1 month.

- Add 4 volumes of ethanol (96–100%) to Buffer RPE for a working solution.

- Remove RNAprotect® stabilized tissue from the reagent using forceps.

- For RNeasy Protect Mini Kit (cat. nos. 74124 and 74126), please start with the Quick-Start Protocol RNAprotect Tissue Reagent, RNAprotect Tissue Tubes, and RNeasy Protect Kits.

1. Cells: Harvest a maximum of 1 x 107 cells, as a cell pellet or by direct lysis in the vessel. Add the appropriate volume of Buffer RLT (Table 1.) and select a suitable method for disruption and homogenization.

Table 1. Volumes of Buffer RLT for sample disruption and homogenization

Sample	Amount	Dish	Buffer RLT (µl)	Disruption and homogenization
Animal cells	$<5 \times 10^6$	<6 cm	350	Add Buffer RLT, vortex ($\leq 1 \times 10^5$ cells); or use
	$<1 \times 10^7$	6–10 cm	600	QIAshredder, TissueRuptor®, or needle and syringe
Animal tissues	<20 mg	–	350	TissueLyser LT; TissueLyser II; TissueRuptor, or mortar and
	≤ 30 mg	–	600	pestle followed by QIAshredder or needle and syringe

2. Add 1 volume of 70% ethanol to the lysate and mix well by pipetting. Do not centrifuge.

Proceed immediately to step 3.

3. Transfer up to 600 µl of the sample, including any precipitate, to a RNeasy Mini spin column placed in a 2 ml collection tube. Close the lid, and centrifuge for 15 s at

≥8000 x g. Discard the flow-through.

4. Add 600 µl Buffer RW1 to the RNeasy spin column. Close the lid and centrifuge for 15 s at ≥8000 x g. Discard the flow-through.

5. Add 500 µl Buffer RPE to the RNeasy spin column. Close the lid and centrifuge for 15 s at ≥8000 x g. Discard the flow-through.

6. Add 500 µl Buffer RPE to the RNeasy spin column. Close the lid and centrifuge for 2 min at ≥8000 x g. Optional: Place the RNeasy spin column in a new 2 ml collection tube (supplied). Centrifuge at full speed for 1 min to dry the membrane.

7. Place the RNeasy spin column in a new 1.5 ml collection tube. Add 40 µl RNase-free water directly to the spin column membrane. Close the lid and centrifuge for 1 min at ≥8000 x g to elute the RNA.

8. If the expected RNA yield is >30 µg, repeat step 7 using another 30–50 µl of RNase-free water or the eluate from step 7 (if high RNA concentration is required). Reuse the collection tube from step 7.

C. *cDNA synthesis*

iScript^{TM} cDNA Synthesis Kit (Cat. #1708890, Bio-Rad)

Components	Volume per Reaction, uL
1. 5X iScript Reaction Mix:	4 ul
2. iScript Reverse Transcriptase:	1 ul
3. RNA template (1 µg total RNA):	Variable

4. Nuclease-free water: Variable

    Total volumen: 20ul

Note: Always include 10% to account for pipetting errors.

Reaction Protocol

Incubate the complete reaction mix in a thermal cycler using the following protocol:

1. Priming: 5 min at 25°C

2. Reverse transcription: 20 min at 46°C

3. RT inactivation: 1 min at 95°C

4. Optional step: Hold at 4°C

Note: Label property and store at -20°C

D. *Real-time PCR*

    Real-time PCR was performed following the iTaq™ Universal SYBR® Green Supermix

    Product Insert provided by Bio-Rad.

E. *Protein extraction*

Cell lysate preparation (Adherent Cells)

1. Wash cells directly in the tissue culture flask or dish by gently adding cold PBS and rocking.

    Aspirate PBS and repeat. Keep the tissue culture dish on ice throughout.

2. Add an appropriate volume of ice-cold lysis buffer (with new protease inhibitors) to the

    plate (approximately 200 ul flask for a 100 mm tissue culture dish).

3. Incubate for 10 minutes on ice, and then scrape cells from the surface using a rubber spatula.

4. Transfer to a microfuge tube and clarify the lysate by spinning for 20 minutes at 12,000 rPM, at 4°C.

5. Transfer the supernatant to a fresh tube and store it on ice or frozen at -20°C or -80°C.

BCA Protein Assay (Thermo Scientific, Cat. No. 23227)

Application: Tecan i-control	Tecan i-control , 2.0.10.0
Device: infinite 200Pro	Serial number: 1507008929
	MAI, V_3.40_01/15_Infinite (Dec 23 2014/12.45.11)
Firmware: V_3.40_01/15_Infinite (Dec 23 2014/12.45.11)	
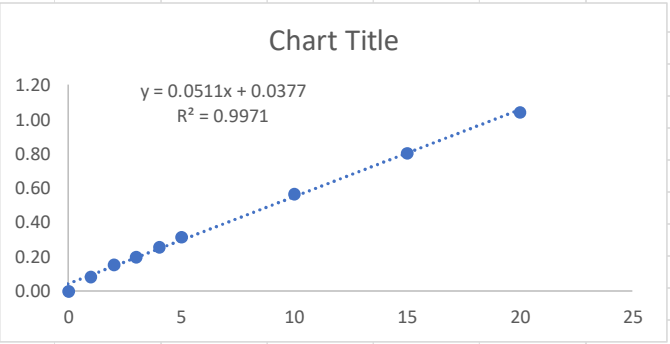
Mode	Absorbance
Measurement Wavelength	562 nm
Bandwidth	9 nm
Number of Flashes	25
Settle Time	0 ms

Sample	A	B	Average	Average-Blank
0	0.08	0.08	0.08	0.00
1	0.17	0.15	0.16	0.08
2	0.23	0.23	0.23	0.15
3	0.27	0.28	0.27	0.19
4	0.35	0.32	0.34	0.26
5	0.41	0.38	0.39	0.31
10	0.66	0.63	0.65	0.57
15	0.91	0.85	0.88	0.80
20	1.12	0.92	1.12	1.04

Chart Title

$y = 0.0511x + 0.0377$
$R^2 = 0.9971$

Sample	A	B	Average	Average-Blank		ug/ul	40ug	Lysis B.	Total	5x Load.	Total
MCF7	0.44	0.43	0.44	0.36	6.28	3.1	12.74	17.83	30.6	7.64	38.2
231	0.52	0.46	0.49	0.41	7.25	3.6	11.04	19.53	30.6	7.64	38.2
SUM149	0.31	0.30	0.31	0.23	3.72	1.9	21.52	9.05	30.6	7.64	38.2
SUM190	0.43	0.41	0.42	0.34	5.93	3.0	13.48	17.08	30.6	7.64	38.2

Steps for calculating protein concentration from the BCA

1. *Average sample A + B.*

2. *Subtract the value of the control group; Blank (0).*

3. *Use the linear equation to solve for x.*

4. *Divide by 2 the µg of the 2 µl sample to obtain the concentration of µg/µl.*

Standard denaturing

1. Mix sample 1:1 by volume with Laemmli 2x sample buffer.

2. Heat to 95°C for 10 minutes.

3. Load 20-50 µg sample per lane, along with appropriate positive and negative controls.

4. Run the gel and transfer it to PVDF or nitrocellulose membrane according to the manufacturer's instructions for the equipment and materials.

F. SDS-PAGE

SDS-PAGE was performed following the Mini-PROTEAN TGX Precast Gels Quick Strat Guide (Bulletin_6048B) provided by Bio-rad.

G. Western blot

Using the Trans-Blot® SD Semi-Dry Transfer Cell

1. Prepare ~ 1 L of a 1x transfer buffer solution by diluting 100 ml 10x Tris/glycine premixed buffer (catalog #161-0734) with 700 ml water and 200 ml methanol.

2. Rinse gel briefly in water and equilibrate in 1x transfer buffer for 15 min

3. Soak two pieces of precut extra-thick filter paper (match the size of the gel) and nitrocellulose membrane in transfer buffer until wet; if PVDF is used, activate the PVDF by soaking in 100% methanol briefly, then equilibrating in transfer buffer

4. Place one filter paper on the anode side of the semi-dry apparatus

5. Place membrane (PVDF or nitrocellulose) on top of the filter paper

6. Carefully place gel on top of the membrane

7. Place the second piece of filter paper on top of the gel; roll out any bubbles that may have formed between the stacks

8. Carefully place the cathode assembly onto the transfer stack and then place the safety cover back onto the unit.

H. *Immunodetection* (immunoblotting)

1. Place blot into blocking solution for 1 hr at RT or overnight at 4°C.

2. Rinse the blot briefly with wash buffer and then add the primary antibody diluted in the wash buffer (check datasheets for precise recommendations). Incubate for 2 hr at RT or overnight at 4°C.

3. Wash the blot extensively in wash buffer (3 x 5 min) with gentle agitation.

4. Add appropriate enzyme-conjugated secondary antibody diluted in wash buffer and incubate for 1 hr at RT with gentle agitation.

5. Wash the membrane 3x 5 min in TBST with gentle agitation.

6. Add appropriate enzyme substrate solution (1 ml mix) and incubate as recommended by the manufacturer to visualize protein bands.

I. 2D-Dose Response Curve (IC50)

1. Two days (100mm plate with cells)- starving medium (1%DCC)

After two days:

2. Perform 2X Serial Dilution of the treatment using a starving medium.
3. Using the 100mm plate of step 1, detach cells using trypsin.
4. Count cells using Trypan Blue.
5. Calculate the number of cells for all the wells (10,000 cells per well)

$$\frac{\text{Number of cells needed}}{\text{Number of cells counted}} = \text{Volume}$$

6. Prepare the sterile tubes with the calculated volume and 1 mL of starving medium. The amount of tubes is based on the number of diluted concentrations of the treatment.
7. Centrifuge all the tubes (1.2rpm for 8-10 minutes).
8. Decant the supernatant in a beaker.
9. Resuspend the pellet with the calculated amount of dilution (starving medium + treatment).
10. Add 200ul of the suspension in their respective wells.
11. Place the 96 wells plate in the incubator for 24, 48, and 72 hours. *Prepare a 96 wells plate for each timepoint.
12. After the timepoint, remove the medium and add 100ul of diluted Alamar Blue (90ul of starving medium + 10ul of Alamar Blue).

> Example: You need 3 wells for each concentration of treatment. *ADD 2 ADDITIONAL WELLS.
>
> **(10,000 cells) x (5 wells) = 50,000 cells**
>
> Calculate the number of cells for all the wells. Example: If the 100mm plate has 1×10^6 cells:
>
> **(50,000 cells) / (1×10^6 cells) = 0.05ml 0.05ml x 1,000 = 50ul**
>
> If you have 8 concentrations of the treatment. Prepare 8 sterile tubes with:
>
> **50ul + 1ml starving medium**
>
> Calculate the amount of starving medium + treatment (dilution):
>
> **(200ul of dilution) x (5 wells) = 1,000ul**
>
> Alamar Blue dilution:
>
> **(90ul starving medium) x (5 wells) = 450ul (10ul Alamar Blue) x (5 wells) = 50ul** *Prepare the dilution in a reservoir.

Important details:

- All the concentrations have been performed in three technical replicates.
- All the timepoints have been performed in three biological replicates.
- All the plates need three technical replicates of:
  - Starving medium (without cells)
  - Cells with starving medium (without treatment)
  - Vehicle (DMSO or EtOH)

J. 3D cell culture in Matrigel

The major components of Corning® Matrigel® matrix are laminin (~60%), collagen IV (~30%), entactin (~8%) and heparan sulfate proteoglycan. Growth factors, collagenases, plasminogen activators, and other undefined components have also been reported in Corning Matrigel matrix.

Reagents and Materials

◗ SUM149 cell line (ATCC)

◗ FBS (Corning Cat. No. 35-015-CV)

◗ PBS (Corning Cat. No. 21-040-CV)

◗ Complete SUM149 growth medium

◗ 0.25% Trypsin/EDTA (Corning Cat. No. 25-053-Cl)

◗ 24-well plate (Corning Cat. No. 3524)

◗ Corning Matrigel matrix (Corning Cat. No. 356234)

◗ Incubator

Protocol

1. Thaw Matrigel matrix overnight by submerging the vial in a 4°C refrigerator before use. Once Matrigel matrix is thawed, swirl vial to ensure the material is dispersed.

2. Add 200 μL of Matrigel matrix into each well of a pre-chilled 24-well plate, spread evenly with a pipet tip, and then incubate at 37°C for 30 min. to allow the Matrigel matrix to gel.
    Note: All culture ware or media in contact with Matrigel matrix should be pre-chilled/ice-cold. Keep Matrigel matrix on ice during the entire process and do not over dry the Matrigel matrix during the gel process.

3.   Wash the SUM149 cells once with PBS. Trypsinize the cells to make a single-cell suspension, and then pellet the cells through centrifugation at 125 x g for 10 min. at room temperature (RT).
    Note: Use cells that are healthy and not more than 85% confluent. SUM149 cells tend to form cell clumps; therefore, it is often necessary to pipet them vigorously to obtain a single cell suspension.

4. Re-suspend the cells with SUM149 complete medium (F12 + 10% FBS) to adjust the final cell density to 1 x 10^5 cells/mL, plate 250 μL prepared cell suspension into each well of the pre-coated 24-well plate, and then incubate at 37°C for 60 min.

   Note: The number of cells may need optimization depending on the growth properties of the cell line.

5. Chill the SUM149 complete medium on ice and prepare treatments solution. Add Matrigel matrix to 5% of the final volume for each treatment. Gently add 250 μL of Matrigel matrix medium mixture to the plated culture. Note: Medium must be thoroughly chilled before the addition of Matrigel matrix to ensure homogenous mixing and even deposition of Matrigel matrix onto cells in culture. Pipet the Matrigel matrix medium mixture down the side of the well to avoid disturbance of the cells or Matrigel Matrix.

6. Continuously culture for 10 days and change Matrigel matrix medium mixture every 2 days.

7. After 10 days of culturing, the morphology of the colonies is verified through a microscope (4X objective). The area/size of the colonies are measured in the 20X objective through ImageJ.

K. RStudio codes

1. Bargraph and bubbleplots

```
library(enrichR)
library(ggplot2)
library(dplyr)
library(stringr)
library(viridis)
library(data.table)
library(tidyverse)
setwd("C:/Users/xbitt/OneDrive/Documents/CCC/Rstudio/RNAseq_analysis/DMSOvs45min")
getwd()
list.files()


####Load dataset with list of sig Genes
XavierList <- read.csv(file="RNAseq_DMSOvs45min.csv",sep=",", header=T, na.strings = "NA")
head(XavierList)
miniXavier <- head(XavierList, 211)
head(miniXavier)
listEnrichrSites()


setEnrichrSite("Enrichr") # Human genes


websiteLive <- TRUE


dbs <- listEnrichrDbs()


if (is.null(dbs)) websiteLive <- FALSE
if (websiteLive) head(dbs)


dbs            <-           c("GO_Molecular_Function_2021",           "GO_Cellular_Component_2021",
"GO_Biological_Process_2021", "KEGG_2021_Human")
```

```
if (websiteLive) {
  enriched <- enrichr(miniXavier$Gene.Symbol, dbs)
}

GOBP<-if (websiteLive) enriched[["GO_Biological_Process_2021"]]
GOCC<-if (websiteLive) enriched[["GO_Cellular_Component_2021"]]
GOMF<-if (websiteLive) enriched[["GO_Molecular_Function_2021"]]
KEGG<-if (websiteLive) enriched[["KEGG_2021_Human"]]

colnames(GOBP)
colnames(GOCC)
colnames(GOMF)
colnames(KEGG)

#####Visualization from enrichR Results
######Add the count column based on the number of gene present per GO term
GOBP$NumberOfGenes <- str_count(GOBP$Genes, ";")+1
GOCC$NumberOfGenes <- str_count(GOCC$Genes, ";")+1
GOMF$NumberOfGenes <- str_count(GOMF$Genes, ";")+1
KEGG$NumberOfGenes <- str_count(KEGG$Genes, ";")+1

######Add a column that contains the -logbase10 of the pValue enriched per GO term
GOBP <- GOBP %>% mutate(log10pValue=-log10(P.value))
GOCC <- GOCC %>% mutate(log10pValue=-log10(P.value))
GOMF <- GOMF %>% mutate(log10pValue=-log10(P.value))
KEGG <- KEGG %>% mutate(log10pValue=-log10(P.value))

#######Rename the columns obtained from enrichR
GOBP <- GOBP %>% rename(GOTerm=Term,
          pValue=P.value,
          OldpValue=Old.P.value,
          AdjpValue=Adjusted.P.value,
```

```
                    OldAdjpValue=Old.Adjusted.P.value)
GOCC <- GOCC %>% rename(GOTerm=Term,
                    pValue=P.value,
                    OldpValue=Old.P.value,
                    AdjpValue=Adjusted.P.value,
                    OldAdjpValue=Old.Adjusted.P.value)
GOMF <- GOMF %>% rename(GOTerm=Term,
                    pValue=P.value,
                    OldpValue=Old.P.value,
                    AdjpValue=Adjusted.P.value,
                    OldAdjpValue=Old.Adjusted.P.value)
KEGG <- KEGG %>% rename(GOTerm=Term,
                    pValue=P.value,
                    OldpValue=Old.P.value,
                    AdjpValue=Adjusted.P.value,
                    OldAdjpValue=Old.Adjusted.P.value)


#####Filter to only have the significant GOTerms
GOBP<- GOBP %>% filter(log10pValue>=1.30103)
GOCC<- GOCC %>% filter(log10pValue>=1.30103)
GOMF<- GOMF %>% filter(log10pValue>=1.30103)
KEGG<- KEGG %>% filter(log10pValue>=1.30103)


#####Sort the dataframes by -log10pValue in descending order.
GOBP<- GOBP %>% arrange(desc(log10pValue))
GOCC<- GOCC %>% arrange(desc(log10pValue))
GOMF<- GOMF %>% arrange(desc(log10pValue))
KEGG<- KEGG %>% arrange(desc(log10pValue))


#####Subset a dataframe that only contains the first top 50 most significant GOTerms
#####This is only if the dataframe exceeds more than 50!!!!!!!
GOBP_p2<-head(GOBP, 10) #Top 50 most enriched
```

```r
GOCC_p2<-head(GOCC, 10) #Top 50 most enriched
GOMF_p2<-head(GOMF, 10) #Top 50 most enriched
KEGG_p2<-head(KEGG, 10) #Top 50 most enriched


#########################BUBBLEPLOTS#####################
#####Make the Bubbleplots
#####Bubleplot for GOBP
ggsave("GOBP_BubblePlotXavier_06162022.png",width = 16,height = 9,dpi = 1200)
a<-ggplot(GOBP_p2,aes(x=log10pValue,y=GOTerm, size=NumberOfGenes, color=log10pValue))+
 geom_point(alpha=0.5)+
 scale_color_viridis(option="turbo", direction=-1)+
 ggtitle("Enrichment analysis from enrichR for GO Biological Process")+
 xlab("-log10pValue")+
 ylab("GO Terms")+
 theme(
  plot.title = element_text(color="black", size=12, face="bold", hjust=+0.5),
  axis.title.x = element_text(color="black", size=12, face="bold"),
  axis.title.y = element_text(color="black", size=12, face="bold")
 )
print(a)
dev.off()


#####Bubleplot for GOCC
ggsave("GOCC_BubblePlotXavier_06162022.png",width = 16,height = 9,dpi = 1200)
b<-ggplot(GOCC_p2,aes(x=log10pValue,y=GOTerm, size=NumberOfGenes, color=log10pValue))+
 geom_point(alpha=0.5)+
 scale_color_viridis(option="turbo", direction=-1)+
 ggtitle("Enrichment analysis from enrichR for GO Cellular Components")+
 xlab("-log10pValue")+
 ylab("GO Terms")+
 theme(
  plot.title = element_text(color="black", size=12, face="bold", hjust=+0.5),
```

```r
    axis.title.x = element_text(color="black", size=12, face="bold"),

    axis.title.y = element_text(color="black", size=12, face="bold")

  )

print(b)

dev.off()

#####Bubleplot for GOMF

ggsave("GOMF_BubblePlotXavier_06162022.png",width = 16,height = 9,dpi = 1200)

c<-ggplot(GOMF_p2,aes(x=log10pValue,y=GOTerm, size=NumberOfGenes, color=log10pValue))+

  geom_point(alpha=0.5)+

  scale_color_viridis(option="turbo", direction=-1)+

  ggtitle("Enrichment analysis from enrichR for GO Molecular Functions")+

  xlab("-log10pValue")+

  ylab("GO Terms")+

  theme(

    plot.title = element_text(color="black", size=12, face="bold", hjust=+0.5),

    axis.title.x = element_text(color="black", size=12, face="bold"),

    axis.title.y = element_text(color="black", size=12, face="bold")

  )

print(c)

dev.off()


#####Bubleplot for KEGG

ggsave("KEGG_BubblePlotXavier_06162022.png",width = 16,height = 9,dpi = 1200)

d<-ggplot(KEGG_p2,aes(x=log10pValue,y=GOTerm, size=NumberOfGenes, color=log10pValue))+

  geom_point(alpha=0.5)+

  scale_color_viridis(option="turbo", direction=-1)+

  ggtitle("Enrichment analysis from enrichR for KEGG Pathways")+

  xlab("-log10pValue")+

  ylab("GO Terms")+

  theme(

    plot.title = element_text(color="black", size=12, face="bold", hjust=+0.5),

    axis.title.x = element_text(color="black", size=12, face="bold"),
```

```
    axis.title.y = element_text(color="black", size=12, face="bold")
  )
print(d)
dev.off()

#########################BUBBLEPLOTS######################


#########################BARPLOTS######################
#####Make the Barplots
#####Barplot for GOBP
summary(GOBP_p2$log10pValue)
ggplot(GOBP_p2,aes(x=NumberOfGenes,y=reorder(GOTerm,+NumberOfGenes), fill=log10pValue))+
  geom_bar(stat = "identity") +
  #scale_color_viridis(option="turbo", direction=-1)+
  scale_fill_gradient2(low="black", mid="lightskyblue2", high="red",
                midpoint=9.839, limits=range(GOBP_p2$log10pValue)) +
  ggtitle("Enrichment analysis for GO Biological Process, E2 45 min")+
  xlab("Number of Genes per GO Term")+
  ylab("GO Terms")+
  theme(
    plot.title = element_text(color="black", size=14, face="bold", hjust=+0.5),
    axis.title.x = element_text(color="black", size=14, face="bold"),
    axis.title.y = element_text(color="black", size=14, face="bold")
  )
#####Barplot for GOCC
summary(GOCC_p2$log10pValue)
ggplot(GOCC_p2,aes(x=NumberOfGenes,y=reorder(GOTerm,+NumberOfGenes), fill=log10pValue))+
  geom_bar(stat = "identity", color= "black") +
  #scale_color_viridis(option="turbo", direction=-1)+
  scale_fill_gradient2(low="black", mid="lightskyblue2", high="red",
                midpoint=2.132, limits=range(GOCC_p2$log10pValue)) +
  ggtitle("Enrichment analysis for GO Cellular Components, E2 45 min")+
  xlab("Number of Genes per GO Term")+
```

```r
  ylab("GO Terms")+
  theme(
    plot.title = element_text(color="black", size=14, face="bold", hjust=+0.5),
    axis.title.x = element_text(color="black", size=14, face="bold"),
    axis.title.y = element_text(color="black", size=14, face="bold")
  )
#####Barplot for GOMF
summary(GOMF_p2$log10pValue)
ggplot(GOMF_p2,aes(x=NumberOfGenes,y=reorder(GOTerm,+NumberOfGenes), fill=log10pValue))+
  geom_bar(stat = "identity", color= "black") +
  #scale_color_viridis(option="turbo", direction=-1)+
  scale_fill_gradient2(low="lightskyblue4", mid="lightskyblue2", high="red",
                midpoint=11.135, limits=range(GOMF_p2$log10pValue)) +
  ggtitle("Enrichment analysis for GO Molecular Functions, E2 45 min")+
  xlab("Number of Genes per GO Term")+
  ylab("GO Terms")+
  theme(
    plot.title = element_text(color="black", size=14, face="bold", hjust=+0.5),
    axis.title.x = element_text(color="black", size=14, face="bold"),
    axis.title.y = element_text(color="black", size=14, face="bold")
  )
#####Barplot for KEGG
summary(KEGG_p2$log10pValue)
ggplot(KEGG_p2,aes(x=NumberOfGenes,y=reorder(GOTerm,+NumberOfGenes), fill=log10pValue))+
  geom_bar(stat = "identity") +
  #scale_color_viridis(option="turbo", direction=-1)+
  scale_fill_gradient2(low="black", mid="lightskyblue2", high="red",
                midpoint=6.087, limits=range(KEGG_p2$log10pValue)) +
  ggtitle("Enrichment analysis for GO KEGG Pathways, E2 45 min")+
  xlab("Number of Genes per GO Term")+
  ylab("GO Terms")+
  theme(
```

```
    plot.title = element_text(color="black", size=14, face="bold", hjust=+0.5),

    axis.title.x = element_text(color="black", size=14, face="bold"),

    axis.title.y = element_text(color="black", size=14, face="bold")

  )
```

#########################BARPLOTS#####################

```
#Save the files
write.csv(GOBP, file="GOBP_enrichRResults_XavierRNAaseq_DMSOvs45min.csv",row.names=FALSE)

write.csv(GOCC, file="GOCC_enrichRResults_XavierRNAaseq_DMSOvs45min.csv",row.names=FALSE)

write.csv(GOMF, file="GOMFP_enrichRResults_XavierRNAaseq_DMSOvs45min.csv",row.names=FALSE)

write.csv(KEGG, file="KEGG_enrichRResults_XavierRNAaseq_DMSOvs45min.csv",row.names=FALSE)
```

2. **Volcano plot code**

```
library(ggplot2)
library(dplyr)
library(ggrepel)


setwd("C:/Users/xbitt/OneDrive/Documents/CCC/Rstudio/RNAseq_analysis/DMSOvs90min")
getwd()
list.files()


genes <- read.csv(file="90min_genes_1.csv",sep=",", header=T, na.strings = "NA")
head(genes)
colnames(genes)


genes$diffexpressed <- "NO"
head(genes)
dim(genes)


genes$diffexpressed[genes$log2.Fold.Change>(0.58) & genes$Adjusted.P.value<0.05] <-"UP"
genes$diffexpressed[genes$log2.Fold.Change<(-0.58) & genes$Adjusted.P.value<0.05] <-"DOWN"
```

```
head(genes)

genes$delabel <-NA
ggplot(data=genes,aes(x=log2.Fold.Change,y=-log10(P.value), col=diffexpressed,label=delabel))+
   geom_point()+
   theme_minimal()+
   geom_text_repel()+
   scale_color_manual(values=c("blue", "black", "red"))+
   geom_vline(xintercept=c(-0.8, 0.8), col="red")+
   geom_hline(yintercept=-log10(0.001), col="red")+
   theme(text=element_text(size=20))

head(genes)

arrange(genes,Adjusted.P.value)
head(arrange(genes,Adjusted.P.value),10)$Adjusted.P.value [10]

thresh=arrange(arrange(genes,Adjusted.P.value),10)$Adjusted.P.value [10]
thresh
head(genes)
head(thresh)
head(arrange(genes,Adjusted.P.value),10)$Gene.Symbol

head(arrange(genes,Adjusted.P.value),10)
genes$delabel[genes$Adjusted.P.value                                    <=thresh]<-
(genes$Gene.Symbol[genes$Adjusted.P.value<=thresh])
head(genes$Gene.Symbol[genes$Adjusted.P.value<=thresh])


ggplot(data=genes,aes(x=log2.Fold.Change,y=-log10(Adjusted.P.value),
col=diffexpressed,label=delabel))+
 geom_point()+
```

```
theme_minimal()+

geom_text_repel()+

scale_color_manual(values=c("blue", "black", "red"))+

ggtitle("Differentialy expressed genes after E2 (90min)")+

#theme(text=element_text(size=16))

theme(

plot.title = element_text(color="black", size=16, face="bold", hjust=+0.5),

axis.title.x = element_text(color="black", size=16, face="bold"),

axis.title.y = element_text(color="black", size=16, face="bold")

)
```